Master's Theses   Master's Theses and Graduate Research

1989

Computer modeling of slug and bail tests

Carrie Anne Cummings
San Jose State University

Follow this and additional works at: https://scholarworks.sjsu.edu/etd_theses

Recommended Citation

INFORMATION TO USERS

The most advanced technology has been used to photograph and reproduce this manuscript from the microfilm master. UMI films the text directly from the original or copy submitted. Thus, some thesis and dissertation copies are in typewriter face, while others may be from any type of computer printer.

The quality of this reproduction is dependent upon the quality of the copy submitted. Broken or indistinct print, colored or poor quality illustrations and photographs, print bleedthrough, substandard margins, and improper alignment can adversely affect reproduction.

In the unlikely event that the author did not send UMI a complete manuscript and there are missing pages, these will be noted. Also, if unauthorized copyright material had to be removed, a note will indicate the deletion.

Oversize materials (e.g., maps, drawings, charts) are reproduced by sectioning the original, beginning at the upper left-hand corner and continuing from left to right in equal sections with small overlaps. Each original is also photographed in one exposure and is included in reduced form at the back of the book.

Photographs included in the original manuscript have been reproduced xerographically in this copy. Higher quality 6" x 9" black and white photographic prints are available for any photographs or illustrations appearing in this copy for an additional charge. Contact UMI directly to order.

Order Number 1339608

Computer modeling of slug and bail tests

Cummings, Carrie Anne, M.S.

San Jose State University, 1989

COMPUTER MODELING OF SLUG AND BAIL TESTS

A Thesis

Presented to

The Faculty of the Department of Geology
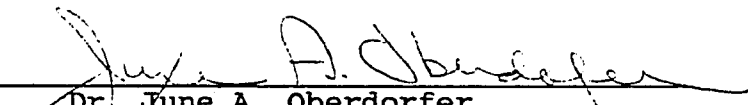
San Jose State University

In Partial Fulfillment

of the Requirements for the Degree
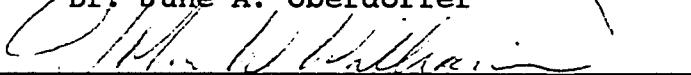
Master of Science

By

Carrie Anne Cummings

December, 1989
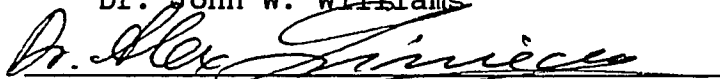
APPROVED FOR THE DEPARTMENT OF GEOLOGY

Dr. June A. Oberdorfer
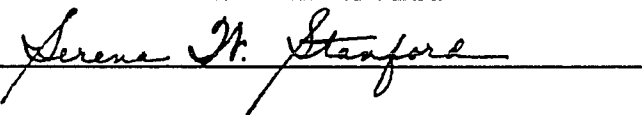
Dr. John W. Williams

Dr. Alex G. Liniecki

APPROVED FOR THE UNIVERSITY

ACKNOWLEDGEMENTS

TABLE OF CONTENTS

LIST OF ILLUSTRATIONS

LIST OF TABLES

ABSTRACT

COMPUTER MODELING OF SLUG AND BAIL TESTS

By Carrie Anne Cummings

Slug and bail tests were performed on monitoring
wells at Lawrence Livermore National Laboratory Site 300.
The wells were located in unconfined aquifers and
constructed with relatively permeable sandpacks. The
analytical methods used to interpret the field data are
not directly applicable to unconfined aquifers and do not
account for the rapid sandpack response that often masks
the aquifer response. The hydraulic conductivities
calculated have varied over two orders of magnitude
between the different methods.

The slug and bail tests were modeled using a computer
program (UNSAT2). The UNSAT2 well recovery curves are
strongly influenced by well geometries, but are not
particularly sensitive to unsaturated properties of the
aquifer and sandpack or initial water level displacement.
The UNSAT2 results generally agree with modified methods
of Hvorslev (1951) and Bouwer and Rice (1976). The method
of Cooper et al. (1967) tends to overestimate the
hydraulic conductivity values.

INTRODUCTION

Lawrence Livermore National Laboratory Site 300

Tritium, a radioactive isotope of hydrogen, was used in explosives experiments during the period 1963 to 1978 at Site 300, a Lawrence Livermore National Laboratory (LLNL) explosives test site. The tritium-contaminated waste generated during the experiments was contained in landfills at Site 300. An initial series of landfill monitoring wells were installed in 1982 to satisfy Resource Conservation and Recovery Act (RCRA) requirements.

Ground water samples were obtained quarterly from the monitoring wells and analyzed for a variety of constituents, including tritium. Samples collected in 1984 showed increasing tritium concentrations that exceeded the State of California drinking water standard (20,000 pCi/l) in some wells. An investigation was conducted to characterize the geology, hydrology, and tritium distribution in the contaminated area. The results of the study include probable tritium source locations, release mechanisms, ground water velocities and directions, and predicted tritium plume migration rates (Buddemeier et al., 1985 and 1986).

The calculated ground water velocities, based on formation hydraulic conductivities and the hydraulic gradient, are a few tens of meters per year. It has been concluded that the tritium contamination, traveling at these velocities, poses no short-term threat to human health or to any drinking water supply, and it is predicted to pose no long-term threat. Further investigation and monitoring are being performed to refine the contaminant transport predictions for the longer term. There is also a need to refine the understanding of the aquifer parameters, including the hydraulic conductivity estimates.

The shallow contaminated aquifer at Site 300 is unconfined, and is dominated by interbedded claystones, siltstones, and sandstones of the Neroly Formation (Buddemeier et al., 1985 and 1986). Slug tests have been chosen as a suitable method for determining the hydraulic conductivity of the aquifer because it is relatively small. An accurate hydraulic conductivity value for the aquifer is essential to predict ground water velocities, but there has been much uncertainty in the results obtained using the existing methods. Several analytical methods have been used to determine the hydraulic conductivities of the contaminated aquifer at Site 300

from slug test results, but none of these methods was developed for the specific type of well at Site 300.

The monitoring wells and piezometers at Site 300 are cased and fully or partially penetrating, with well screen extending both above and below the water table. The distance over which water flows into or out of the well varies during slug testing because of this well screen placement. Additionally, a sandpack is installed between the well casing and the aquifer. The sandpack is highly permeable relative to the aquifer and will drain or saturate relatively quickly (Bouwer, 1989). The sandpack response may partially mask the aquifer response during slug testing.

None of the analytical methods is valid for all these conditions. The hydraulic conductivities calculated using four common methods vary over two orders of magnitude (Buddemeier et al., 1985) and introduce a proportional uncertainty in the calculated ground water velocity values. The purpose of this study is to develop a reliable method of analyzing slug test results for the type of monitoring wells and aquifer under investigation at Site 300, thereby improving or confirming the accuracy of the contaminant transport predictions.

Computer Model UNSAT2

Slug tests are modeled for this study using the finite element program, UNSAT2. The program was created by Shlomo P. Neuman for the analysis of flow in unsaturated, partially saturated, or fully saturated porous media. UNSAT2 is documented in Neuman (1973, 1975b) and a user's guide and program listing is provided in Davis and Neuman (1983). The program was developed to simulate flow systems that involve variably unsaturated and saturated conditions, such as infiltration, evaporation, water uptake by plants, and flow to or from a well. Unsaturated flow above the water table is included in the theory, allowing gravity drainage from the unsaturated zone to be a factor in some flow situations.

UNSAT2 is directly applicable to the simulation of slug and bail tests. Flow may be simulated in a three dimensional region with radial symmetry about a vertical axis, as is the case with well simulations. The program can incorporate boundaries exposed to atmospheric conditions such as seepage faces which may form along the well casing during slug tests. The program can analyze flow to a fully or partially penetrating well of finite radius.

Multiple material types may be simulated by UNSAT2. Each element is assigned constant values of saturated vertical and horizontal hydraulic conductivity, specific storage, and porosity, corresponding to either the aquifer or the sandpack material. The characteristic curves for negative pressure head or relative hydraulic conductivity versus volumetric water content are also assigned to each element depending on the material type. The elements surrounding the well are assigned the values corresponding to the sandpack, and the others are assigned values corresponding to the aquifer. This permits the determination of both the aquifer and the sandpack responses because the sandpack elements may drain or saturate more rapidly than the aquifer elements in response to a gradient.

UNSAT2 simulates the response of an unconfined aquifer with a moving water table. The water content at individual nodes varies during transient conditions, and the water table is defined by an internal isobar where the pressure head equals zero. The program can simulate monitoring wells and piezometers with well screen extending both above and below the water table. The water level in the well and the saturated thickness of the aquifer along the well determine the length over which water flows into or out of the well.

Previous Numerical Approaches

The effect of unsaturated flow on aquifer behavior has been investigated and applied to well testing by Taylor and Luthin (1969), Brutsaert et al. (1971), Guitjens and Luthin (1971), and Cooley (1971), among others. These works, like the program used in this study, attribute gravity drainage to unsaturated flow above the water table, causing "delayed yield", the release of water from the unsaturated zone over a period of time. Other factors have been proposed to cause delayed yield, including elastic storage effects in the aquifer (Neuman, 1972), and restricted air movement in the unsaturated zone (Bouwer and Rice, 1978). Depending on the specific flow situation, any of these factors may play a role in delayed yield, though the relative importance of each remains unclear (El-Kadi and Brutsaert, 1986). Pump test simulations using the unsaturated flow theory have shown good agreement with experimental data (Cooley, 1983), as have drainage and infiltration simulations (Neuman and Davis, 1983).

An earlier program by Neuman (1972) neglects the unsaturated zone and treats the zero-pressure head surface as a moving boundary. This "free surface" approach was determined to be unsuitable for problems where the water

table has an irregular shape. This method cannot accurately predict the rate of advance of the zero-pressure head surface because it neglects the pre-existing moisture conditions in the unsaturated zone (Neuman, 1975). The variably saturated theory was applied in developing UNSAT2 (Davis and Neuman, 1983) for better accuracy.

Both the finite difference and finite element methods have been used for numerical modeling of well testing. The finite element method appears to result in a more stable solution than the finite difference method for variably saturated flow simulations (Cooley ,1983; Neuman, 1975). The nonuniform parameters of the unsaturated zone and the treatment of seepage faces along a well casing are more easily handled by the finite element method.

Objectives of This Study

The specific well construction details and the aquifer and sandpack geometries for some Site 300 wells are used for UNSAT2 slug and bail test simulations. Field data from Site 300 are evaluated using the results of the computer sumulations, and compared with the interpretations using various other slug test methods. The conclusions of this study will reduce the uncertainty

in hydraulic conductivity estimates and ground water velocity calculations for the aquifer at Site 300.

HYDRAULIC CONDUCTIVITY

Ground water pore velocities are estimated for the aquifer at Site 300 to predict the tritium migration rate. Pore velocity is the actual velocity at which ground water travels through pore spaces, and may be expressed as:

$$v_p = \frac{v}{n_e} = \frac{Q}{A\,n_e} \qquad (1)$$

in which:

v_p is the pore velocity (LT^{-1}),

v is the discharge velocity (LT^{-1}),

n_e is the effective porosity ( ),

Q is the volume flow rate (L^3T^{-1}), and

A is the cross-sectional area of

flow (L^2).

Darcy's Law relates the volume flow rate to hydraulic conductivity for saturated ground water flow:

$$\frac{Q}{A} = - K \frac{dh}{dl} \qquad (2)$$

in which:

K is the hydraulic conductivity (LT^{-1}), and

dh/dl is the hydraulic gradient ( ).

Hydraulic conductivity is a function of the properties of the aquifer and the fluid flowing through it. The standard value of K is defined for pure water at 15°C (Fetter, 1980). The standard K is a function of the size and shape of the aquifer pore openings.

Combining Equation (1) with Darcy's Law, pore velocity is described by:

$$v_p = -\frac{K}{n_e} \frac{dh}{dl} \qquad (3)$$

Porosity values can be determined experimentally or obtained from the literature. The hydraulic gradient is calculated from water levels in monitoring wells or piezometers. The hydraulic conductivity for a particular type of soil or rock may vary over several orders of magnitude (Morris and Johnson, 1967) and must be determined accurately for each geologic material.

Hydraulic Conductivity Testing

The hydraulic conductivity of a porous media can be determined by laboratory or field testing.

Laboratory Testing

Hydraulic conductivity is determined in the laboratory using a chamber that holds a small, undisturbed sample of soil or rock (Klute, 1965a). The sample is brought to saturation, and a hydraulic gradient is imposed across it. Noncohesive soils are tested in a constant-head permeameter. The discharge rate is measured as water flows through the soil sample under a constant hydraulic gradient. Cohesive material is tested in a

falling-head permeameter. The change in hydraulic gradient across the sample is measured over a known time interval. The hydraulic conductivity is calculated from a variation of Darcy's Law.

Laboratory results can be inaccurate if the samples do not retain their original structure. The permeability of soil and rock can change significantly if samples are disturbed during sampling. Laboratory results can be misleading because of the small size of the test sample. Heterogeneities, such as cracks and voids, can greatly affect the hydraulic conductivity results on this small scale. Some test samples may contain the cracks and voids, and others may not. A sufficient number of samples must be tested to obtain a regional average.

Field Testing

Field tests are generally considered a more accurate method for determining hydraulic conductivities and are performed at Site 300. Two common field methods are pump tests (Thiem, 1906 in Fetter, 1980; Theis, 1935; Neuman, 1975a) and slug tests (Kirkham, 1945; Luthin and Kirkham, 1949; Hvorslev, 1951; Cooper et al., 1967; Bouwer and Rice, 1976). Pump tests are performed by pumping water from a well and measuring the change in water levels at different times in the pumping well or in one or more

observation wells. The hydraulic conductivity is
calculated using mathematical equations involving the rate
of water level change in the well(s).

Slug tests are another common field method for
determining hydraulic conductivity. The water level in a
well is instantaneously raised or lowered. The rate at
which the water in the well returns to the original level
is measured. The hydraulic parameters of the aquifer, the
aquifer thickness, and the well radius affect the rate at
which the water level returns to equilibrium. Graphic
methods and/or mathematical equations are used to
calculate the hydraulic conductivity. The remainder of
this paper refers to tests involving the removal of water
as bail tests and to those involving injection as slug
tests.

Slug and bail tests are often used to determine the
hydraulic conductivity of low-permeability aquifers. Pump
tests are not always a suitable method for
low-permeability aquifer testing because of the excessive
drawdowns that result from constant pumping. The
monitoring wells at Site 300 have very low sustainable
pumping rates, typically less than 0.5 gallon per minute
(Buddemeier et al., 1985). For this reason, it is often
impossible to perform pump tests in these wells.

Slug and bail tests are also preferable to pump tests when the aquifer has been contaminated, and disposal of discharge water is a problem. No water is removed during slug tests, and a relatively small amount of water is withdrawn from the well during bail tests. An alternate method of performing bail tests is to submerge a displacement object of known volume in the well. After the water in the well has recovered to the equilibrium level, the object is quickly removed. The water level in the well falls immediately, and no contaminated water is removed from the well. The displacement object can also be lowered into the well at the start of a slug test to cause a rise in the water level.

Slug and bail tests have been performed at Site 300 because of the reasons mentioned above: the aquifer has a low permeability, and the ground water is contaminated.

SLUG AND BAIL TESTS

When slug and bail tests are performed in confined aquifers, ground water flows through a constant aquifer thickness and well screen length. The entire aquifer remains saturated throughout testing. Equations have been developed to describe well recovery during slug and bail testing in a confined aquifer (Cooper et al., 1967; Hvorslev, 1951).

When slug and bail tests are performed in unconfined aquifers, the ground water flow is more complex. Both unsaturated and saturated flow occur. Immediately following the start of a bail test, the water table drops to form a cone around the well. The thickness through which water flows into the well decreases during this early stage of the test. The water table eventually begins to rise along with the water level in the well, and the saturated thickness along the casing increases until the well recovers fully. The water table is the internal isobar that separates the saturated and unsaturated zones of the earth material. The unsaturated portion, above the water table, continues to change in water content throughout testing as water drains downward, contributing to the rise of the water table.

Immediately following the start of a slug test, the water table rises to form a reverse cone around the well. Water flows out of the well both above and below the static water table, at different rates depending on the different water contents in the material along the well. The length through which water flows out of the well is therefore equal to the changing height of water in the well throughout testing. Eventually the water table begins to fall along with the water level in the well.

If there is a relatively permeable sandpack surrounding the well casing, an abrupt head difference exists at the interface between the sandpack and the aquifer for both slug and bail tests. During a bail test a seepage face forms along the well casing, above the water surface in the well, and below the water table in the sandpack. Water leaves the sandpack along the seepage face, and trickles down into the well (Bear, 1972).

Existing Methods for Analyzing Slug and Bail Test

Four methods have been used to calculate the hydraulic conductivity of the aquifer at Site 300: the method of Hvorslev (1951), the method of Cooper et al. (1967), the method of Bouwer and Rice (1976), and the "Navy" method (1982).

Hvorslev Method

In the Hvorslev method (1951), the hydraulic conductivity, K, is calculated by:

$$K = \frac{r^2 \ln(L/R)}{2 L T_0} \qquad (4)$$

in which:

    r is the unscreened casing radius (L),

    R is the screened casing radius (L),

    L is the screen (or uncased) length (L),
     and

    T_0 is the basic time lag (T).

Figure 1 shows a schematic diagram of the flow system. The basic time lag is determined from a plot of log $(H-h)/(H-H_0)$ vs. time, in which:

    h is the water level at time t during
     testing (L),

    H_0 is the water level immediately after the
     injection or withdrawal of the slug
     (L), and

    H is the equilibrium water level (L).

T_0 is defined as the time at which log $(H-h)/(H-H_0) = 0.37$. The Hvorslev method was developed for a piezometer with a screened interval located entirely below the water table for the duration of testing. The L value is therefore constant. A
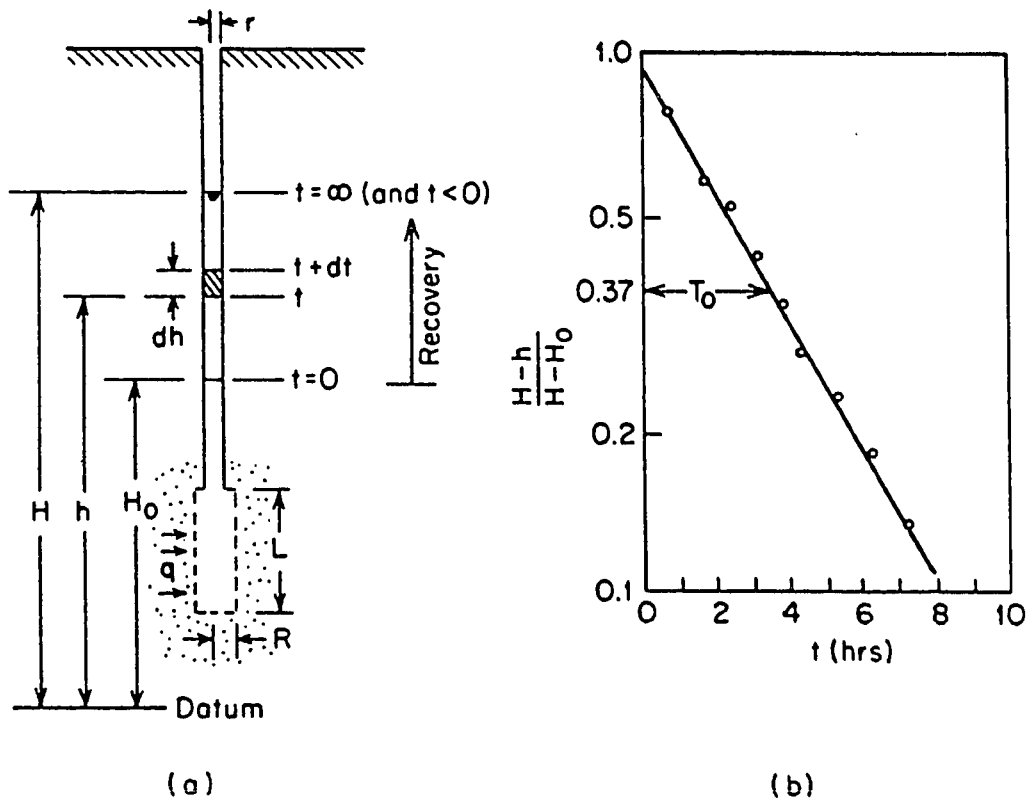
Figure 1. Hvorslev piezometer test. (a) Geometry;
(b) method of analysis (from Hvorslev, 1951 in Freeze and
Cherry, 1979).

time-averaged value of L is used for Site 300 wells since the saturated thickness along the well casing varies with time.

Method of Cooper et al.

In the method of Cooper et al. (1967), the value of H/H_0 is plotted verses log t in which:

> H is the water level displacement at
> > time t (L),
>
> H_0 is the initial water level
> > displacement (L), and
>
> t is time (T).

Figure 2 shows a schematic diagram of the flow system. The plot is matched to a set of type curves that plot H/H_0 verses log (Tt/r_c^2) for different values of storage coefficient (fig. 3) in which:

> T is the transmissivity (L^2T^{-1}),
>
> r_c is the casing radius (L).

The time corresponding to $Tt/r_c^2 = 1$ is determined on the matching type curve. The hydraulic conductivity, K, is calculated by:

$$K = \frac{r_c^2}{b\,t} \tag{5}$$

in which b is the aquifer thickness (L). This method was developed for a piezometer with a screened interval

Instantaneous Charge
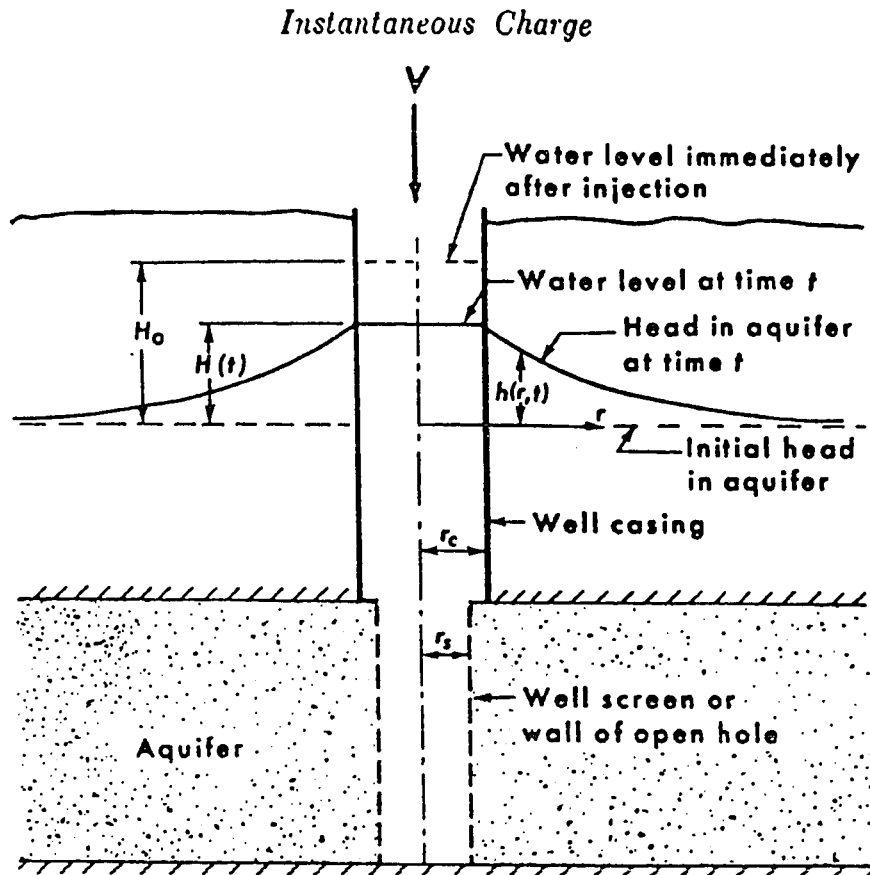
Figure 2. Idealized representation of a well into which a volume, V, of water is suddenly injected (Cooper et al., 1967).
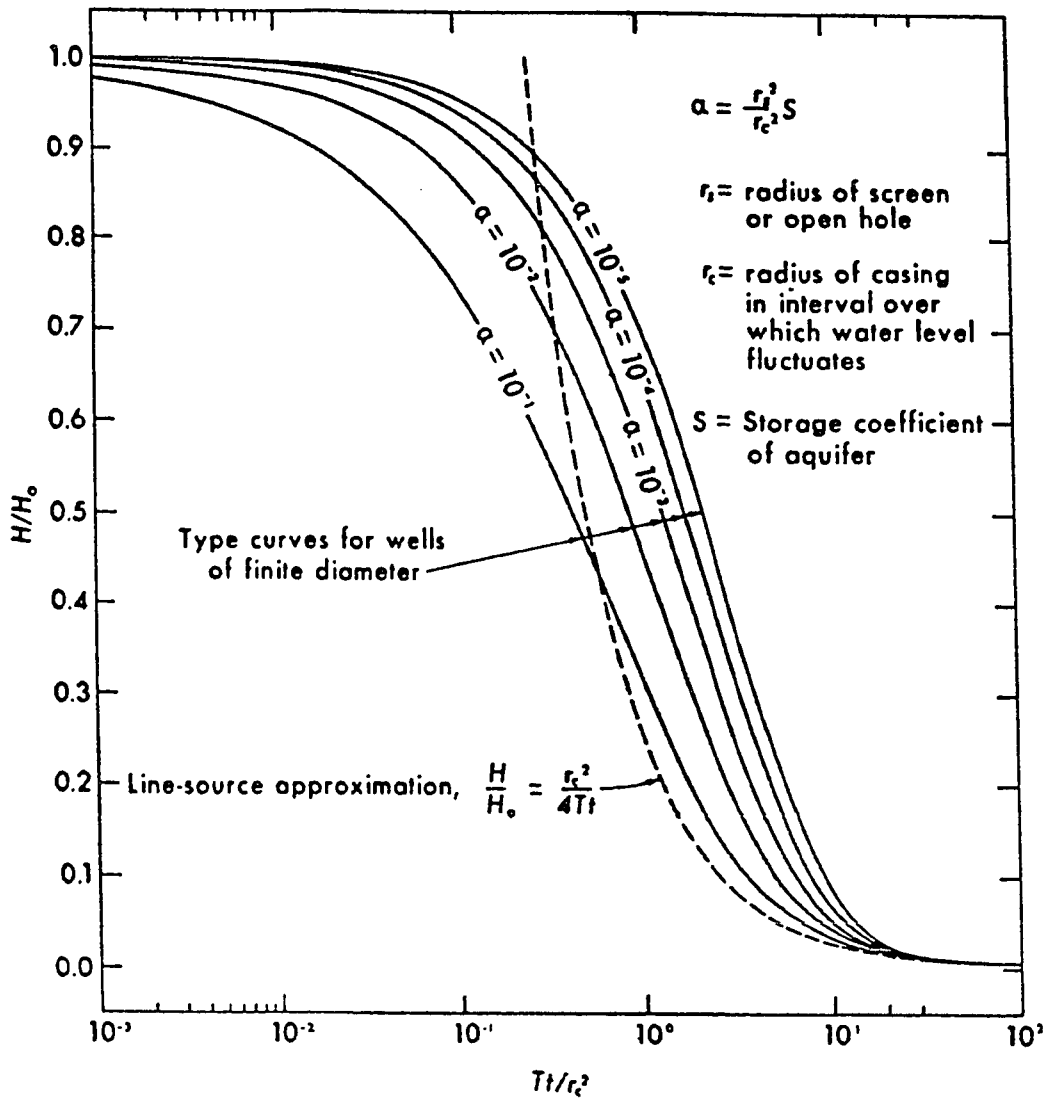
Figure 3. Type curves for instantaneous charge in well of finite diameter (Cooper et al., 1967).

located entirely below the water table for the duration of the test, for which the thickness, b, is constant. A time-averaged value of b is used for unconfined aquifers because the saturated thickness along the well casing varies with time. If there is a relatively permeable sandpack surrounding the well, the borehole radius is used for r, thereby neglecting the sandpack response.

The Cooper et al. method was modified for the Site 300 wells. A modified radius is calculated to account for the volume of pore space in the sandpack using the following equation. The portion of the equation that involves r_{od} and r_{id} is used only in the special case when a displacement object is submerged during a slug test.

$$r_m^2 = n_s \ (r_b^2 - r_o^2) + r_i^2 - (r_{od}^2 - r_{id}^2) \qquad (6)$$

in which: r_m is the modified radius (L),

n_s is the sandpack porosity (L),

r_b is the borehole radius (L),

r_o is the outside diameter of the

casing (L),

r_i is the inside diameter of the

casing (L),

r_{od} is the outside diameter of the

displacement object, if submerged

during a slug test (L), and

r_{id} is the inside diameter of the

displacement object, if submerged

during a slug test (L).

It is then assumed that no sandpack exists surrounding the well. The portion of the curve that represents primarily the sandpack response is graphically subtracted and the time scale of the remaining portion of the curve is set to zero. The formation response is rescaled so that H_0 equals the water level displacement at the time reset to zero.

Method of Bouwer and Rice

The method of Bouwer and Rice (1976) was developed for unconfined aquifers. The hydraulic conductivity is calculated by:

$$K = \frac{r_c^2 \ln \left(\frac{R_e}{r_c}\right) \ln \left(\frac{Y_0}{Y_t}\right)}{2Lt} \tag{7}$$

in which: r_c is the casing radius (L),

R_e is the effective radius over which the

head change is dissipated in the flow

system (L),

L is the height of the screened or uncased

zone (L),

Y_t is the water level displacement at

time t (L),

Y_0 is the initial water level displacement

(L), and

t is time (T).

The value of effective radius, R_e, depends on the geometry of the flow system. The water level displacement, Y, is plotted against time on a semi-logarithmic plot. The best fitting straight line is drawn through the points, and t and Y_t are chosen arbitrarily from this line. The early data points are ignored when the presence of a sandpack causes a "double straight line" (Bouwer, 1989). Only the later straight line portion is used for calculating hydraulic conductivity. If there is a relatively permeable sandpack surrounding the well, the borehole radius is used for r, thereby neglecting the sandpack response. A constant value is used for L even though the saturated thickness of the aquifer along the casing varies with time. Equation (7) is based on the assumption that the water table drawdown near the well is negligible. The drawdown in the aquifer may significantly affect test results when relatively thin aquifers are tested.

Navy Method

The "Navy" method (1982) was developed for an uncased hole. The hydraulic conductivity, K, is calculated by the following equation:

$$K = \frac{R\ (h_2 - h_1)}{16\ D\ S\ (t_2 - t_1)} \tag{8}$$

in which: R is the borehole radius (L),

D is the height of static water table above the bottom of the casing (L),

S is the shape factor ( ),

h_1 is the water level change at time $= t_1$ (L), and

h_2 is the water level change at time $= t_2$ (L).

The value of the shape factor, S, depends on the geometry of the flow system. This equation applies for D/R less than 50. The sandpack effects are neglected since R is the borehole radius.

The hydraulic conductivity values determined by the four methods described above have varied over two orders of magnitude (Buddemeier et al., 1985). The method presented in this paper was developed to more accurately determine the hydraulic conductivity at Site 300.

APPLICATION OF UNSAT2 TO SLUG AND BAIL TESTS

Flow Equations

Conservation of mass states that the net outflow of mass from an elemental volume equals the decrease of mass within the volume. The continuity equation expresses this principle for variably saturated porous material by the equation:

$$- \frac{\partial}{\partial x_i} (\rho \, v_i) = \frac{\partial}{\partial t} (\rho \, n \, S_w) \tag{9}$$

in which: ρ is the density of water (FT^2L^{-1}

or ML^{-3}),

v_i is the Darcy velocity (LT^{-1}),

n is the porosity of the porous material

( ), and

S_w is the relative water saturation

$(0 \leq S_w \leq 1)$.

An indicial notation is used whereby quantities with a single subscript represents components of vectors, and quantities with two subscripts represent components of second rank matrices or tensors (Neuman, 1973). The three Cartesian coordinates x, y and z are represented by x_i where i = 1, 2, and 3, respectively.

Darcy's Law can be expressed for a variably saturated porous medium by:

$$v_i = -K_{ij}K_r \frac{\partial H}{\partial x_j} \qquad (10)$$

in which: K_{ij} is the saturated hydraulic conductivity

         tensor (LT^{-1}),

     K_r is the relative hydraulic conductivity

         ( ), and

     H is the hydraulic head (L).

K_r is a scalar function of the degree of saturation that equals one at saturation $(0 \leq K_r \leq 1)$. Hysteresis is not accounted for in Equation (10). Combination of Equations (9) and (10) gives:

$$\frac{\partial}{\partial x_i}\left(\rho\ K_{ij}K_r \frac{\partial H}{\partial x_j} \right) - \frac{\partial}{\partial t}(\rho\ n\ S_w) = 0 \qquad (11)$$

Expansion of the time derivative in Equation (11) gives:

$$\frac{\partial}{\partial x_i}\left(\rho\ K_{ij}K_r \frac{\partial H}{\partial x_j} \right) = \rho\ n\ \frac{\partial S_w}{\partial t} + n\ S_w \frac{\partial \rho}{\partial t} + \rho\ S_w \frac{\partial n}{\partial t} \qquad (12)$$

An empirical relationship for the change in porosity (Cooley, 1971) leads to the definition for formation compressibility:

$$c_f = \frac{1}{\rho\ n\ g}\ \frac{\partial n}{\partial H} \qquad (13)$$

in which: c_f is the formation compressibility

         $(L^2 F^{-1})$, and

g is the acceleration due to gravity

(LT^{-2}).

Combining Equation (13) with the last term of Equation (12) gives:

$$\rho \, S_w \, \frac{\partial n}{\partial t} = \rho^2 \, S_w \, c_f \, g \, n \, \frac{\partial H}{\partial t} \qquad (14)$$

The time derivative of density can be expressed by the Equation of State (Pinder and Gray, 1977):

$$\frac{\partial \rho}{\partial t} = \rho \, g \, c_w \, \frac{\partial H}{\partial t} \qquad (15)$$

in which: c_w is the compressibility of water (L^2F^{-1}).

Substitution of Equations (14) and (15) into Equation (11) gives:

$$\frac{\partial}{\partial x_i} \left(\rho \, K_{ij} K_r \, \frac{\partial H}{\partial x_j} \right) = \rho \, n \, \frac{\partial S_w}{\partial t} + S_w \rho^2 n g \, (c_w + c_f) \, \frac{\partial H}{\partial t} \qquad (16)$$

The specific storage, S_s, (L^{-1}), can be defined as:

$$S_s = \rho \, n \, g \, (c_w + c_f) \qquad (17)$$

Specific storage is the volume of water instantaneously released from or taken into storage per unit volume of a porous medium per unit drop or rise in head.

Substituting Equation (17) into Equation (16) and assuming that the spatial variations in ρ are negligible due to the slight compressiblity of water gives:

$$\frac{\partial}{\partial x_i} \left(K_{ij} K_r \, \frac{\partial H}{\partial x_j} \right) = n \, \frac{\partial S_w}{\partial t} + S_w \, S_s \, \frac{\partial H}{\partial t} \qquad (18)$$

The volumetric water content, θ, is a dimensionless quantity defined as:

$$\theta = S_w \, n \qquad (19)$$

Substituting Equation (19) into Equation (18), the flow equation becomes:

$$\frac{\partial}{\partial x_i} \left(K_{ij} K_r \frac{\partial H}{\partial x_j} \right) = n \frac{\partial (\theta/n)}{\partial t} + \frac{\theta}{n} S_s \frac{\partial H}{\partial t} \qquad (20)$$

The specific moisture capacity, C, (L^{-1}), is defined as:

$$C = \frac{\partial \theta}{\partial \psi} \qquad (21)$$

in which: ψ is the pressure head (L).

The specific moisture capacity is the change in water content of the soil per unit pressure head change and is related to the pore size distribution of the soil (Klute, 1965b).

Substituting Equation (21) into the flow equation, and rewriting the equation in terms of pressure head, ψ, and elevation head, z, it becomes:

$$\frac{\partial}{\partial x_i} \left(K_{ij} K_r \frac{\partial \psi}{\partial x_j} + K_{i3} K_r \right) = \left(C + \frac{\theta S_s}{n} \right) \frac{\partial \psi}{\partial t} \qquad (22)$$

Equation (22) is used by UNSAT2 to described variably saturated flow. The first term is an advection term, which accounts for ground water flow in response to a pressure head gradient. The second term is a drainage

term, which accounts for gravity effects. The third term, containing the specific moisture capacity, C, and the specific storage, S_s, is the storage term. For saturated portions of the flow region, C is zero and S_s is the only storage coefficient that applies. For unsaturated portions, where θ/n is less than one, UNSAT2 neglects the specific storage term by assigning a value of zero to θ/n. The effect of compressibility on storage is assumed negligibly small compared to the effect of changes in the water content, θ (Neuman, 1975b).

Verification

Two sample problems are simulated using UNSAT2 to verify that the program accurately simulates well testing for the input control data to be used in the slug and bail test simulations for Site 300 wells (Davis and Neuman, 1983). The dimensions of the general finite element grid are verified as sufficiently small to model the slug and bail tests performed at Site 300. The initial time interval and successive time steps are verified as sufficiently small for accurate results. The output values from the computer runs are compared to analytical solutions for the problems.

Slug Test Example

A slug test is modeled using UNSAT2, and the results
are compared with the analytical solution for slug tests
presented by Cooper et al. (1967). The verification
problem simulates a well located in a homogeneous
isotropic confined aquifer of uniform thickness. The well
is fully penetrating and screened throughout the aquifer
thickness. A schematic diagram of the system is shown in
figure 4.

The horizontal and vertical hydraulic conductivities
are both equal to 0.01 cm/sec (3.28×10^{-4} ft/sec). The
porosity of the soil is 35%. The well diameter is 30.5 cm
(12 inches). The program was run five times with specific
storage values varying from 1.0×10^{-5} to 0.1 cm^{-1}
(3.0×10^{-4} to 3.0 ft^{-1}).

The finite element grid developed for the slug test
problem is shown in figure 5. The grid represents a
vertical cross-section through the sandpack and aquifer.
The nodes are assigned x_1 and x_3 coordinates (horizontal
and vertical, respectively) that are fixed in space. The
left vertical edge coincides with the well casing. The
lower edge lies along the lower boundary of the aquifer,
and the upper edge lies along the upper aquifer boundary.
The right edge of the grid represents a vertical surface
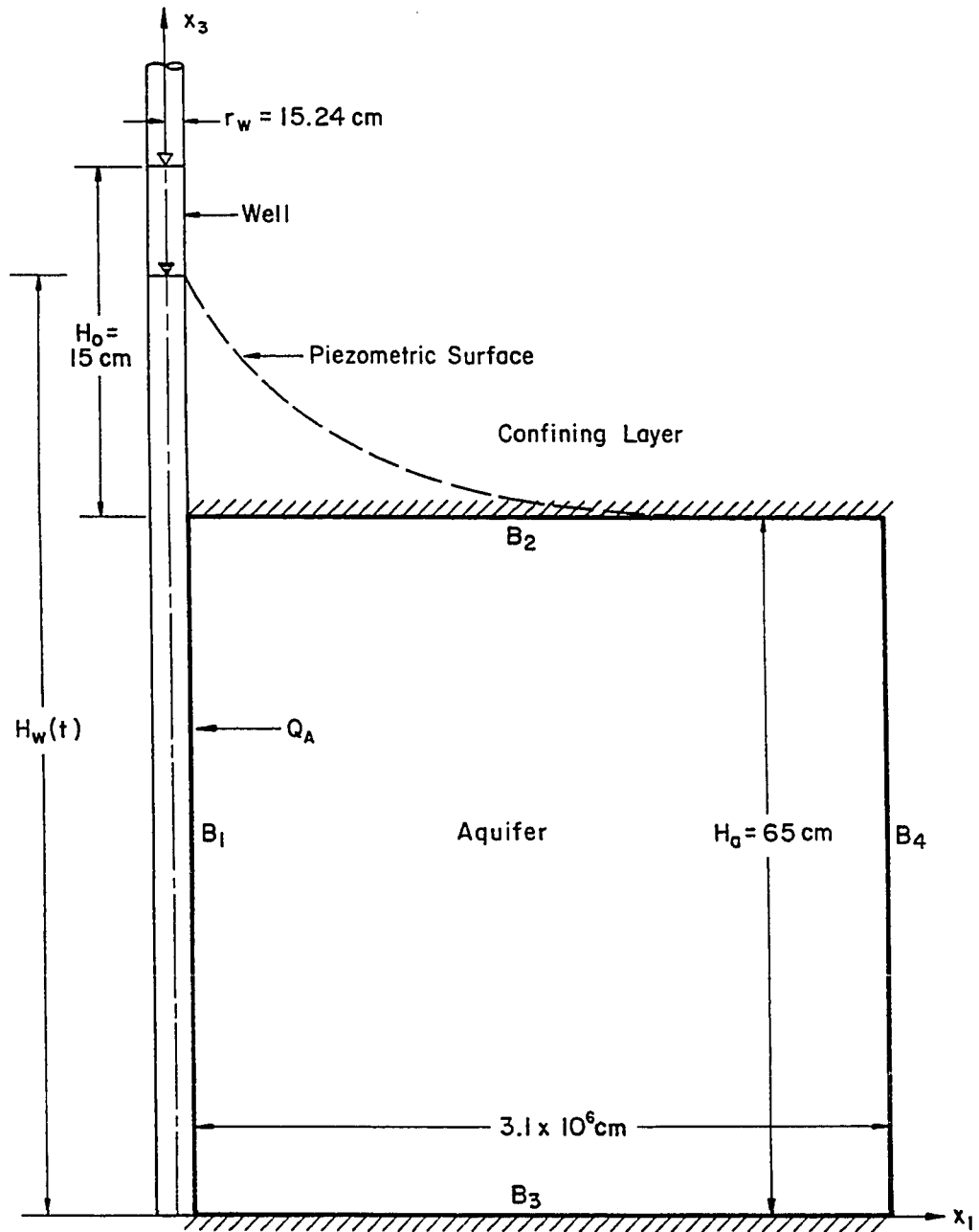
Figure 4. Verification slug test geometry.
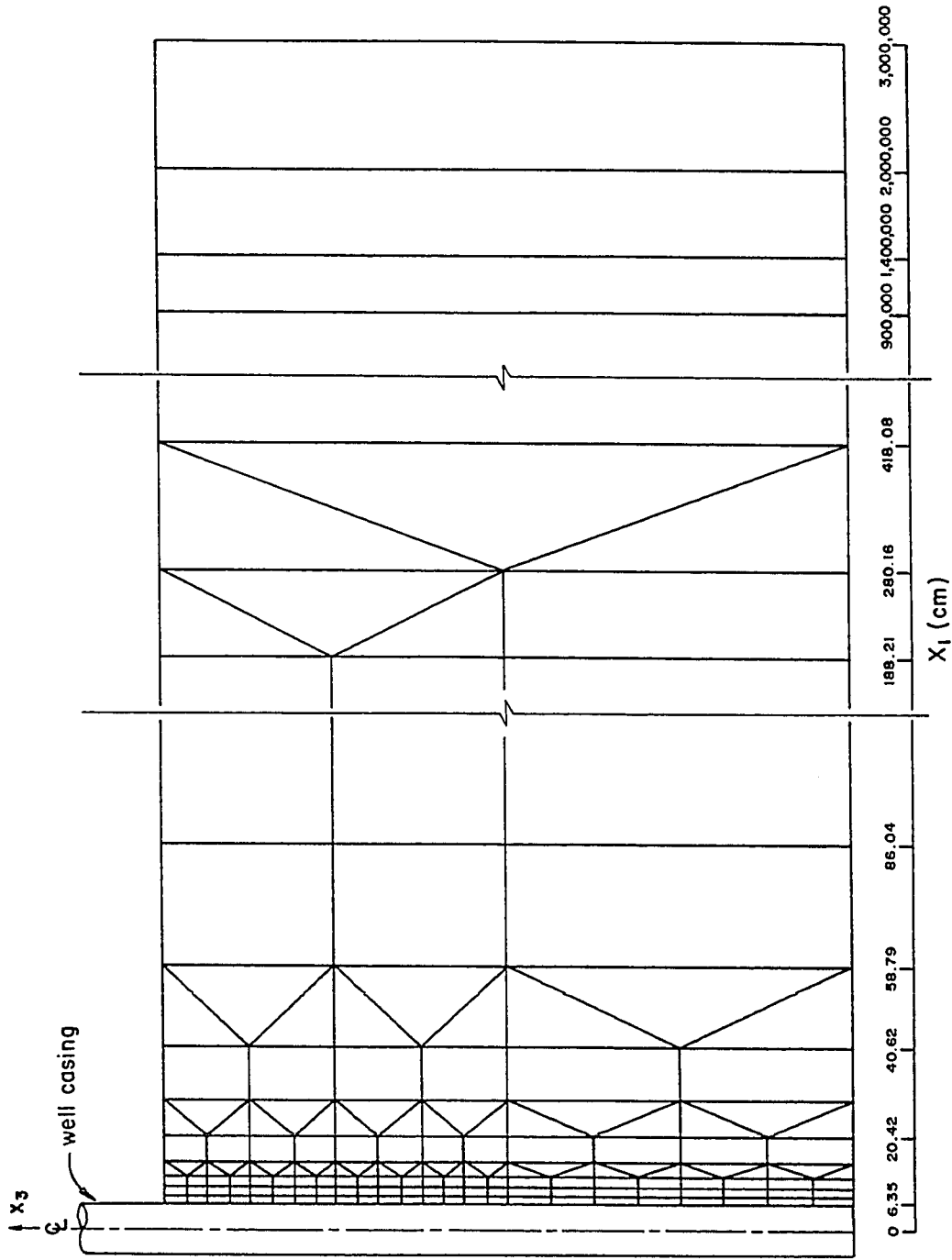
Figure 5. Finite element grid for 12.7 cm diameter well.

32

within the aquifer where the hydraulic head remains at the static level throughout testing.

The initial and boundary conditions for the problem are:

$$H(x_i,0) = 65.0 \text{ cm } (2.13 \text{ ft}) \qquad x_1 > 15.24 \text{ cm} \qquad (23)$$

$$H(x_i,0) = 80.0 \text{ cm } (2.63 \text{ ft}) \qquad \text{on } B_1 \qquad (24)$$

$$H(x_i,t) = H_w(t) \qquad \text{on } B_1 \qquad (25)$$

$$\frac{\partial H}{\partial x_3} = 0 \qquad \text{on } B_2 \text{ and } B_3 \qquad (26)$$

$$H(x_i,t) = 65.0 \text{ cm } (2.13 \text{ ft}) \qquad \text{on } B_4 \qquad (27)$$

Before testing, the aquifer is assumed to be uniform and at a constant head, 65.0 cm (2.13 ft). Equation (23) states that there is initially no head change in the aquifer outside of the monitoring well. Equation (24) states that initially the head is 80.0 cm (2.63 ft) along the well casing (B_1). Equation (25) states that the head along the well casing equals the water level in the well. Equation (26) states that boundaries B_2 and B_3 are no-flow boundaries. Boundary B_4 represents an infinitely distant, constant head boundary with a hydraulic head of 65.0 cm (2.13 ft) (Equation 27). The nodes on this boundary are located 3,095,521 cm (101,559 ft) from the well, a distance sufficiently great to simulate the condition of an infinite aquifer. If the right surface is located closer than approximately 500,000 cm (16,404 ft) to the

well, the constant head boundary condition causes the well
to recover prematurely, and the output does not match the
analytical curves of Cooper et al. (1967). Equation (28)
calculates the change in water level in the well, ΔH_w, for
each time interval, Δt:

$$\Delta H_w = \frac{Q_A \; \Delta t}{\pi \; r_w^2} \tag{28}$$

in which: Q_A is the discharge from the well to the
                aquifer $(L^3 T^{-1})$, and

            r_w is the well radius (L).

The verification input data file and the output for
several time steps generated by UNSAT2 are presented in
Appendix A. The relative response of the well, H/H_0, is
plotted versus a dimensionless time parameter, Tt/r^2,
similar to the curves presented by Cooper et al. (1967).
Five curves were plotted, each corresponding to a
different specific storage value (fig. 6). The curves are
the same for different r and T values when plotted with
dimensionless axes. The computer simulated response
curves match the curves generated by the analytical method
with the exception of a slight deviation during the
beginning of testing for the specific storage of 10^{-1}.
This difference is not significant relative to the level
of curve matching error with the Site 300 curves.
Variation of the porosity or the initial change of water
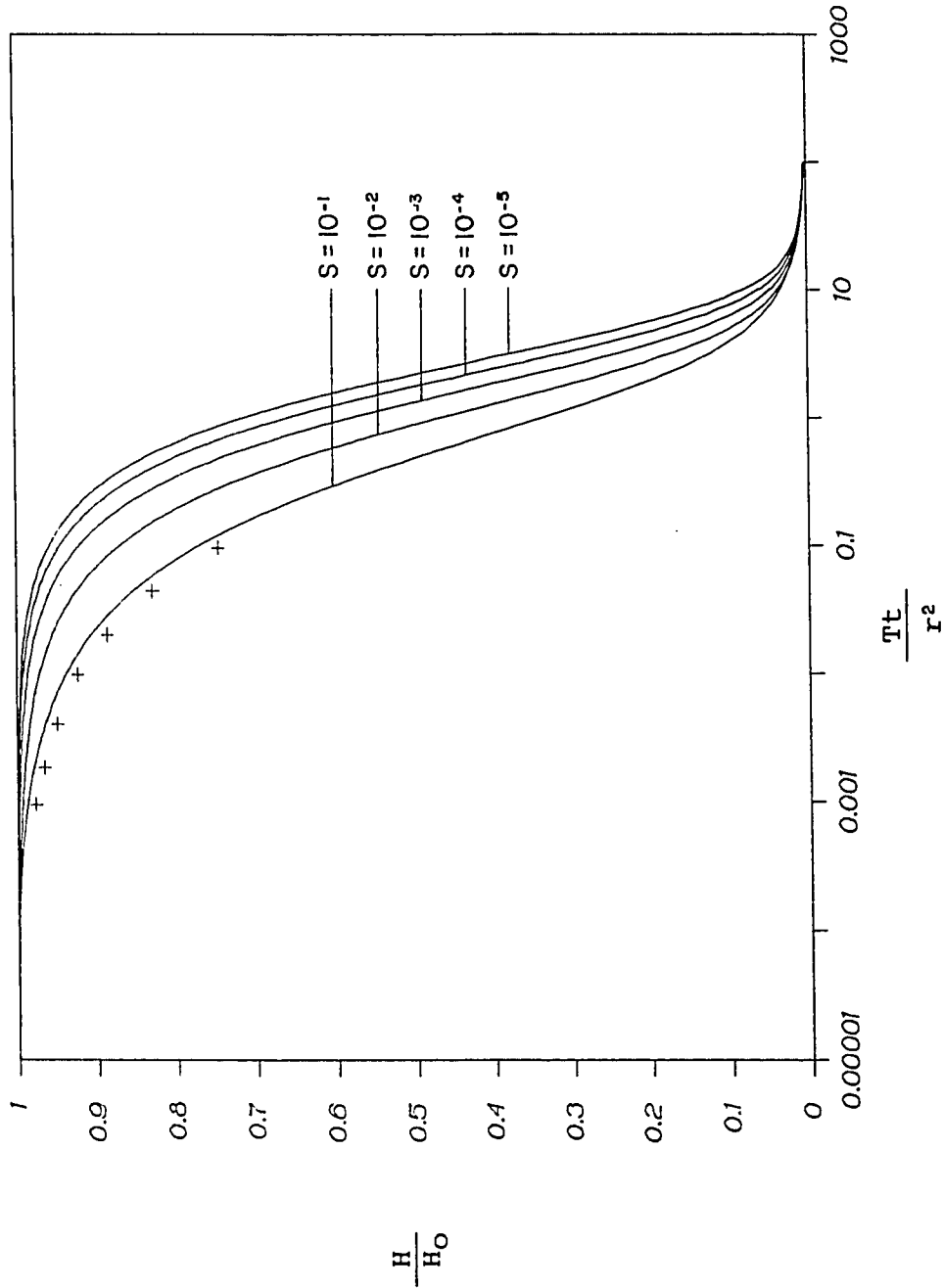
Figure 6. Well recovery curves for confined slug test simulation using UNSAT2. Symbols show curve where UNSAT2 differs from Cooper et al. (1967).

level in the well do not affect the relative recovery
curves as long as the flow system remains saturated
throughout testing.

Pump Test Example

A pump test is modeled using UNSAT2, and the results
are compared with the Jacob straight-line method for pump
tests presented by Cooper and Jacob (1946). This
verification problem simulates a pump test performed on a
well of infinitesimally small diameter. The well is
located in a homogeneous isotropic confined aquifer of
uniform thickness. The aquifer is 60.96 cm (2.0 ft) thick
and the equilibrium hydraulic head is 90.0 cm (2.95 ft).
The well is fully penetrating and screened throughout the
aquifer thickness. A schematic diagram of the system is
shown in figure 7.

The input horizontal and vertical hydraulic
conductivities are both equal to 0.01 cm/sec
(3.28×10^{-4} ft/sec). An input porosity of 35% is used.
As with the slug test example, the output is not affected
by porosity. The pump test was simulated twice, with two
different specific storage values for the aquifer: 10^{-3}
and 10^{-5} cm^{-1} (0.03 and 3.0×10^{-4} ft^{-1}). A pumping well
diameter of 0.2 cm (0.08 in) is used to approximate an
infinitesimally small diameter. The pumping rate is
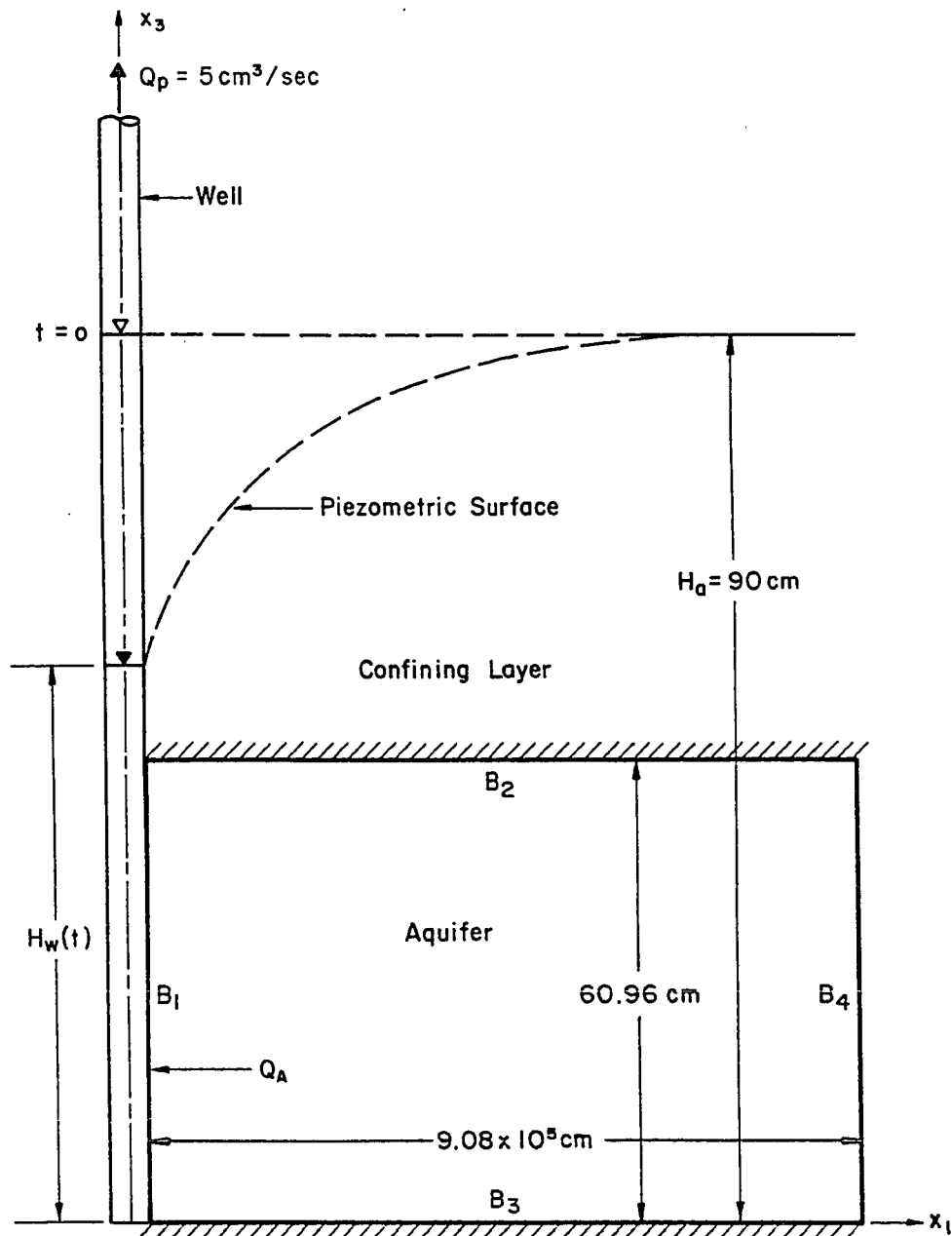
Figure 7. Verification pump test geometry.

5.0 cm³/sec (1.77 x 10⁻⁴ ft³/sec). The output data are based on a hypothetical observation well located 130.89 cm (4.29 ft) from the central axis of the pumping well.

The finite element mesh developed for the slug test problem (fig.5) is also used for the pump test problem. The initial and boundary conditions for the problem can be described mathematically by:

$$H(x_1, 0) = 90.0 \text{ cm } (2.95 \text{ ft})\tag{29}$$

$$H(x_i, t) = H_w(t) \qquad\qquad\qquad \text{on } B_1\tag{30}$$

$$\frac{\partial H}{\partial x_3} = 0 \qquad\qquad\qquad \text{on } B_2 \text{ and } B_3\tag{31}$$

$$H(x_i, t) = 90.0 \text{ cm } (2.95 \text{ ft}) \qquad \text{on } B_4\tag{32}$$

Equation (29) states that the initial hydraulic head in the aquifer and in the monitoring well is 90.0 cm. Along boundary B_1 the hydraulic head equals H_w, the water level in the well (Equation 30). There is no vertical flow across boundaries B_2 and B_3 (Equation 31). The boundary B_4 represents an infinitely distant, constant head boundary (Equation 32).

Equation (33) calculates the change in water level in the well, ΔH_w, during each time step, Δt:

$$\Delta H_w = \frac{\Delta t (Q_A - Q_P)}{\pi \, r_w^2} = \frac{\Delta t (Q_A - 5.0 \text{ cm}^3/\text{sec})}{\pi \, (0.2 \text{ cm})^2}\tag{33}$$

in which: r_w is the monitoring well radius (L),

Q_A is the discharge from the well to the

aquifer (L^3T^{-1}), and

Q_p is the pumping rate (L^3T^{-1}).

It is assumed that the cross sectional area of the production tubing is of infinitely small diameter, and is neglected in well volume calculations.

The input data file and the output for several time steps generated by UNSAT2 are presented in Appendix A. The water level in the well is plotted versus log time (fig. 8). This plot will be a straight line on the semilogarithmic scale for $t > 5r^2S/T$ (Cooper and Jacob, 1946). A straight line is drawn through the curves and extended back to the zero-drawdown axis. The line intercepts this axis at a time t_0. Hydraulic conductivity, K, and storativity, S, can be calculated by the following equations:

$$K = \frac{2.3\ Q}{4b\pi\ (h_2-h_1)} \qquad (34)$$

$$S = \frac{2.25\ Tt_0}{r^2} \qquad (35)$$

where: Q is the pumping rate (L^3T^{-1}),

b is the aquifer thickness (L),

(h_2-h_1) is the drawdown per log cycle of time (L),

T is the transmissivity (L^2T^{-1}),

t_0 is the time at the straight line
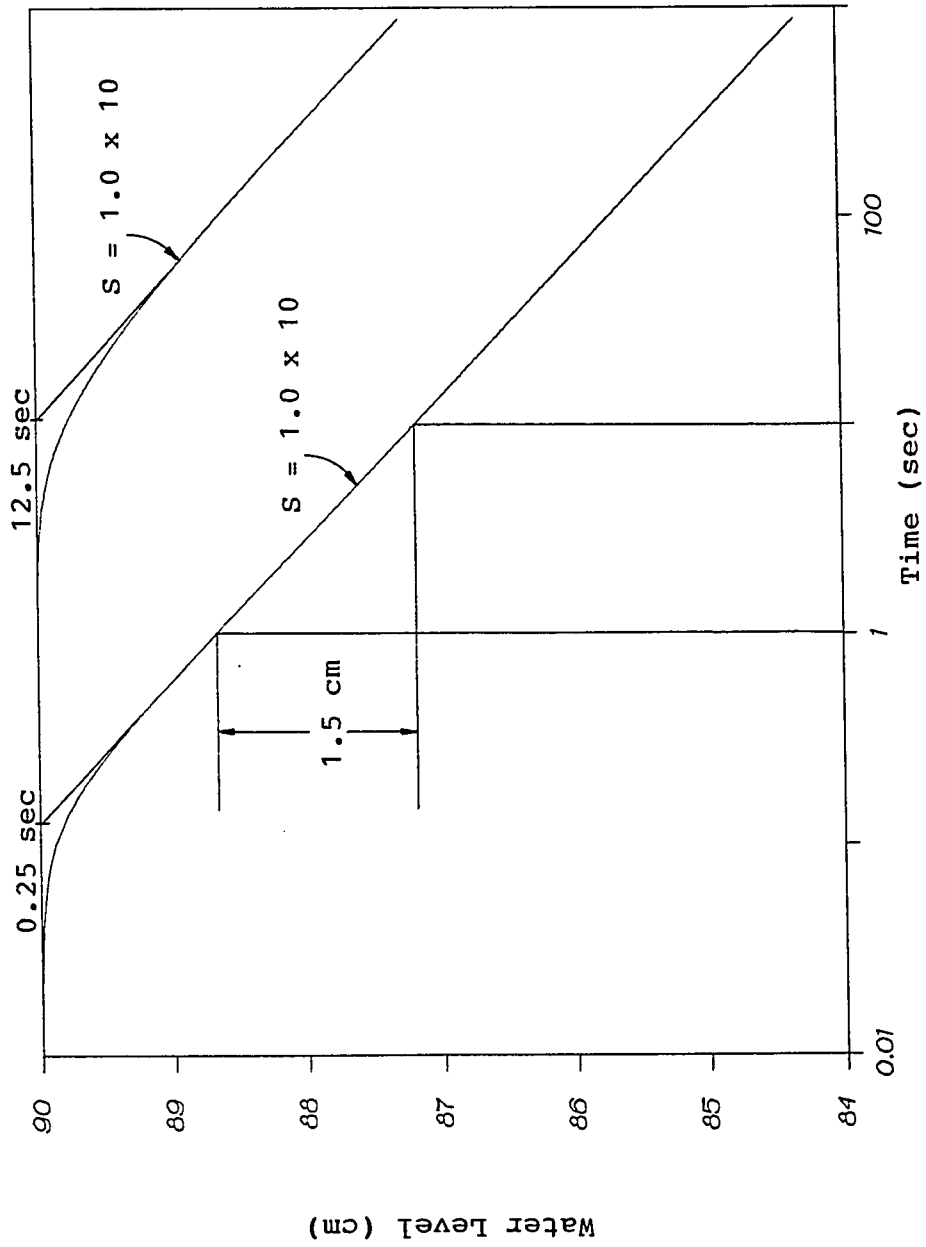
Figure 8. Drawdown curves for pump test verification problem.

intercept (T), and

r is the distance to the observation

well (L).

The drawdown per log cycle and t_0 values from UNSAT2

are:

Curve 1: (input S = 0.00001)

(h_2-h_1) = 1.5 cm = 0.05 ft

t_0 = 0.125 sec

Curve 2: (input S = 0.001)

(h_2-h_1) = 1.5 cm = 0.05 ft

t_0 = 12.5 sec

The calculated values of K and S are in agreement

with the input values:

Curve 1: $K = \dfrac{(2.3)(5 \text{ cm}^3/\text{sec})}{(4)(3.14)(1.5 \text{ cm})(60.96 \text{ cm})} = 0.01 \text{ cm/sec}$

$S = \dfrac{(2.25)(0.61 \text{ cm}^2/\text{sec})(.125 \text{ sec})}{(130.89)^2} = 1.0 \times 10^{-5}$

Curve 2: $K = \dfrac{(2.3)(5 \text{ cm}^3/\text{sec})}{(4)(3.14)(1.5 \text{ cm})(60.96 \text{ cm})} = 0.01 \text{ cm/sec}$

$S = \dfrac{(2.25)(0.61 \text{ cm}^2/\text{sec})(12.5 \text{ sec})}{(130.89)^2} = 1.0 \times 10^{-3}$

The success of these two verification problems indicates

that UNSAT2 can adequately and accurately describe radial

flow to a well.

Finite Element Grid

The finite element grid used to represent the problem domain for Site 300 slug and bail test modeling is the same as shown in figure 5. The grid represents a vertical cross-section through the sandpack and aquifer. The nodes are assigned x_1 and x_3 coordinates (horizontal and vertical, respectively) that are fixed in space. The element sizes and locations are therefore constant.

The left vertical edge of the grid coincides with the well casing. The lower edge lies along the lower impermeable boundary of the aquifer. The upper edge lies within the unsaturated zone, above the water table. The right edge of the grid represents a vertical surface within the aquifer where the water table remains at the static level throughout testing. The actual boundary is theoretically located an infinite distance from the well. The nodes on this surface of the grid are located approximately 30 km from the well for slug and bail test simulation. The height of the grid is large enough to include the capillary zone above the water table. It varies with the aquifer thickness for each test simulation.

Elements with the smallest horizontal dimensions are located near the well, where the radial hydraulic

gradients are the greatest. The radial distance between adjacent nodes increases by a factor of about 1.5 away from the well. The elements located near the top of the grid have smaller vertical dimensions. These elements surround the injected or withdrawn column of water, where the vertical gradients are greatest because of the sudden change in water level in the well.

The governing equation is applied to radial flow problems by using an axisymmetric system of elements. UNSAT2 considers the finite element grid to be a cross-sectional view of a network of concentric rings with the axis of revolution at the center of the well (Pinder and Gray, 1977).

Initial Conditions

Slug Test

Before testing, the aquifer is assumed to be uniform and at a constant head, H_a, relative to the datum at the bottom of the aquifer. The initial conditions for slug tests are defined by the hydraulic head, and can be described mathematically by $(i=1,2,3)$:

$$H(x_i,0) = H_a \qquad\qquad x_1 > r_w \qquad (36)$$

$$H(x_i,0) = H_a + H_0 = H_a + \frac{V}{\pi\, r_w^2} \qquad x_1 \leq r_w \qquad (37)$$

where x_1 is the horizontal coordinate on the finite

element grid (fig. 9) and V is the volume added to or displaced within the well. Equation (36) states that there is initially no head change in the aquifer and sandpack at a radial distance greater than the monitoring well radius, r_w. The total hydraulic head within both saturated and unsaturated zones equals the initial saturated thickness of the aquifer. The input data for hydraulic head are expressed as pressure head. All nodes below the water table, in the saturated zone, are assigned a positive initial pressure head corresponding to the water depth. Nodes coinciding with the water table are assigned an initial pressure head of zero. Nodes above the water table, in the unsaturated zone, are assigned a negative pressure head, equal in magnitude to the height of the node above the water table. The pressure head is assigned for all nodes such that the sum of pressure head and the elevation head equals H_a. The initial pressure heads assigned to the nodes in the unsaturated and saturated zones therefore represent an equilibrium condition.

Equation (37) states that immediately following the slug injection, the head in the well and in the sandpack at the face of the well is equal to the equilibrium value, H_a, plus the height, H_0, of the injected volume of water, V. Nodes along the well casing have a pressure head equal
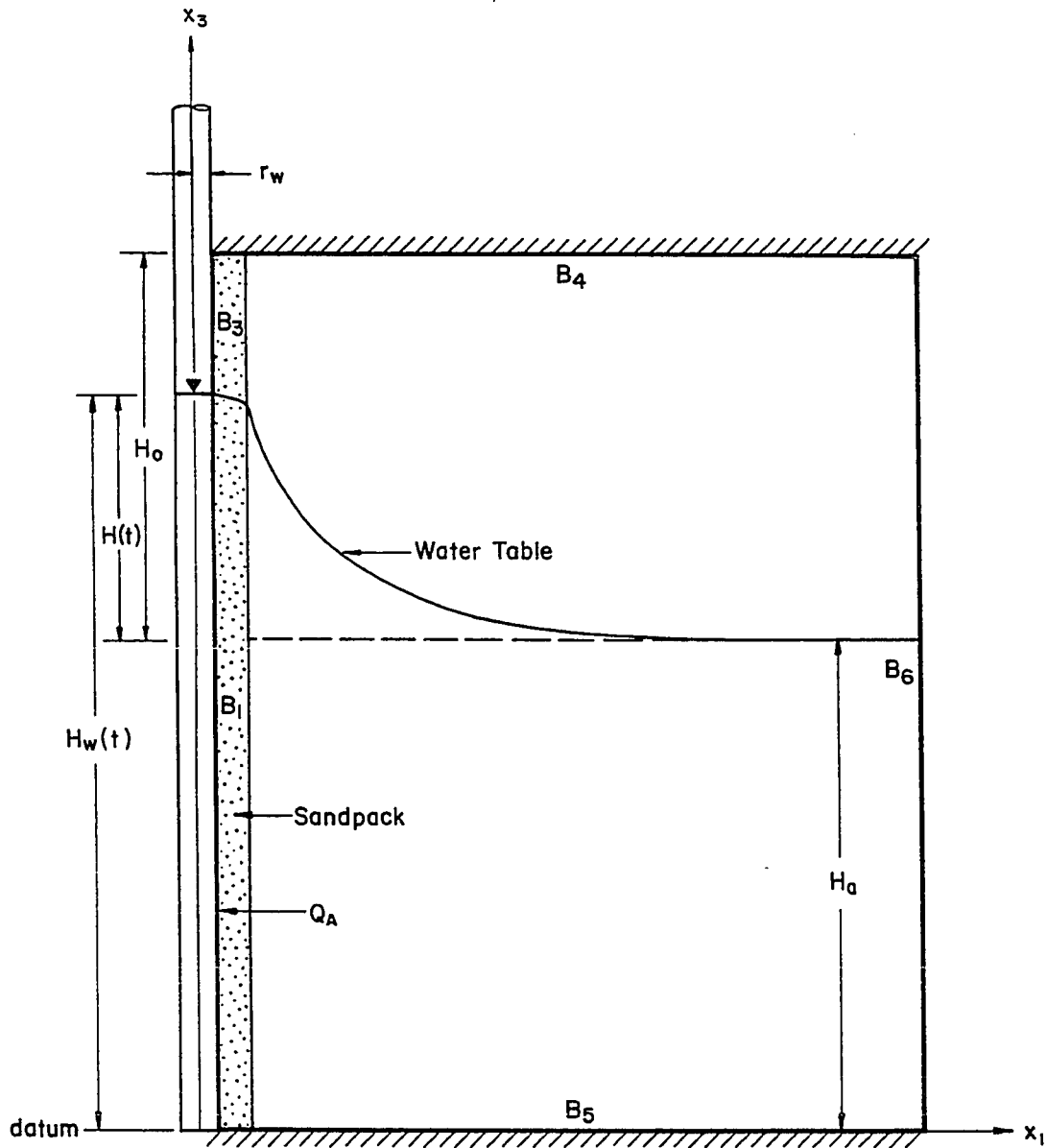
Figure 9. Slug test geometry at time greater than zero.

to the depth of the node below the water table in the
well. The total hydraulic head at these nodes relative to
the datum is equal to the depth of water in the well.

Bail Test

The initial conditions for bail tests can be
described mathematically by Equation (35) and by
(i=1,2,3):

$$H(x_i,0) = H_a - H_0 = H_a - \frac{V}{\pi \, r_w^2} \qquad x_1 \leq r_w \qquad (38)$$

Equation (38) states that initially the head in the
well and in the aquifer at the face of the well is equal
to H_a minus the height, H_0, of the volume of water
bailed (fig. 10).

At the start of a bail test, the upper surface of the
finite element grid corresponds to the water table. Nodes
below the water table were assigned a postive initial
pressure head corresponding to the water depth. Nodes
coinciding with the water table and on the initial seepage
face along the well casing were assigned an initial
pressure head of zero.
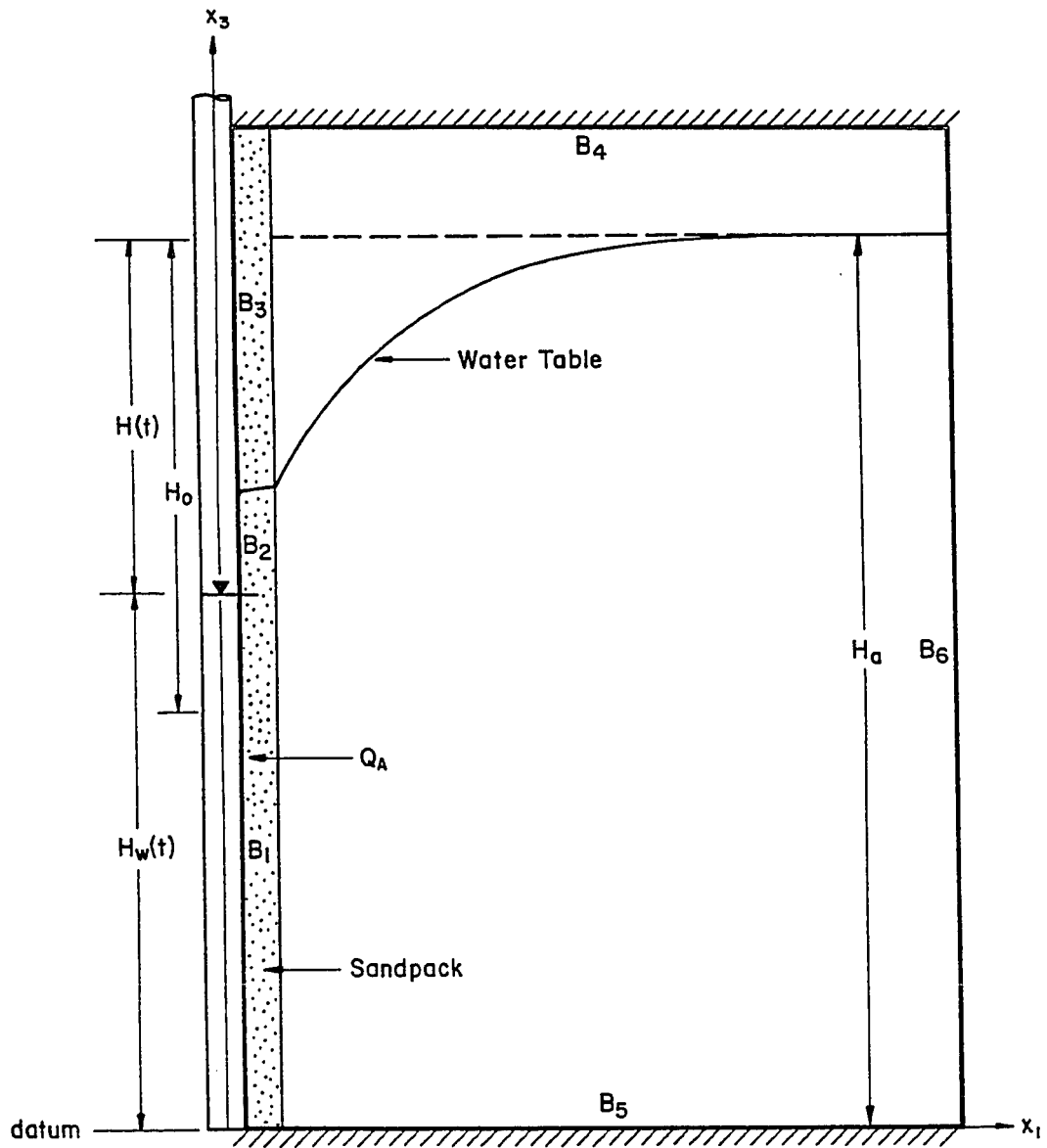
Figure 10. Bail test geometry at time greater than zero.

Boundary Conditions

The boundary conditions for slug and bail tests
(fig. 9 and fig. 10) can be described mathematically by:

$$H(x_i,t) = H_w(t) \qquad \text{on } B_1 \qquad (39)$$

$$H(x_i,t) = x_3 \qquad \text{on } B_2 \qquad (40)$$

$$\frac{\partial H}{\partial x_1} = 0 \qquad \text{on } B_3 \qquad (41)$$

$$\frac{\partial H}{\partial x_3} = 0 \qquad \text{on } B_4 \text{ and } B_5 \qquad (42)$$

$$H(x_i,t) = H_a \qquad \text{on } B_6 \qquad (43)$$

At saturated nodes along the monitoring well casing
(boundary B_1) the hydraulic head equals H_w, the water
level in the well (Equation 39). Equation (40) states
that the pressure head along a seepage face, B_2, is zero.
The hydraulic head equals the elevation head, x_3, along
this boundary. Equation (40) applies only to bail tests
because a seepage face does not form during a slug test.
Equation (42) states that there is no flow between the
aquifer and the monitoring well along B_3, the unsaturated
portion of the monitoring well casing. The upper and
lower boundaries, B_4 and B_5, are no-flow boundaries
(Equation 42). The right vertical surface, B_6, is a
constant head boundary that remains at a hydraulic head of
H_a throughout testing (Equation 43). This boundary is

completely saturated during a bail test. A portion of B_6 is unsaturated during a slug test. Above the water table (for the slug test), the elevation head, x_3, is greater than H_a, but the pressure head is negative, and the sum of the components gives a total head of H_a. The boundary B_6 is located far enough from the monitoring well that the hydraulic head is free to respond to testing at any distance from the well, but the head remains unchanged at an infinite radius.

A seepage face is a boundary with a pressure head of zero where water leaves the system. The position of the seepage face varies with time during a bail test and cannot be predicted (Neuman, 1975b). The saturated portion along the well is treated as a prescribed pressure head boundary with $\psi = 0$. The unsaturated part is treated as a prescribed flux boundary with a discharge $Q = 0$, where Q is the vector representing the nodal fluxes into the system. The lengths of each segment of the boundary are continually adjusted during the iterative process until the calculated values of Q along the saturated portion and of ψ along the unsaturated portion are consistent with these boundary conditions. The node locations are not shifted, but as the length of the seepage face changes, the number of nodes lying on this boundary changes.

The rate of flow into or out of the aquifer equals the rate of change of volume of water in the well. Equation (44) calculates the change in water level in the well during each time step, Δt:

$$\Delta H_w = \frac{Q_A \ \Delta t}{\pi \ r_w^2} \tag{44}$$

in which: ΔH_w is the change in height of the water

level (L),

r_w is the radius of the well (L),

Q_A is the discharge from the aquifer to the

well (negative value for flow from the

well to the aquifer) (L^3T^{-1}).

Aquifer Properties

All elements lying within the portion of the grid representing the aquifer are assigned a porosity, specific storage, and hydraulic conductivity correlative to the aquifer material as it has been logged during field investigation (Buddemeier et al., 1985 and 1986). The elements lying within the region representing the sandpack are assigned properties appropriate for Aquarium #3 sand, the type used in monitoring well construction. The aquifer and filterpack are assumed to be homogeneous and isotropic. A specific storage of zero is assigned to all aquifer and sandpack elements, because the aquifer under

consideration is shallow and the compressibility is assumed negligible (Davis and Neuman, 1983).

The saturated hydraulic conductivity assigned to the sandpack elements was determined by laboratory testing of Aquarium #3 sand. A falling head permeability test, performed by Terratech, Inc., determined the hydraulic conductivity of the sand to be 0.15 cm/sec (5.0×10^{-3} ft/sec). A range of hydraulic conductivities is assigned to the aquifer to determine the closest match. The specific values depend on the relative recovery rate of the well to be modeled.

In unsaturated soil, the pressure head, ψ, and hydraulic conductivity, K, are functions of the water content, θ (Childs, 1969). These relationships must be supplied as input data for each material so that unsaturated flow may be simulated by UNSAT2. These functions are characteristic for each soil and are determined in the laboratory (Klute, 1965a, 1972; Richards, 1965). The $\psi(\theta)$ function is strongly hysteretic and $K_r(\theta)$ is mildly so. There are an infinite number of secondary scanning curves that lie within the region between the boundary wetting and drying curves (fig. 11).

Hysteresis is not considered by UNSAT2, so the input data points for $K_r(\theta)$ and $\psi(\theta)$ must define single valued functions of water content. A single curve that
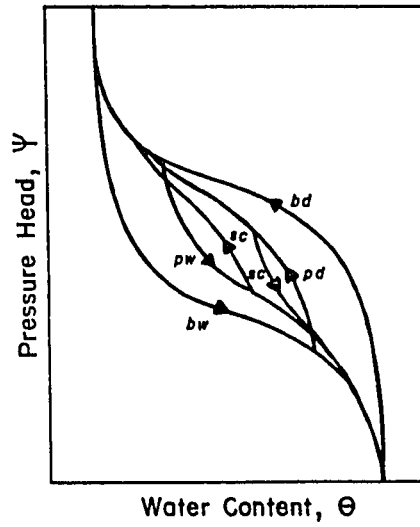
bd, boundary drying curve
bw, boundary wetting curve
pd, primary drying curve
pw, primary wetting curve
sc, scanning curve

Figure 11. Hysteresis of the soil moisture
Characteristic (Childs, 1969).

approximates the wetting and drying curves is used to represent the $K_r(\theta)$ and $\Psi(\theta)$ relationships for both wetting and drying conditions. The $\Psi(\theta)$ and $K_r(\theta)$ curves used to represent the aquifer are shown in figure 12, and the curves used for the sandpack are shown in figure 13. The $K_r(\theta)$ and $\Psi(\theta)$ curves used for the sandpack and aquifer materials are averages of curves from the literature for the corresponding soil types (Mualem, 1976).

A porosity of 30% was determined for the sandpack by laboratory tesing of Aquarium (3) sand by Terratech, Inc. The porosity of the aquifer is assumed to be 35% for wells screened primarily in sandstones and 40% for wells screened primarily in siltstones and claystones based on literature data (Mualem, 1976). The effective porosities in the unsaturated zone are actually lower than these values and are controlled by the characteristic curve for pressure head verses water content.

Example Slug and Bail Test Simulations

Bail Test

Consider a 12.7 cm (5 inch) diameter monitoring well in an unconfined aquifer with a hydraulic conductivity of 1×10^{-6} cm/sec (3×10^{-8} ft/sec). It is assumed that the aquifer has an equilibrium saturated thickness of 152.4 cm
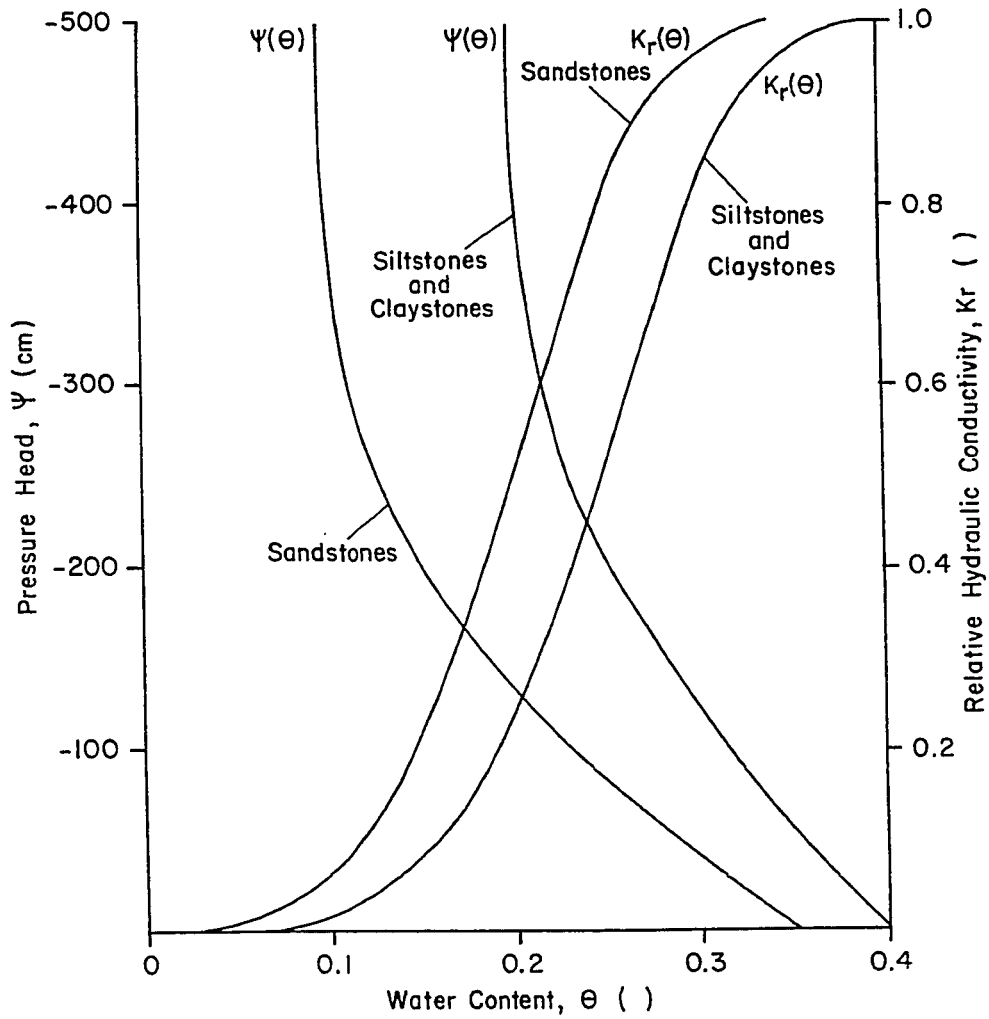
Figure 12. Characteristic curves for the aquifer at Site 300 used for UNSAT2 simulations, based on the literature (Mualem, 1976).
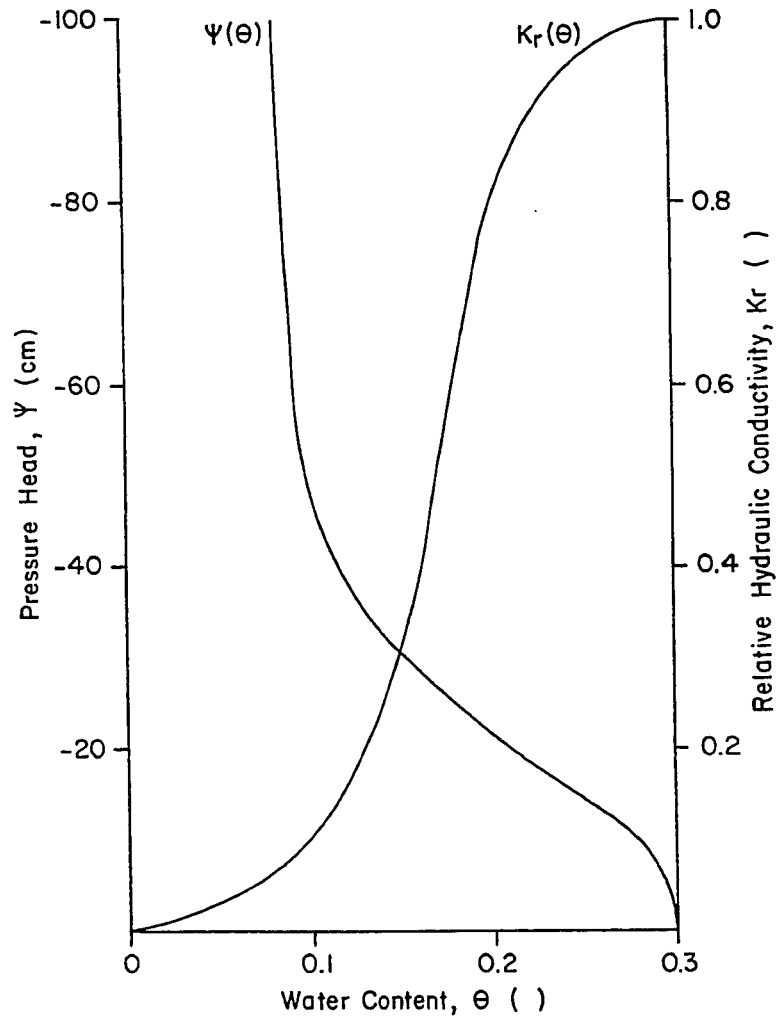
Figure 13. Characteristic curves for the sandpack at Site 300 wells used in UNSAT2 simulations, based on the literature (Mualem, 1976).

(5 ft.). A 5.08 cm (2 inch) thick (radially) sandpack
with a hydraulic conductivity of 1 x 10^{-2} cm/sec
(3 x 10^{-4} ft/sec) surrounds the well. A bail test is
modeled using UNSAT2 to observe the changing water table.
Figure 14 shows the water table in the monitoring well,
sandpack, and aquifer at times t= 53.8 seconds,
133,700 seconds, and 1,088,300 seconds. The water table
position is defined as the boundary between saturated and
unsaturated regions, where the pressure head equals zero.

When the slug of water is removed, the water surface
drops to 76.2 cm (2.5 ft) below the equilibrium level.
The water level rises immediately as water flows into the
well. The sandpack drains quickly compared to the
aquifer. The water content of the unsaturated areas above
the water table decreases with time as water drains
downward. A seepage face forms along the well casing,
connecting the water surfaces in the well and the
sandpack.

Water flows into the well along the saturated portion
of the sandpack, along and below the seepage face. At
t=53.8 seconds, the saturated thickness of the sandpack
decreases as the water table falls. There is an abrupt
head difference across the boundary between the sandpack
and aquifer. The seepage face length decreases with time,
and nearly disappears after t=600 seconds. At
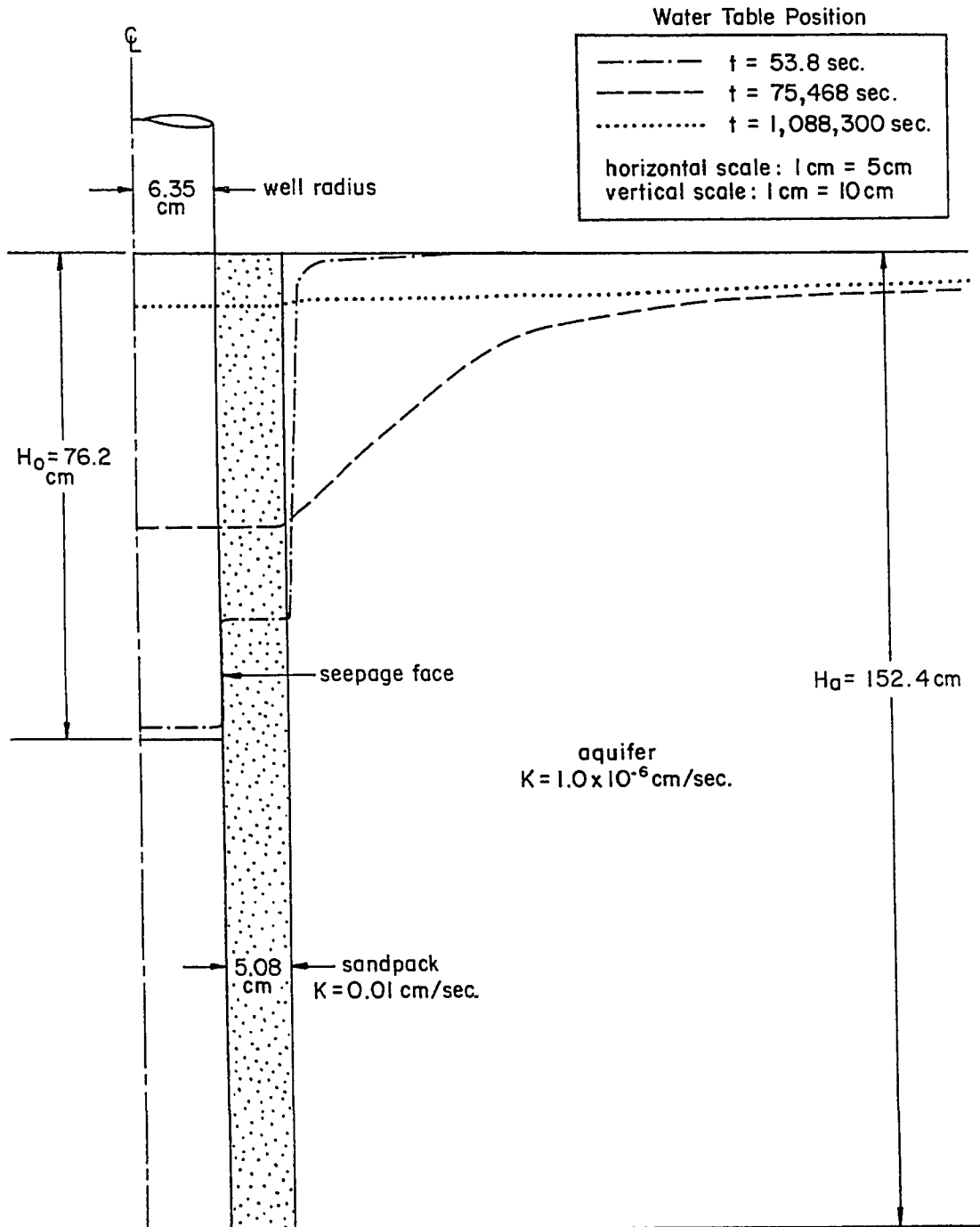
Figure 14. Water table position at various times during a bail test.

t=75,468 seconds, the water table is rising in the
sandpack, but continues to fall in the aquifer. The head
change at the boundary between the sandpack and aquifer is
less abrupt. The saturated thickness of the sandpack
increases at this time. At t=1,088,300 seconds, the water
table is rising in the aquifer, the sandpack, and the
well.

Slug Test

Ground water flow during slug testing differs
slightly from flow during bail testing. UNSAT2 is used to
model a slug test in a 12.7 cm (5 inch) diameter
monitoring well in an unconfined aquifer. The aquifer has
a hydraulic conductivity of 1×10^{-6} cm/sec
$(3 \times 10^{-8}$ ft/sec). The aquifer is assumed to have an
equilibrium saturated thickness of 76.2 cm (2.5 ft). A
5.08 cm (2 inch) thick (radially) sandpack with a
hydraulic conductivity of 1×10^{-2} cm/sec
$(3 \times 10^{-4}$ ft/sec) surrounds the well. Figure 15 shows the
water table in the monitoring well, sandpack, and aquifer
at times t= 48.9 seconds, 21,860 seconds, and
1,316,900 seconds.

When the slug of water is injected into the well, the
water surface rises 76.2 cm (2.5 ft) above the equilibrium
level. The water level falls immediately as water flows
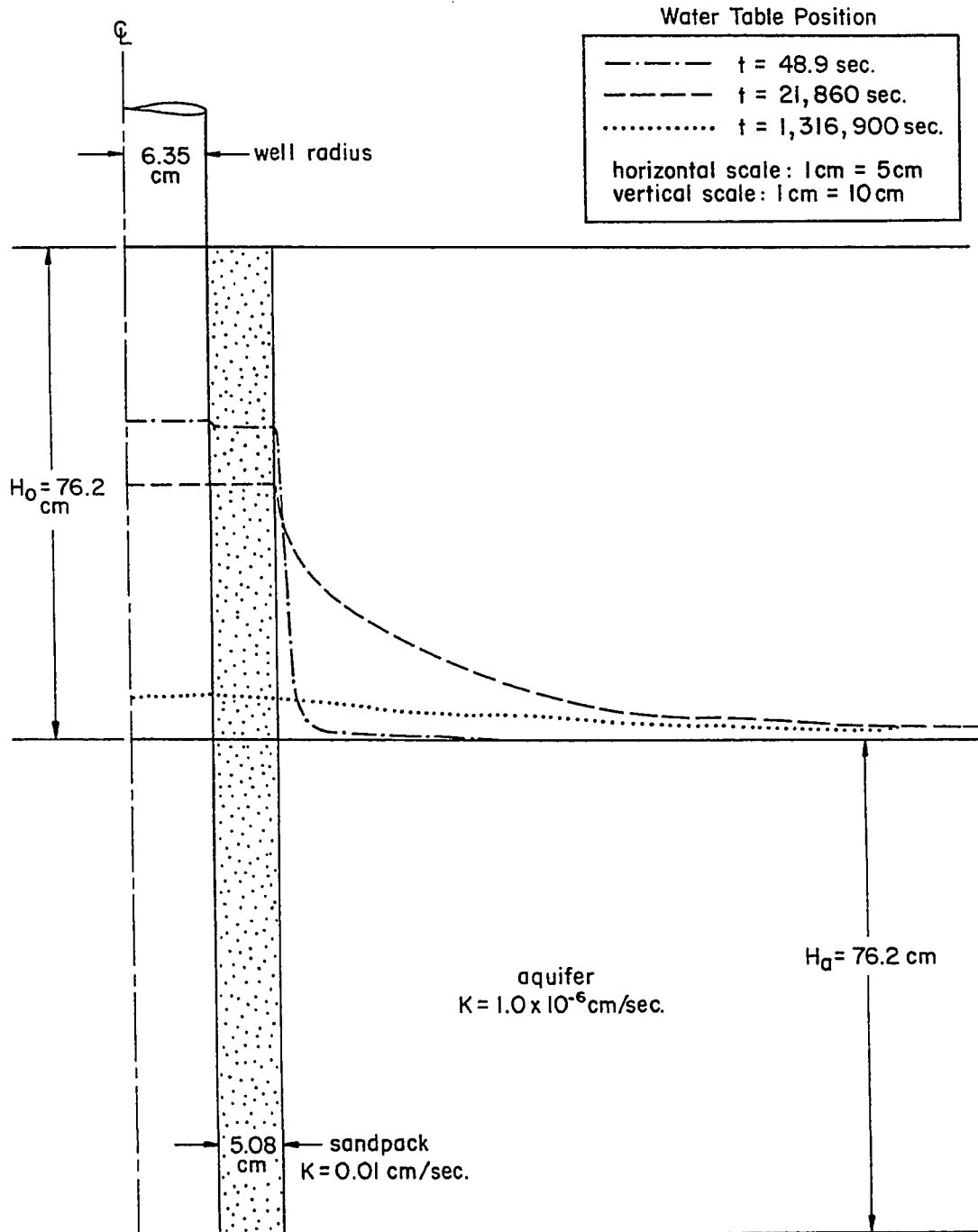
Figure 15. Water table position at various times during slug test.

into the sandpack above and below the water table. Water flows quickly into the sandpack compared to into the aquifer.

At t=48.9 seconds, the screen length through which water flows decreases as the water level falls in the well. There is an abrupt head difference across the boundary between the sandpack and aquifer. At t=21,860 seconds, the water table is falling in the sandpack, but continues to rise in the aquifer. The head difference between the sandpack and aquifer is less abrupt. At t=1,316,900 seconds, the water table is falling in the aquifer, the sandpack, and the well. The screen length through which water flows decreases throughout testing because water leaves the well both above and below the water table.

SENSITIVITY ANALYSIS

The output of the UNSAT2 runs is plotted with relative well recovery, H/H_0, on a vertical arithmetic scale, and time on a horizontal logarithmic scale. When a sandpack exists around the well, the recovery curves for field tests appear to be a combination of two different S-curves. Slug and bail test simulations using UNSAT2 also result in curves that appear to be a combination of two S-curves.

The first part of the curve is dominated by the properties of the sandpack. The sandpack material is more permeable than the aquifer, and much quicker to take in or give off water in response to the water level change in the well. The final portion of the curve is dominated by the properties of the aquifer. The influence of variations in sandpack and aquifer properties and well geometry on well recovery is displayed in the sensitivity analysis curves.

Slug and bail tests show a similar response to variations in aquifer properties and aquifer and well dimensions. Figures are included for the modeling of both slug and bail tests using different aquifer permeabilities to illustrate this similarity. All other sensitivity curves were generated from bail test simulations only.

The input data for each curve, unless stated otherwise, are as follows: the saturated hydraulic conductivity of the aquifer is 1×10^{-5} cm/sec, the saturated hydraulic conductivity of the sandpack is 0.01 cm/sec, the well diameter is 12.7 cm (5 in), the saturated aquifer thickness is 152.4 cm (60 in), the initial water displacement is 76.2 cm (30 in), the sandpack is 5.08 cm (2 in) thick (radially), the porosity of the aquifer is 0.35, and the porosity of the sandpack is 0.30. The unsaturated properties of the aquifer are as illustrated for sandstones on figure 12, and the unsaturated properties of the sandpack are illustrated on figure 13.

Hydraulic Conductivity

Saturated Hydraulic Conductivity

Relative well recovery time is indirectly proportional to hydraulic conductivity. The greater the hydraulic conductivity of the aquifer, the faster the wells recover to the equilibrium level. The final portions of two curves corresponding to two different aquifer hydraulic conductivities are offset along the time axis. Figure 16 shows bail test relative well recovery curves for aquifer hydraulic conductivities equal to 1.0×10^{-3} cm/sec, 1.0×10^{-4} cm/sec, and
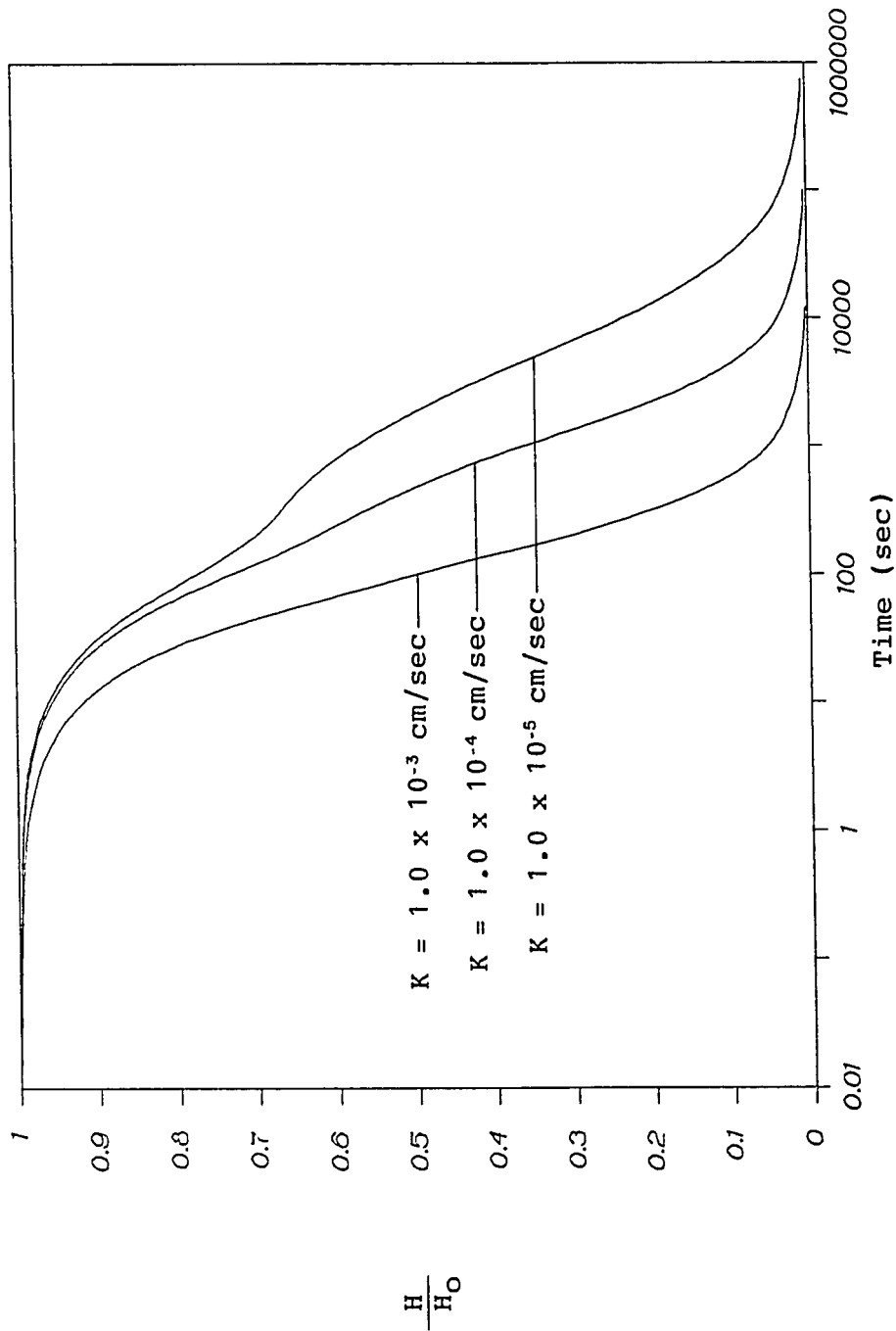
Figure 16. Sensitivity of well recovery curves for a bail test to variation in the saturated hydraulic conductivity of the aquifer. The hydraulic conductivity of the sandpack is 0.01 cm/sec.

1.0×10^{-5} cm/sec. The offset in the latter portion of the curves is proportional to the ratio of the hydraulic conductivities whenever all other monitoring well and aquifer parameters are equal.

Figure 17 shows slug test relative well recovery curves for aquifer hydraulic conductivities equal to those in figure 16. The offset in the latter portion of the curves is similarly proportional to the ratio of the hydraulic conductivities.

The sandpack response is affected by the difference in permeability between the sandpack and the aquifer (see figure 16 and figure 17). The recovery rate is slower during the sandpack dominated portion of the curve for lower permeability aquifers. This indicates that the early portion of the response curve is affected by both the sandpack and aquifer characteristics.

The sandpack shows a stronger influence during a slug test than during a bail test with identical sandpack and aquifer input parameters, as seen by comparing figures 16 and 17. The difference may be explained by the different hydraulic gradients set up along the well casing. The hydraulic gradient between the sandpack and the well is smaller for a bail test than for a slug test. At the start of a bail test, the air inside the well and the surface of the saturated sandpack along the well casing
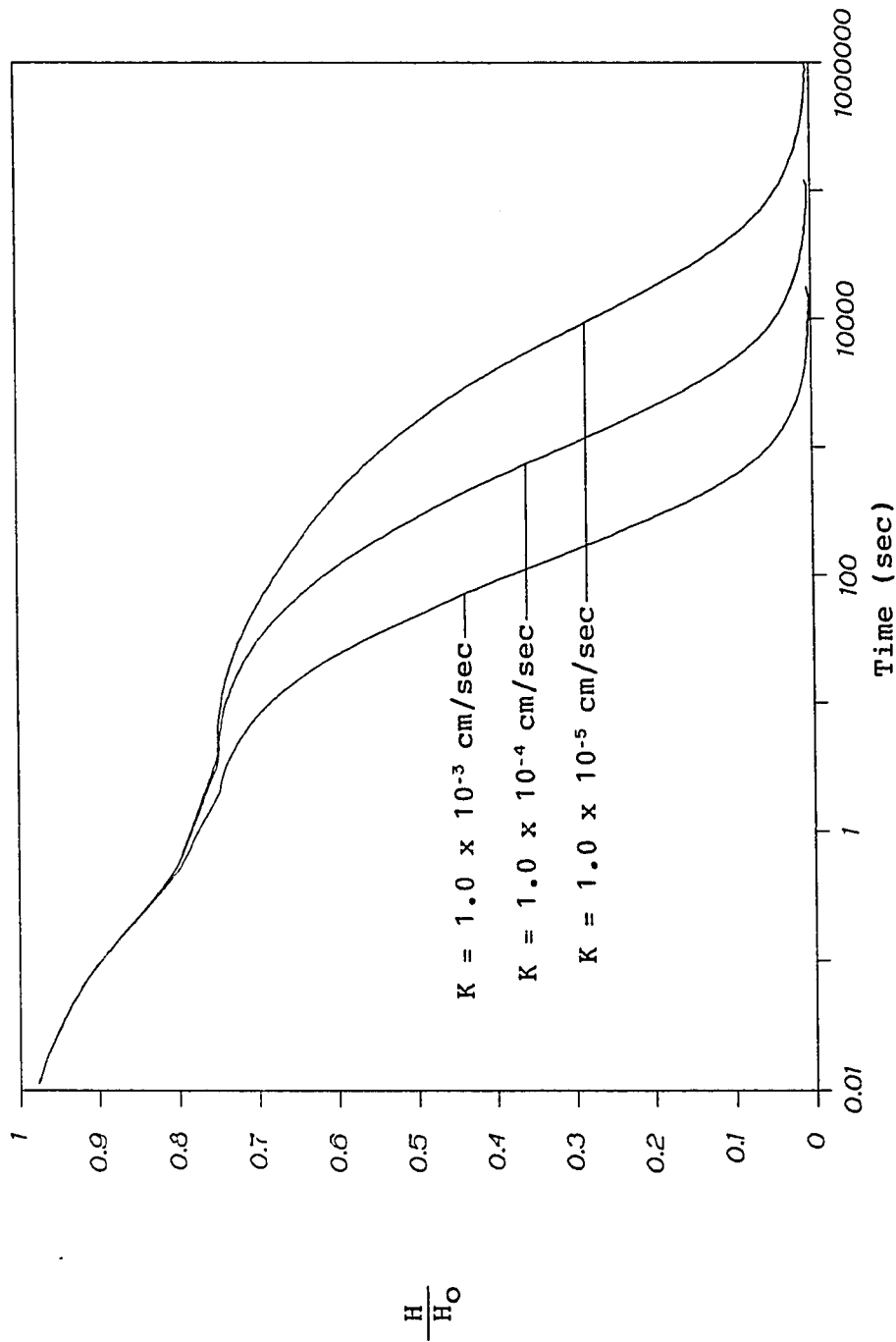
Figure 17. Sensitivity of well recovery curve for a slug test to variation in the saturated hydraulic conductivity of the aquifer. The hydraulic conductivity of the sandpack is 0.01 cm/sec.

are at atmospheric pressure. The remainder of the
saturated sandpack is subjected to the hydrostatic
pressure of the aquifer. At the start of a slug test, the
unsaturated sandpack next to the injected slug is at a
negative pressure head. There is a relatively large head
difference beween the unsaturated zone and the hydrostatic
pressure of the added slug in the well. The unsaturated
zone acts like a sponge, causing the sandpack response to
occur more quickly than with a bail test.

The initial portion of the curves is offset by
variation in the sandpack hydraulic conductivity, similar
to the offset caused by variations in aquifer hydraulic
conductivity. Figure 18 shows the relative well recovery
curves for sandpack hydraulic conductivities equal to
1.0 cm/sec, 0.1 cm/sec, 0.01 cm/sec, and 1×10^{-3} cm/sec.
The offset in the early portion of the curves is
proportional to the ratio of the hydraulic conductivities
whenever all other monitoring well and aquifer parameters
are equal. The greater the difference in permeability
between the sandpack and the aquifer, the more the
sandpack influences the later portion of the curve. A
more permeable sandpack causes an earlier recovery in the
latter portion of the curve. This indicates that the
presence of a sandpack affects the portion of the recovery
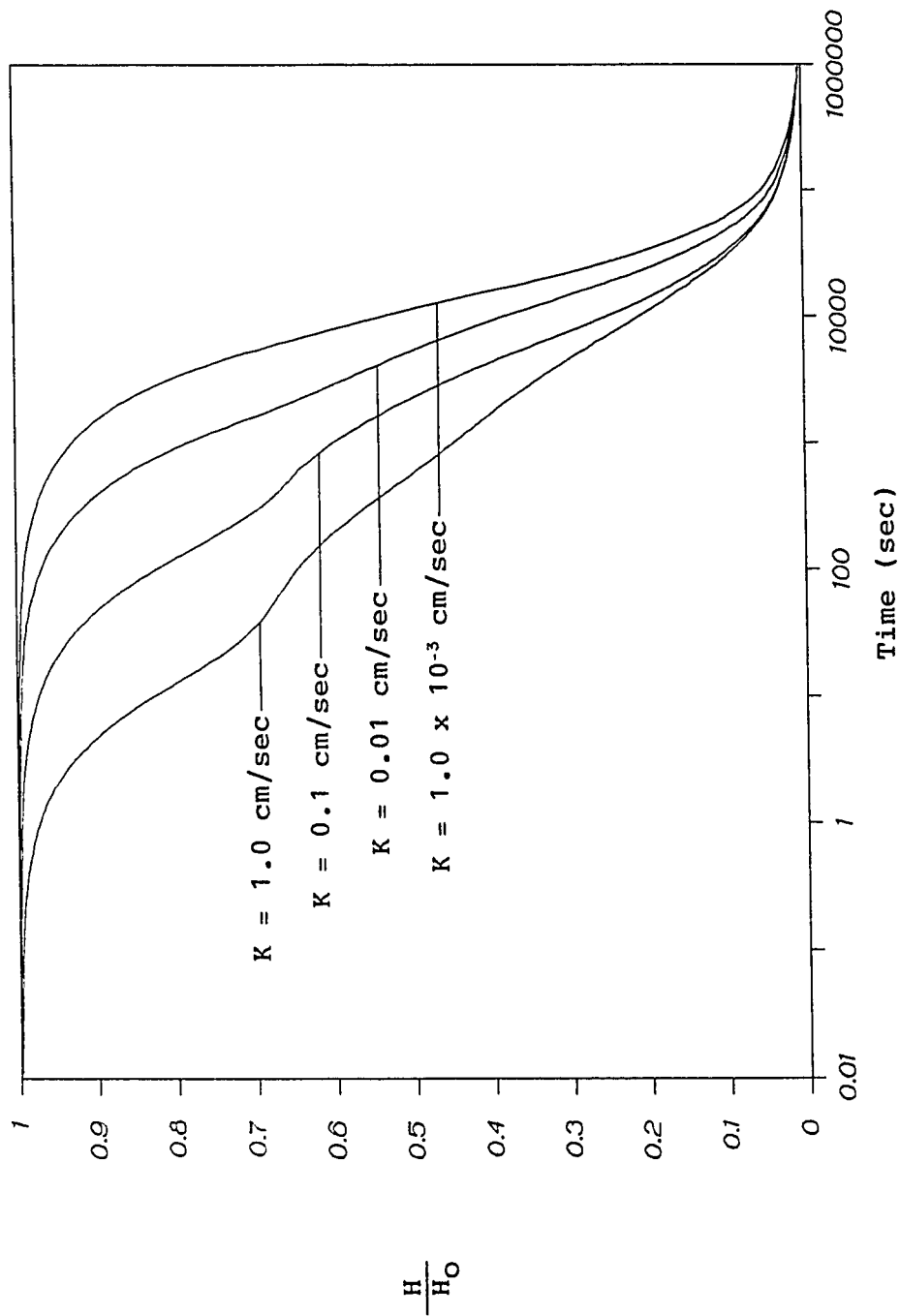
Figure 18. Sensitivity of well recovery curves for a bail test to variation in the saturated hydraulic conductivity of the sandpack. The hydraulic conductivity of the aquifer is 1.0×10^{-2} cm/sec.

curve dominated by the aquifer, and may lead to inaccurate calculation of the aquifer permeability.

If the contrast in permeabilities between the sandpack and the aquifer is less than approximately three orders of magnitude, it is difficult to distinguish the sandpack response from the aquifer response in the well recovery curve. For very permeable aquifers the sandpack response would not be apparent, but it could still influence the aquifer dominated portion of the curve.

Unsaturated Hydraulic Conductivity

The shape of the recovery curves varies slightly with different $K_r(\theta)$ relationships for the aquifer. Figure 19 shows several $K_r(\theta)$ curves for sandstones similar to the aquifer material found at Site 300 (Mualem, 1976). Bail tests were simulated with UNSAT2 using these $K_r(\theta)$ functions for the aquifer. The corresponding relative well recovery curves for bail testing are shown in figure 20.

Curve 1 results in a slightly faster well response then curve 2 and curve 3 because of the greater relative hydraulic conductivity, K_r, of the aquifer for all volumetric water contents. This means that all unsaturated portions of the aquifer are more permeable with curve 1 than with the other two curves, and the water
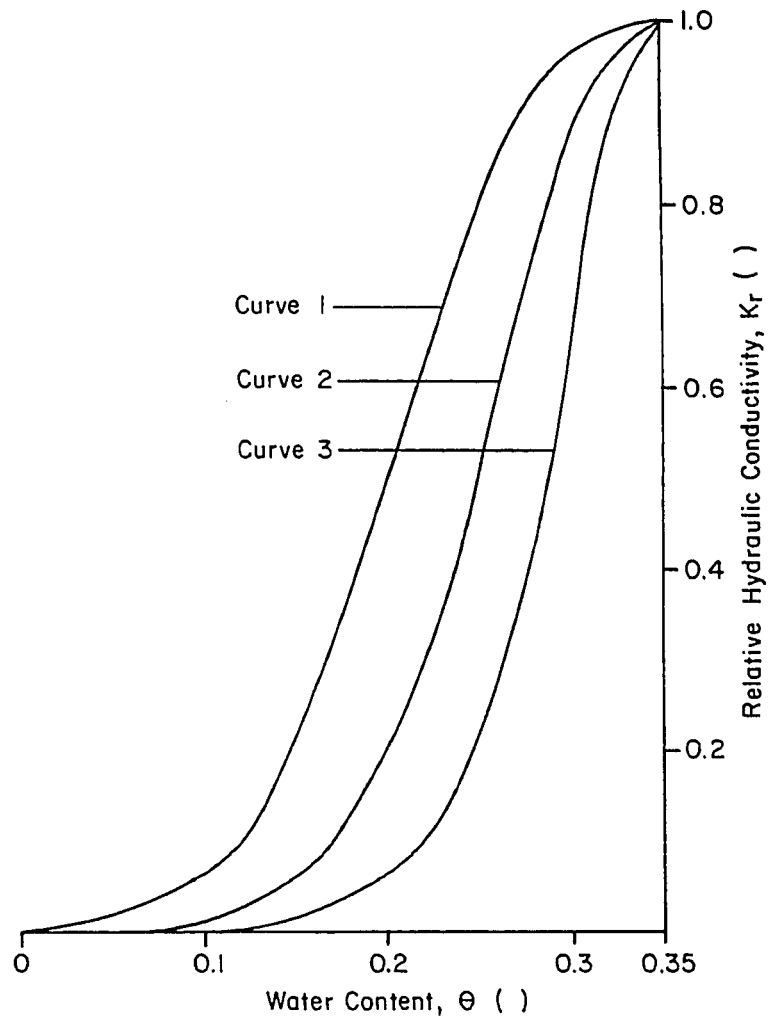
Figure 19. Sample relative hydraulic conductivity functions for sandstone aquifer (Mualem, 1976).
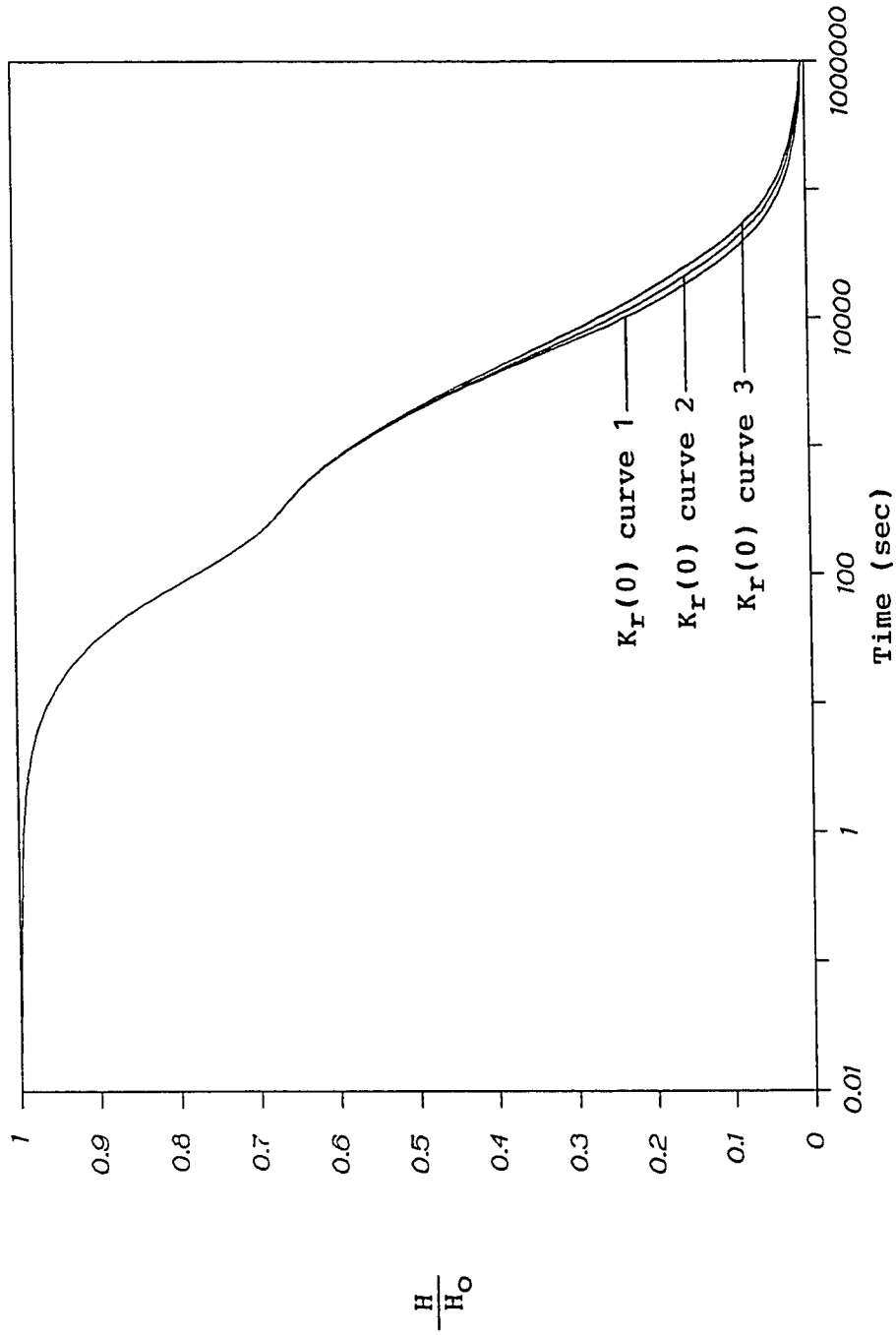
Figure 20. Sensitivity of well recovery curves for a bail test to variation in the unsaturated hydraulic conductivity of the aquifer. The $K_r(0)$ curves are shown on figure 19.

from the unsaturated zone drains into the well slightly
faster. Curve 1 is chosen for the sandstone aquifer
material because it is closest to the majority of curves
in the literature (Mualem, 1976), and a similar curve was
chosen for the siltstone and claystone aquifer material
(see figure 12).

Figure 21 shows several $K_r(\theta)$ curves for sandy soil
similar to the sandpack material used at Site 300 (Mualem,
1976). Slug and bail tests were simulated with UNSAT2
using these $K_r(\theta)$ functions for the sandpack. The
corresponding relative well recovery curves for bail
testing are shown in figure 22. The curves are not
particularly sensitive to variations in the unsaturated
hydraulic conductivity functions.

The same trend is found with variations in the $K_r(\theta)$
curve for the sandpack that was found with the aquifer
variations. Curve 1 is chosen for the sandpack because it
is closest to the majority of curves in the literature
(Mualem, 1976).

Well Diameter

Relative well recovery time is affected by the well
diameter. Smaller diameter wells recover faster than
larger wells. The ratio of well volume to flow rate into
or out of the well is smaller for smaller diameter wells.
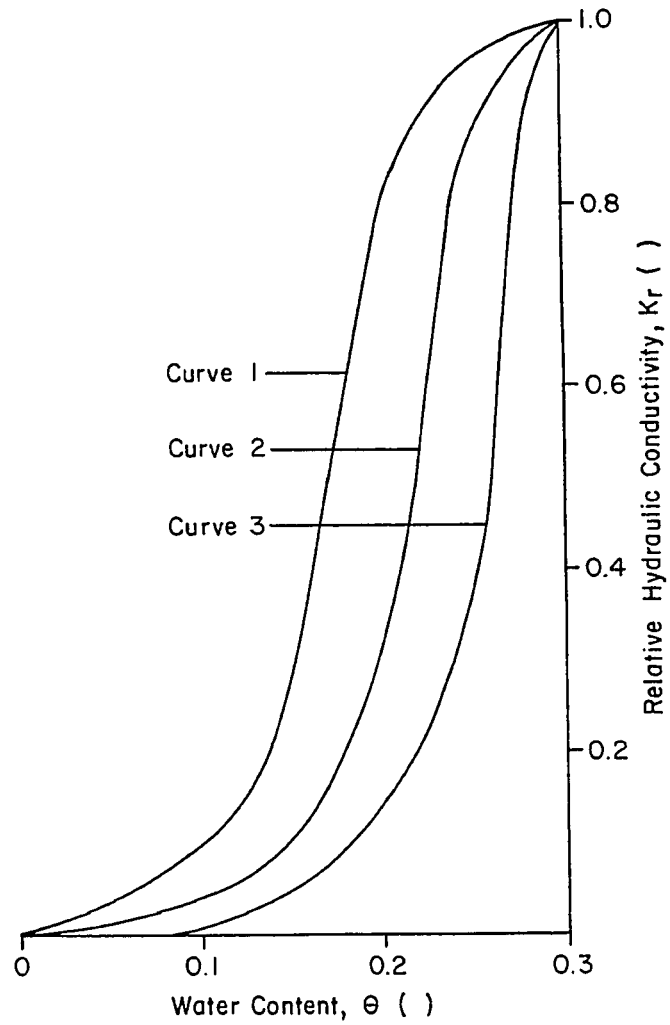
Figure 21. Sample relative hydraulic conductivity functions for sandpack (Mualem, 1976).
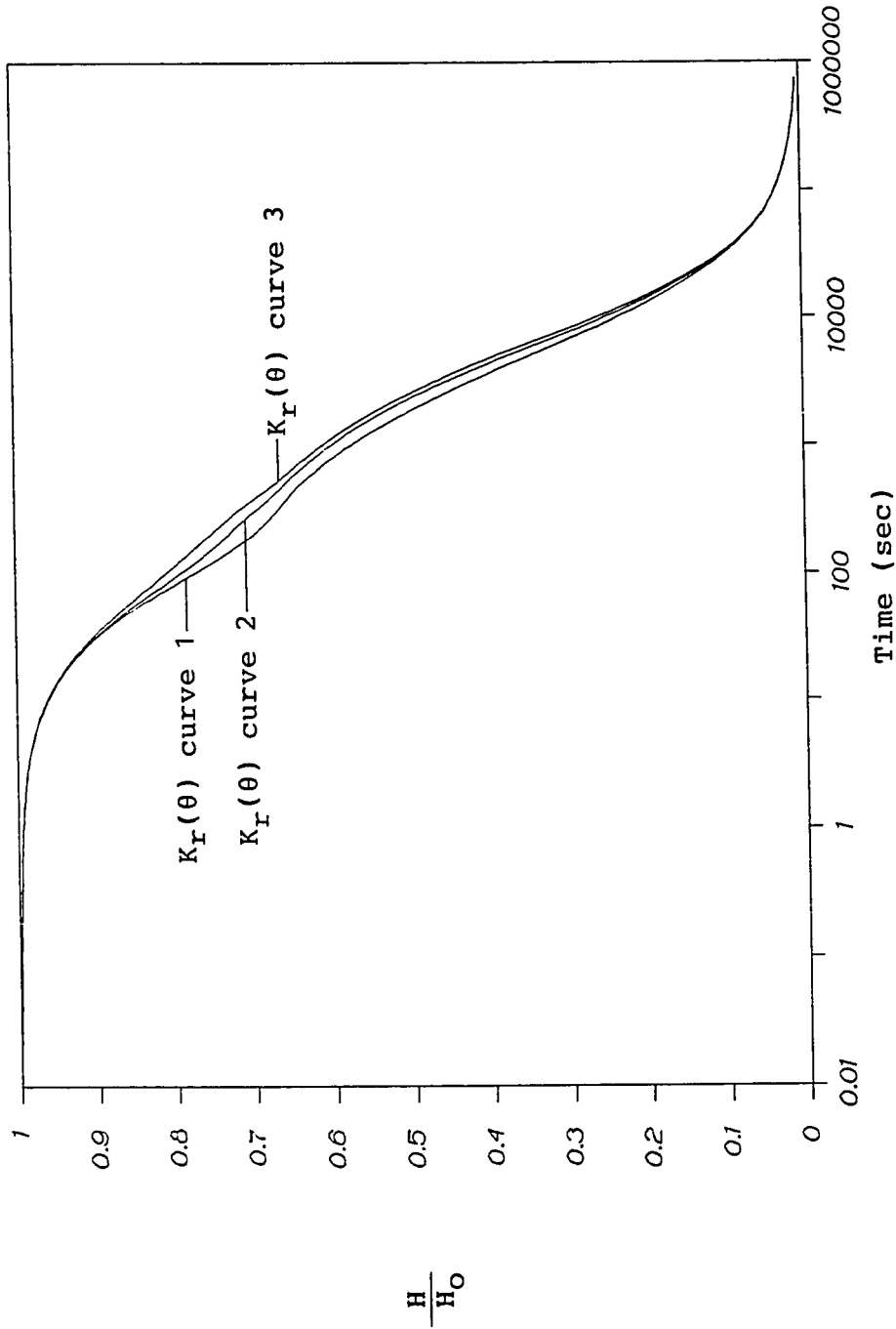
Figure 22. Sensitivity of well recovery curves for a bail test to variation in the unsaturated hydraulic conductivity of the sandpack. The $K_r(0)$ curves are shown on figure 21.

Therefore, for any hydraulic gradient, a smaller well
recovers faster whenever all other well and aquifer
parameters are equal.

Figure 23 shows the relative well recovery curves for
wells with diameters equal to 5.08 cm (2 in), 10.16 cm
(4 in), and 12.70 cm (5 in). The final portions of the
curves are offset proportional to the ratio of the squares
of the well diameters. The smaller the well diameter, the
greater the relative recovery during all stages of well
recovery. This is consistent with the method of
Cooper et al. (1967). Additionally, the sandpack response
is more dominant for the smaller diameter wells because
the ratio of sandpack pore space to well volume is larger.
There is more water available relative to the well volume
during the initial rapid response.

For the 5.08 cm (2 in.) well, the later portion of
the curve is not only offset proportional to the well
diameter, but the slope of this portion is also visibly
affected by the influence of the more dominant sandpack
response. The sandpack response pulls the early portion
of the aquifer response to the left and flattens the slope
of the aquifer response. This may lead to inaccurate
calculation of the aquifer hydraulic conductivity.
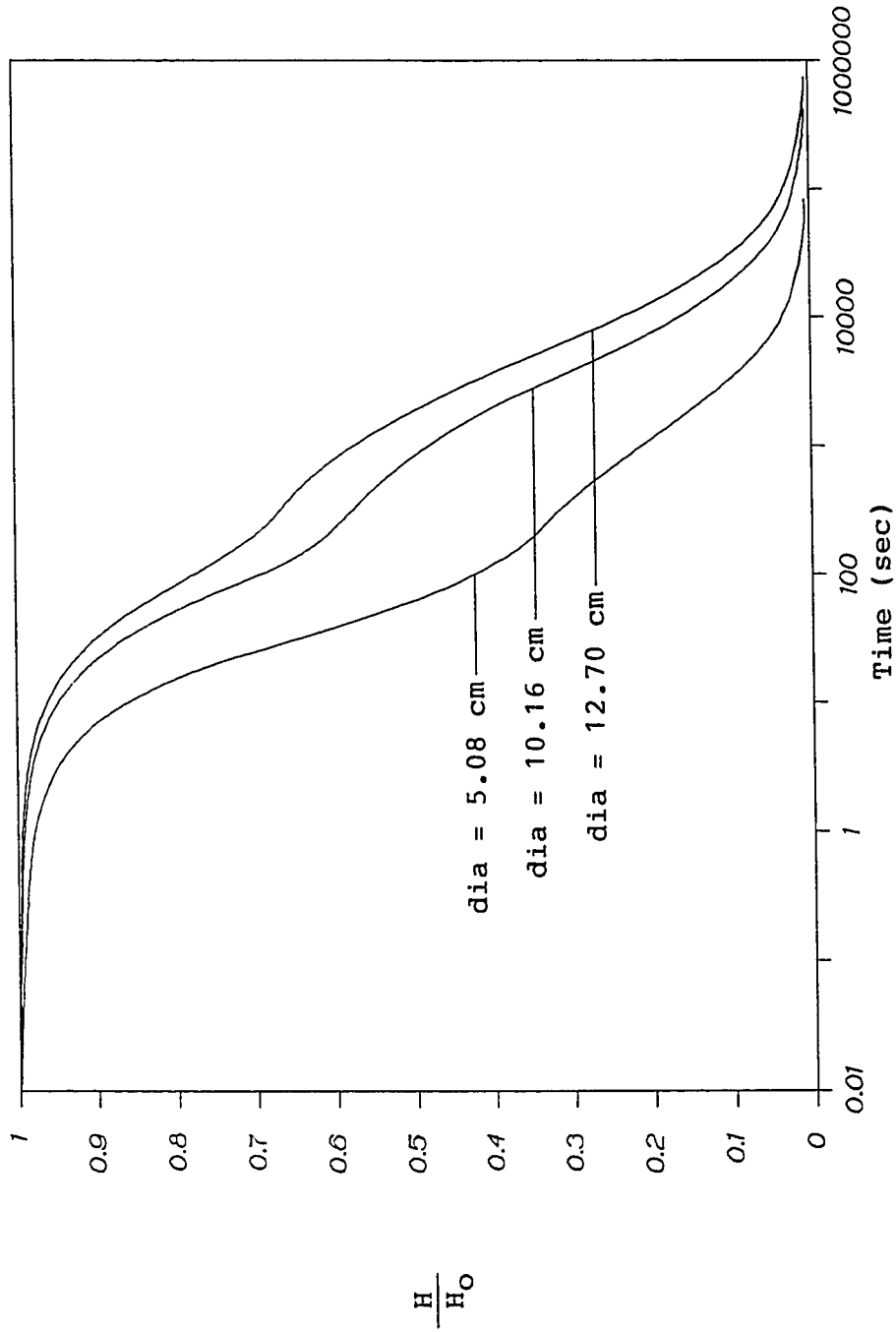
Figure 23. Sensitivity of well recovery curves for a bail test to variation in well diameter.

Radial Sandpack Thickness

Radial sandpack thickness affects the recovery rate during slug and bail tests. Figure 24 shows relative well recovery curves for radial sandpack thicknesses equal to 1.06 cm (0.42 in), 2.65 cm (1.04 in), and 5.08 cm (2 in).

The greater the radial thickness of the sandpack, the faster the well recovery when all other aquifer and well parameters are equal. The thicker sandpacks dominate a greater portion of the curve, and mask the aquifer response more completely. The aquifer response is shifted to the left, proportional to the sandpack thickness. The presence of a sandpack therefore leads to the calculation of an erroneously high aquifer hydraulic conductivity.

Aquifer Thickness

Relative well recovery time is inversely proportional to aquifer thickness. The final portions of curves representing different aquifer thickness are offset along the time axis. Figure 25 shows relative recovery curves for aquifers 457.2 cm (180 in) and 152.4 cm (60 in) thick. The offset is directly proportional to the aquifer thickness. This is consistent with the method of Cooper et al.
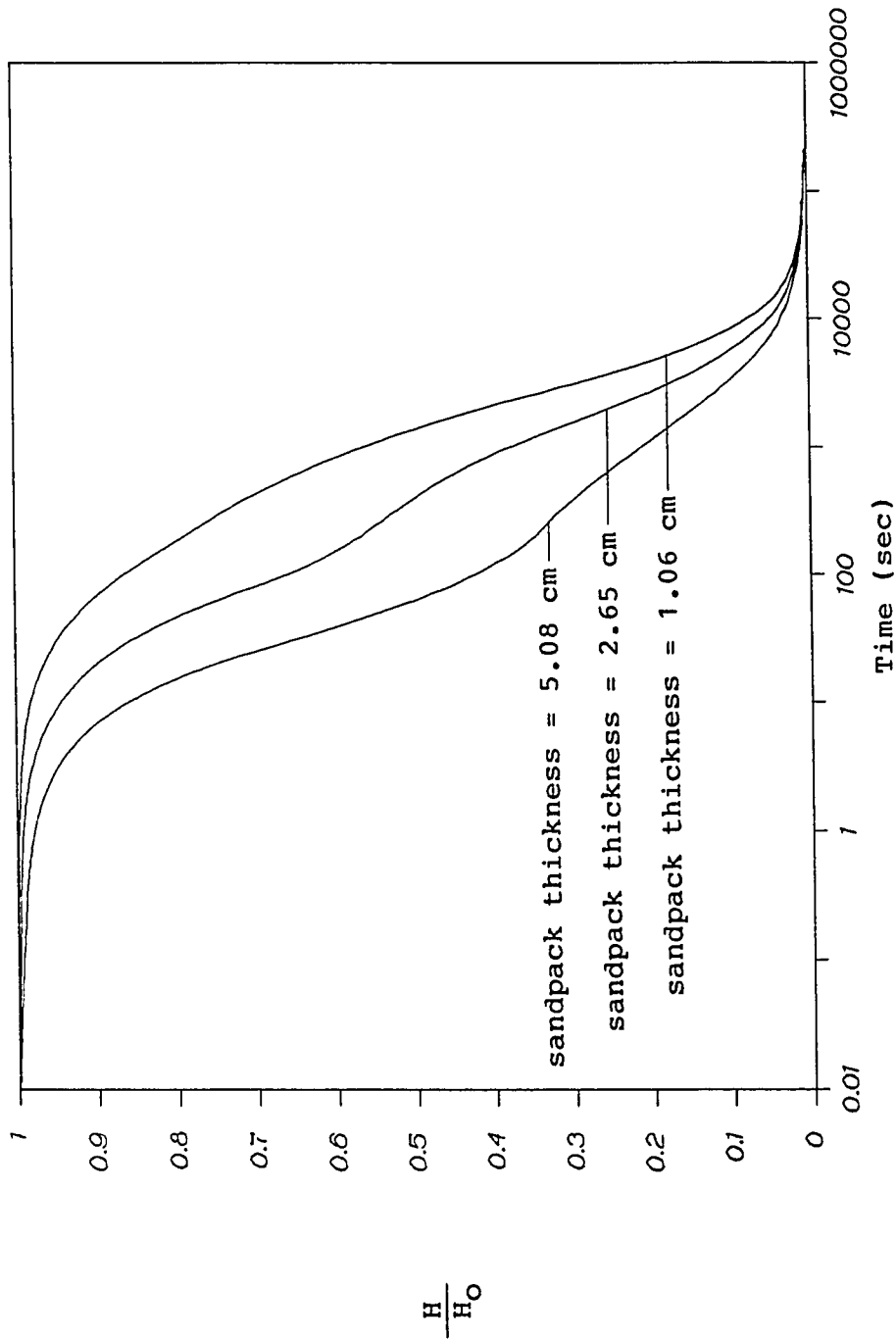
Figure 24. Sensitivity of well recovery curves for a bail test to variation in radial sandpack thickness.
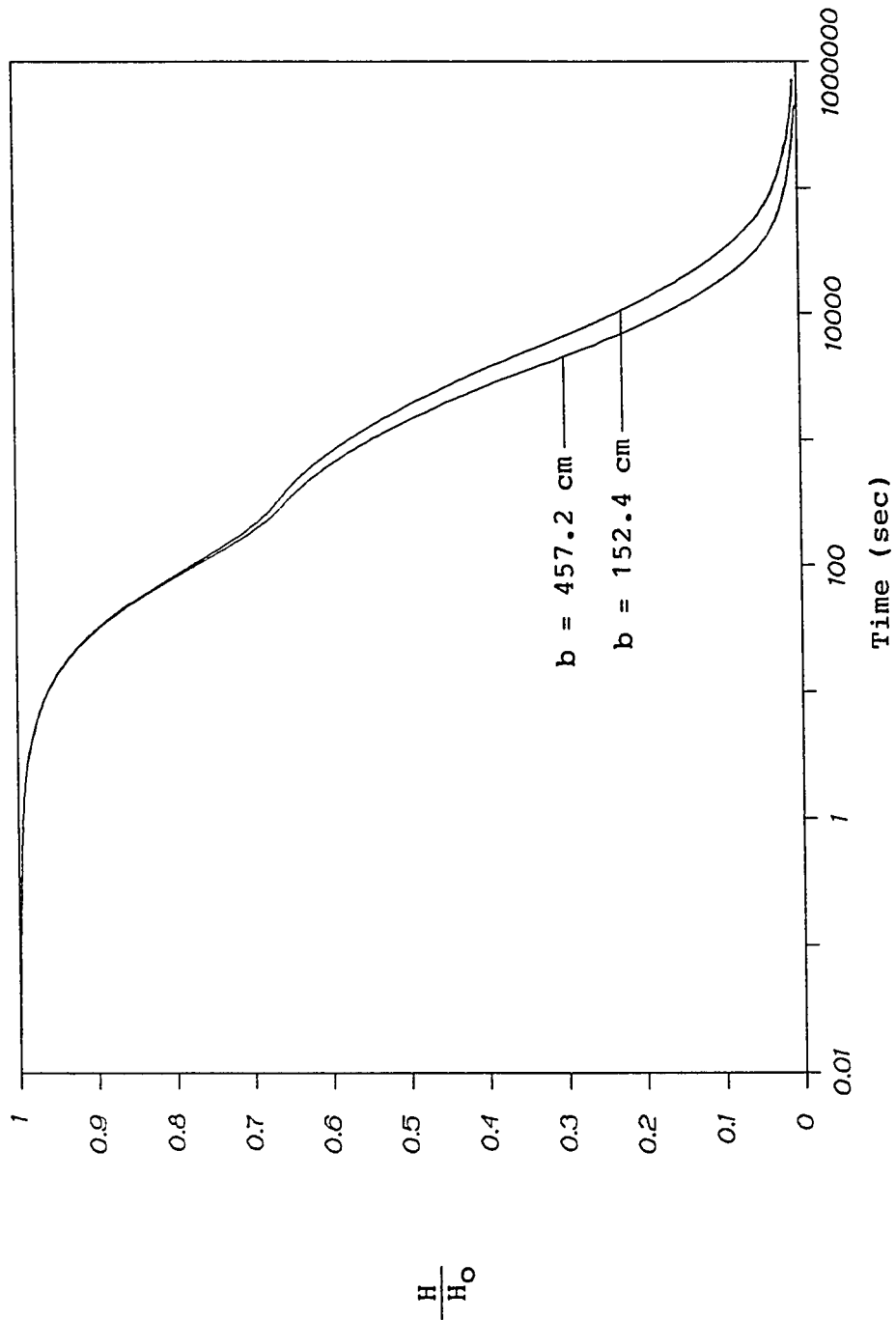
Figure 25. Sensitivity of well recovery curves for a bail test to variation in the aquifer thickness.

Initial Water Level Displacement

Variations in the length of the initial water level displacement in the well change the shape of the relative recovery curves. This is a departure from the method of Cooper et al. Figure 26 shows relative recovery curves for slug lengths of 38.1 cm (15 in), 76.2 cm (30 in), and 152.4 cm (60 in).

The greater the initial water level displacement in the well, the faster the recovery. This may be caused by the greater relative influence of the unsaturated properties of the sandpack and aquifer. The aquifer response is shifted along the time axis by variations in initial water level displacement and must be modeled separately for each test.

Specific Moisture Capacity

The shape of the recovery curves varies with different $\Psi(\theta)$ relationships for the aquifer. Figure 27 shows several empirically determined $\Psi(\theta)$ curves for sandy aquifer material similar to that present at Site 300 (Mualem, 1976). Bail tests were simulated with UNSAT2 using these $\Psi(\theta)$ functions for the aquifer. The corresponding relative well recovery curves are shown in figure 28.
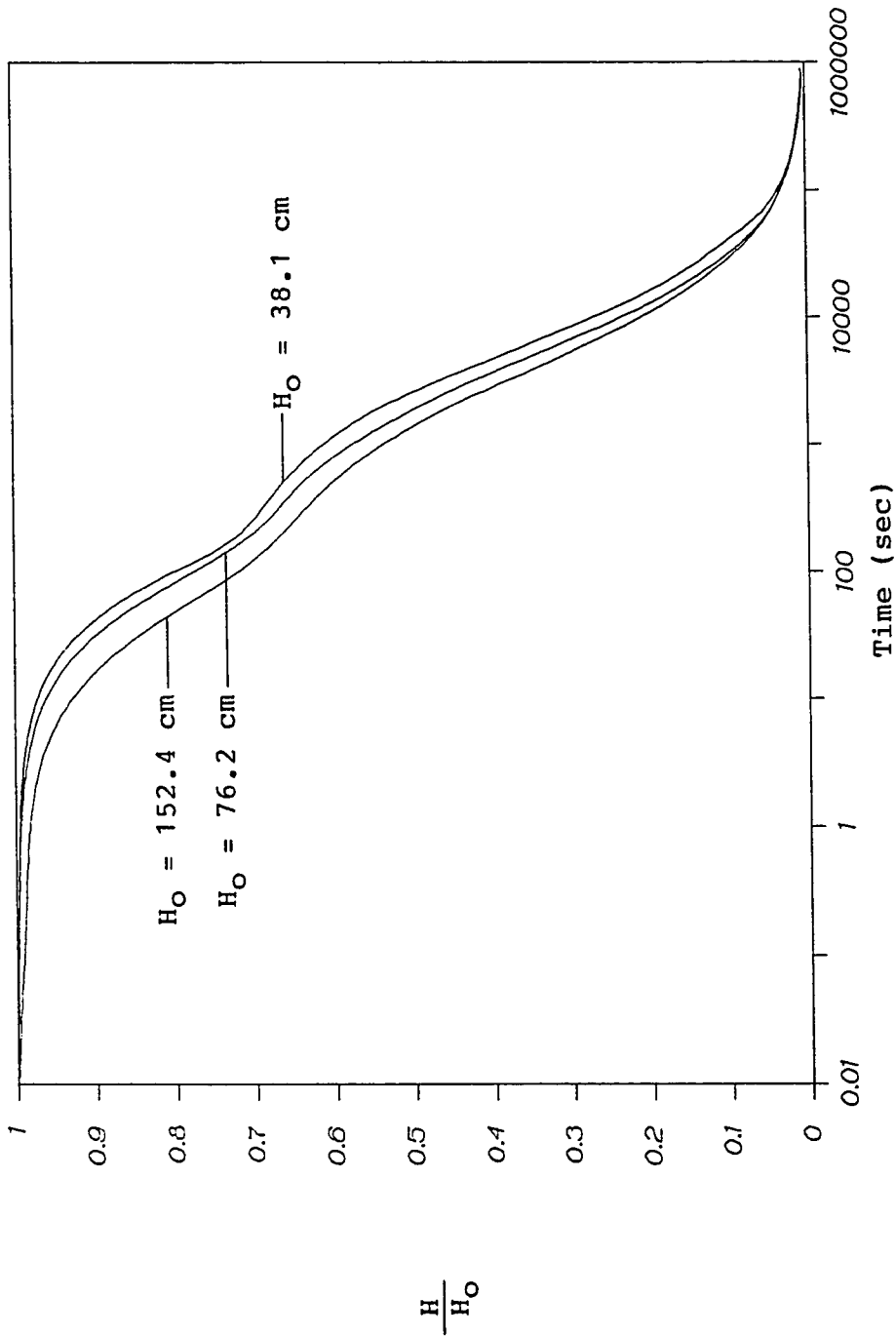
Figure 26. Sensitivity of well recovery curves for a bail test to variation in the initial water level displacement.
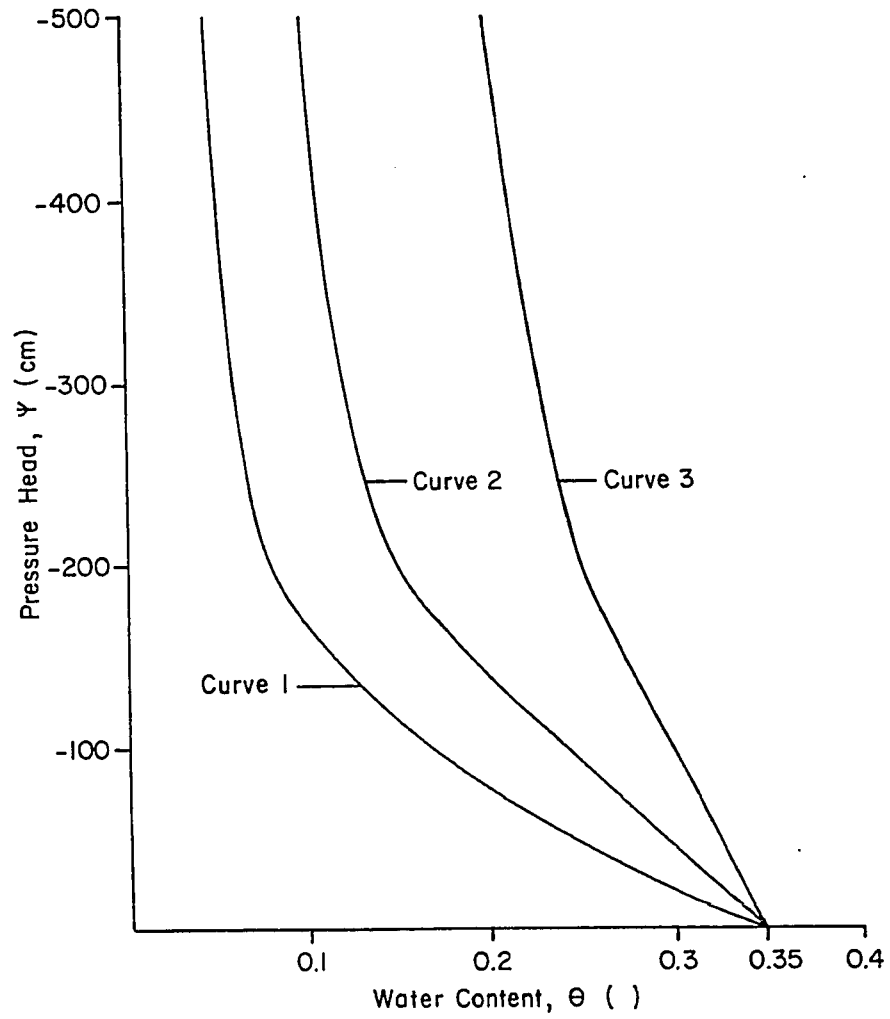
Figure 27. Sample relative hydraulic conductivity functions for sandstone aquifer (Mualem, 1976).
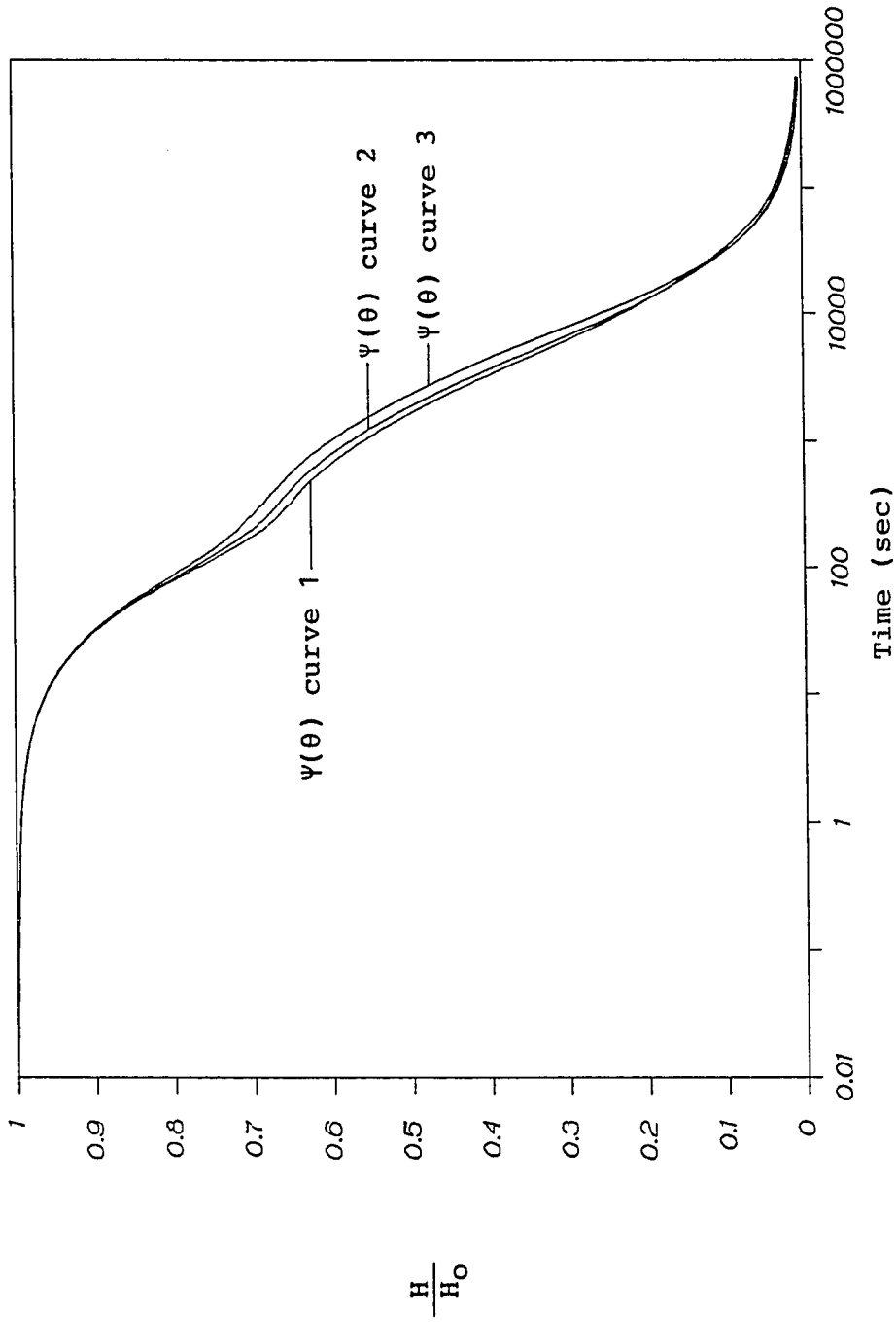
Figure 28. Sensitivity of well recovery curves for a bail test to variation in the negative pressure head function of the aquifer. The $\psi(\theta)$ curves are shown on figure 27.

Curve 1 shows the fastest well response during the aquifer-dominated portion of the curve. Aquifer material with the characteristic curve 1 drains at a lower suction (negative pressure head) than with curve 2 and curve 3. Water is held in the unsaturated zone by tension. Material corresponding to curve 1 loses most of its water at a suction of 200 cm water. Sand that follows the relationship of curve 3 will retain over 50% of the saturated water content when subjected to 500 cm suction.

During a bail test, the aquifer is initially saturated. The aquifer drains faster with characteristic curve 1 than with curve 3 as the suction in each portion of the unsaturated zones increases. Curve 2 is chosen for sandy aquifer material because it most closely matches the curves found in the literature (Mualem, 1976). Similar curves were chosen for siltstone and claystone aquifer material (see figure 12).

The shape of the recovery curves also varies with different $\Psi(\theta)$ relationships for the sandpack. Figure 29 shows several empirically determined $\Psi(\theta)$ curves for sandy soil similar to the sandpack material used at Site 300 (Mualem, 1976). Slug and bail tests were simulated with UNSAT2 using these $\Psi(\theta)$ functions for the sandpack. The corresponding relative well recovery curves are shown in figure 30.
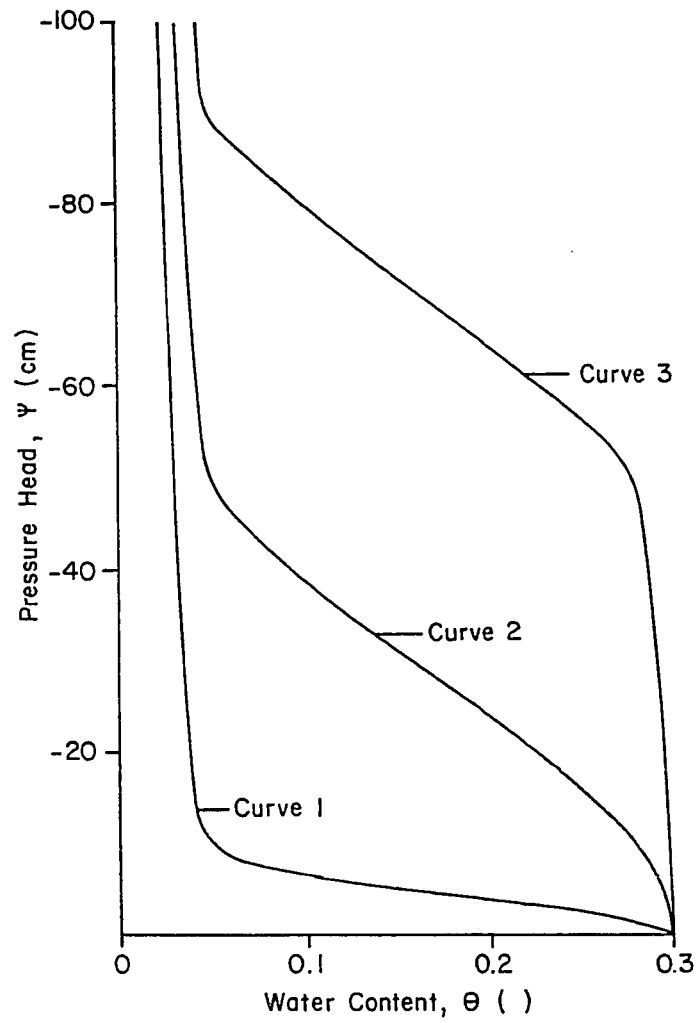
Figure 29. Sample negative pressure head functions for sandpack (Mualem, 1976).
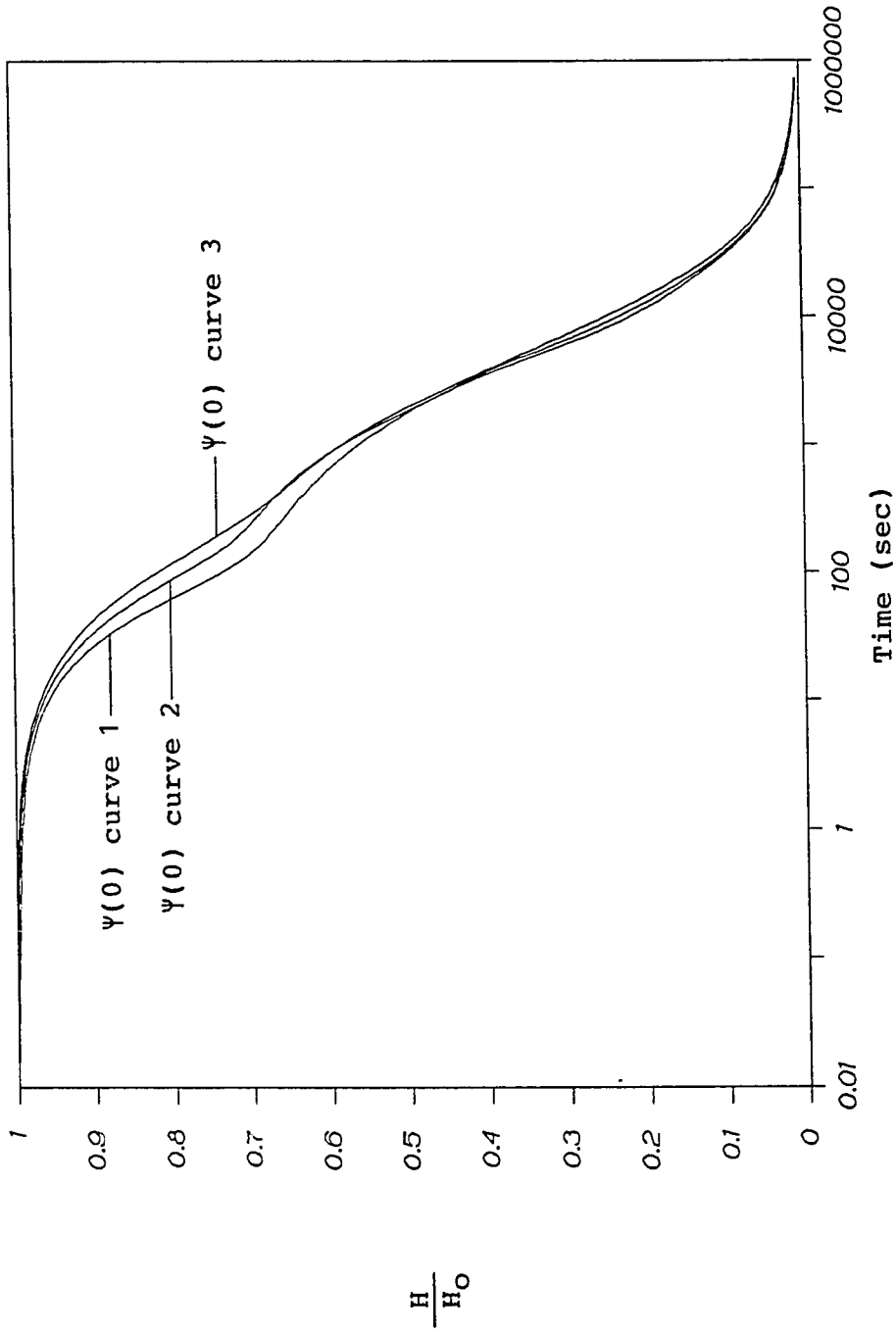
Figure 30. Sensitivity of well recovery curves for a bail test to variation in the negative pressure head function of the sandpack. The Ψ(0) curves are shown on figure 29.

Curve 1 shows the fastest well response during the sandpack-dominated portion of the curve. Sandpack material with the characteristic curve 1 drains at a lower suction (negative pressure head) than with curve 2 and curve 3. Water is held in the unsaturated zone by tension. Sand corresponding to curve 1 loses most of its water at a suction of 15 cm water. Sand that follows the relationship of curve 3 will remain nearly saturated when subjected to 50 cm suction.

During a bail test the sandpack is initially saturated. The sand drains faster with characteristic curve 1 than with curve 3 as the suction in each portion of the unsaturated zones increases. Similarly, during a slug test, the newly saturated areas of the sandpack drain faster to the aquifer with characterisic curve 1 than with curve 3. The initial filling of the sandpack during a slug test should be more rapid for sands that follow the greater suction relationship of curve 3, but the difference appears to be trivial on this short time scale. Curve 2 is chosen for the sandpack because it most closely matches the curves found in the literature (Mualem, 1976) for sand similar to that used in the Site 300 wells.

MODELING OF SITE 300 WELLS

Slug and bail tests have been performed on selected Site 300 wells. The tests were simulated with UNSAT2, incorporating the specific Site 300 aquifer and well geometries into the input data for each run. The well logs, including well completion data, are provided in Buddemeier et al. (1985 and 1986).

The aquifer material is assumed to be homogeneous and isotropic for all test simulations. Most of the wells at Site 300 are screened over a zone that includes more than one type of earth material. The hydraulic conductivity values determined by UNSAT2 curves should be considered weighted averages of the actual hydraulic conductivities of all materials through which water flows during testing.

The UNSAT2 curves all show a gradual recovery at the last stage where the curves representing different aquifer hydraulic conductivities converge. This "tail" is also present in the Cooper et al. curves. The field test curves, however, all recover more abruptly at the extreme end, probably because of the limitation in the instrument sensitivity to measure these very small head changes. The very last portion of the field data is ignored during curve matching.

The Site 300 curves cannot be matched to a dimensionless set of type curves developed by UNSAT2 simulations because of the sandpack influence and flow within the unsaturated zone during slug and bail testing. As was shown in the sensitivity analysis, the curve shapes are controlled by the unsaturated zone relationships and the sandpack properties, particularly the sandpack geometry.

The unsaturated flow is described by a set of highly non-linear equations, and it is difficult to solve for the flow using analytical methods. The characteristic curves for negative pressure head and relative hydraulic conductivity are determined empirically for each earth material, and as was shown on figure 11, there are an infinite number of secondary scanning curves that lie within the the region between the boundary wetting and drying curves. These functions cannot be incorporated into a mathematical description of the slug and bail test flow systems. The unsaturated flow and the relative well recovery rate are dependent on these empirical curves, so they must be modeled separately for each aquifer type.

The presence of a sandpack around the well may have a large influence on the relative recovery curves, as was shown in the sensitivity analysis. The curves are not S-curves like the curves of Cooper et al. (1967), but are

a combination of two different S-curves. The first
portion, dominated by the sandpack response, was shown to
influence the position of the aquifer dominated portion,
depending on the sandpack properties and geometry.
Different sandpack properties and geometries also must be
modeled separately.

The UNSAT2 simulations are plotted with an absolute
time scale on the horizontal axis, and relative recovery,
H/H_0, on the vertical scale. The hydraulic conductivity
values for the Site 300 aquifer materials are determined
by curve matching of the field test results to several
UNSAT2 simulations for different aquifer hydraulic
conductivities. The hydraulic conductivity values
determined from curve matching of the field test results
and UNSAT2 simulations are summarized in table 1.

Well NC7-25

Monitoring well NC7-25 is screened primarily in
sandstone, with smaller amounts of claystone and siltstone
in the screened zone. The program input data for UNSAT2
simulations is as follows: the saturated hydraulic
conductivity of the sandpack is 0.01 cm/sec, the well
diameter is 11.04 cm (4.35 in), the saturated aquifer
thickness is 135.0 cm (53.1 in), the initial water
displacement is 237.7 cm (93.58 in) for the slug test and

Table 1. Comparison of hydraulic conductivity values (cm/sec) determined for field data using different analytical methods and UNSAT2.

Well and Test	UNSAT2 Simulation	Cooper et al.	Cooper et al. modified	Hvorslev	Hvorslev modified	Bouwer and Rice	Bouwer and Rice modified
NC7-25 Slug	2.0E-05	1.2E-04	2.4E-04	9.0E-05	7.0E-05	6.8E-05	5.0E-05
NC7-25 Bail	3.0E-05	1.6E-04	3.2E-04	3.0E-05	4.0E-05	5.8E-05	4.3E-05
NC7-23 Slug	1.0E-06	4.0E-06	7.4E-06	3.0E-06	3.0E-06	2.5E-06	2.3E-06
NC7-23 Bail	1.5E-06	5.0E-06	3.0E-06	5.0E-06	5.0E-06	3.4E-06	3.2E-06
NC2-08 Slug	4.0E-04	9.0E-04	5.9E-04	3.6E-04	3.5E-04	3.5E-04	3.3E-04
NC2-08 Bail	5.0E-04	8.4E-04	5.5E-04	3.8E-04	4.0E-04	3.3E-04	3.4E-04

134.11 cm (52.8 in) for the bail test, the sandpack is
5.91 cm (2.33 in) thick radially, the porosity of the
aquifer is 40%, the porosity of the sandpack is 30%, the
unsaturated properties of the aquifer are as illustrated
for siltstones and claystones on figure 12, and the
unsaturated properties of the sandpack are illustrated on
figure 13. The effective radius of the displacement
object for the slug test is 4.43 cm (1.74 in). The slug
and bail tests do not meet all the assumptions made in
UNSAT2 simulations because the displacement object was not
completely submerged after the slug test began. The
removal and insertion of the displacement object is also
not instantaneous for the slug and bail tests.

The water displacement, H_0, is smaller for the bail
test than for the slug test because the cross-sectional
area in the well surrounding the displacement object
(34.0 cm^2) is substantially smaller than the
cross-sectional area of the object (61.7 cm^2). At the
start of a bail test, the water initially surrounding the
object flows downward to fill a volume equal to H_0
multiplied by 95.7 cm^2, the cross-sectional area of the
well. At the start of the slug test, the water displaced
by the object fills a volume equal to H_0 multiplied by
34.0 cm^2. This results in a higher value of H_0 for the

slug test even when the object is submerged to equal depths for both the slug and bail tests.

Slug Test

The input data file for the NC7-25 slug test and output data for several time steps are presented in Appendix B. Figure 31 presents the output from the UNSAT2 simulation for aquifer hydraulic conductivities of 2.0×10^{-5} cm/sec, 3.0×10^{-5} cm/sec, and 4.0×10^{-5} cm/sec as solid lines. The field test data are represented by symbols. The curve corresponding to 2.0×10^{-5} cm/sec most closely matches the field data. The curve matching error is approximately 1.0×10^{-5} cm/sec.

A displacement tube was lowered into the well to cause the water level rise at the start of the slug test. The expected change in water level was calculated using the displacement tube dimensions and the final depth of the tube below the equilibrium water level. The calculated length H_0 is 237.7 cm (7.8 ft). The highest recorded rise in the well during testing was 149.7 cm (4.9 ft). The difference in calculated and observed slug length exists because the displacement tube is not instantaneously lowered into the well. The water level increased for a period of 8 seconds while the tube was
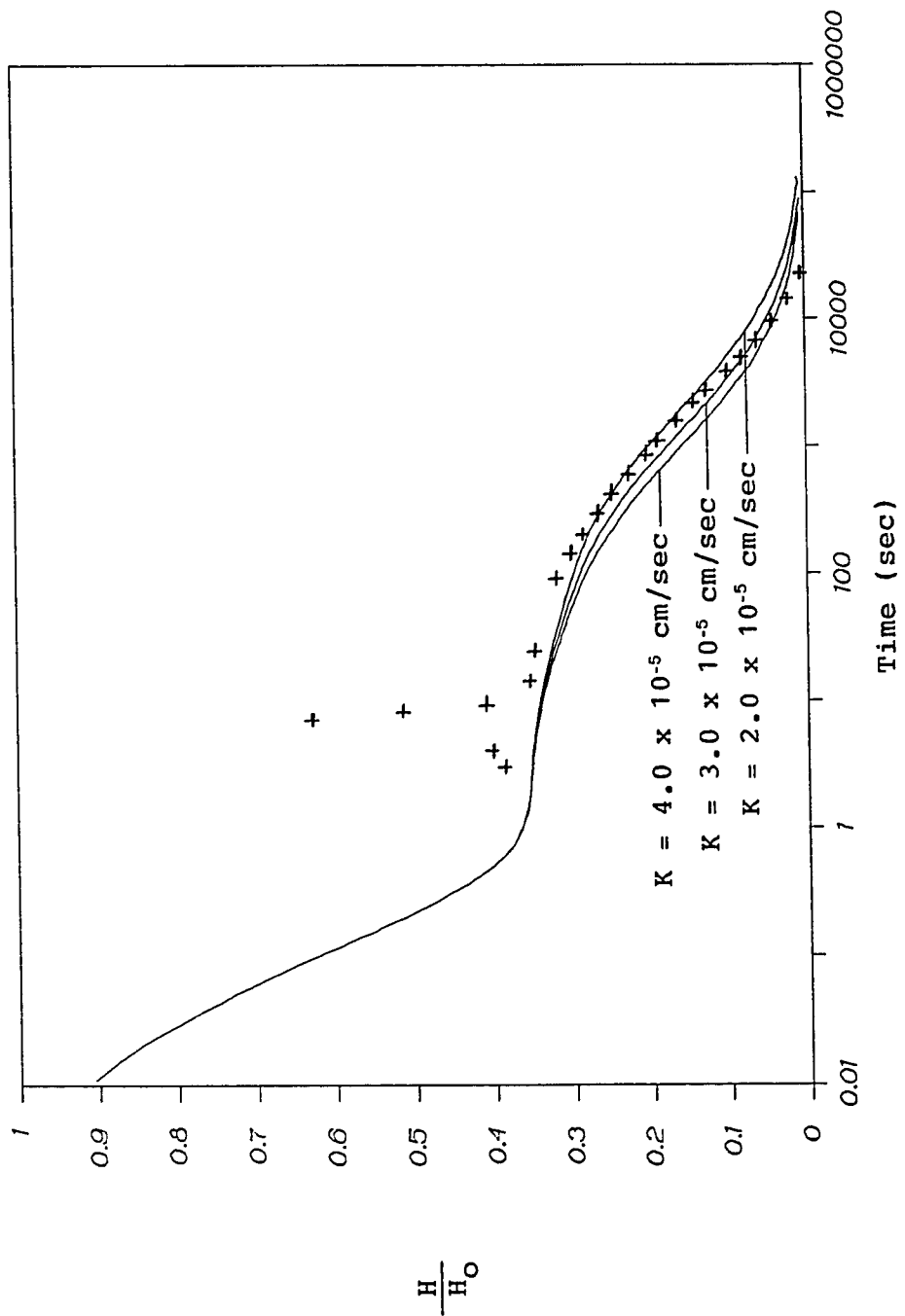
Figure 31. UNSAT2 simulation results for a slug test of Site 300 well NC7-25 shown by solid lines. Field slug test data are shown by symbols.

lowered into position. During this time, water was also draining into the sandpack in response to the increasing level in the well, and the full slug length was never reached in the well. Ideal slug test conditions were modeled with UNSAT2, so the full 237.7 cm slug length was used. The inertial effects of the water column cause some oscillating of the water level at the beginning of the test. The results match the field test data fairly closely from approximately 10 seconds, after oscillations of the water level have been damped. The first part of the UNSAT2 curves show a rapid sandpack response, within the first second of testing. The field data are unable to define the early portion of the curve because the water does not rise instantaneously in the well.

Bail Test

The input data file for the NC7-25 bail test and output data for several time steps are presented in Appendix B. Figure 32 presents the output from the UNSAT2 sumulation for aquifer hydraulic conductivities of 2.0×10^{-5} cm/sec, $3.0 \times 10\text{-}5$ cm/sec, and 4.0×10^{-5} cm/sec as solid lines. The field test data are represented by symbols. The curve corresponding to 3.0×10^{-5} cm/sec matches the field data fairly well
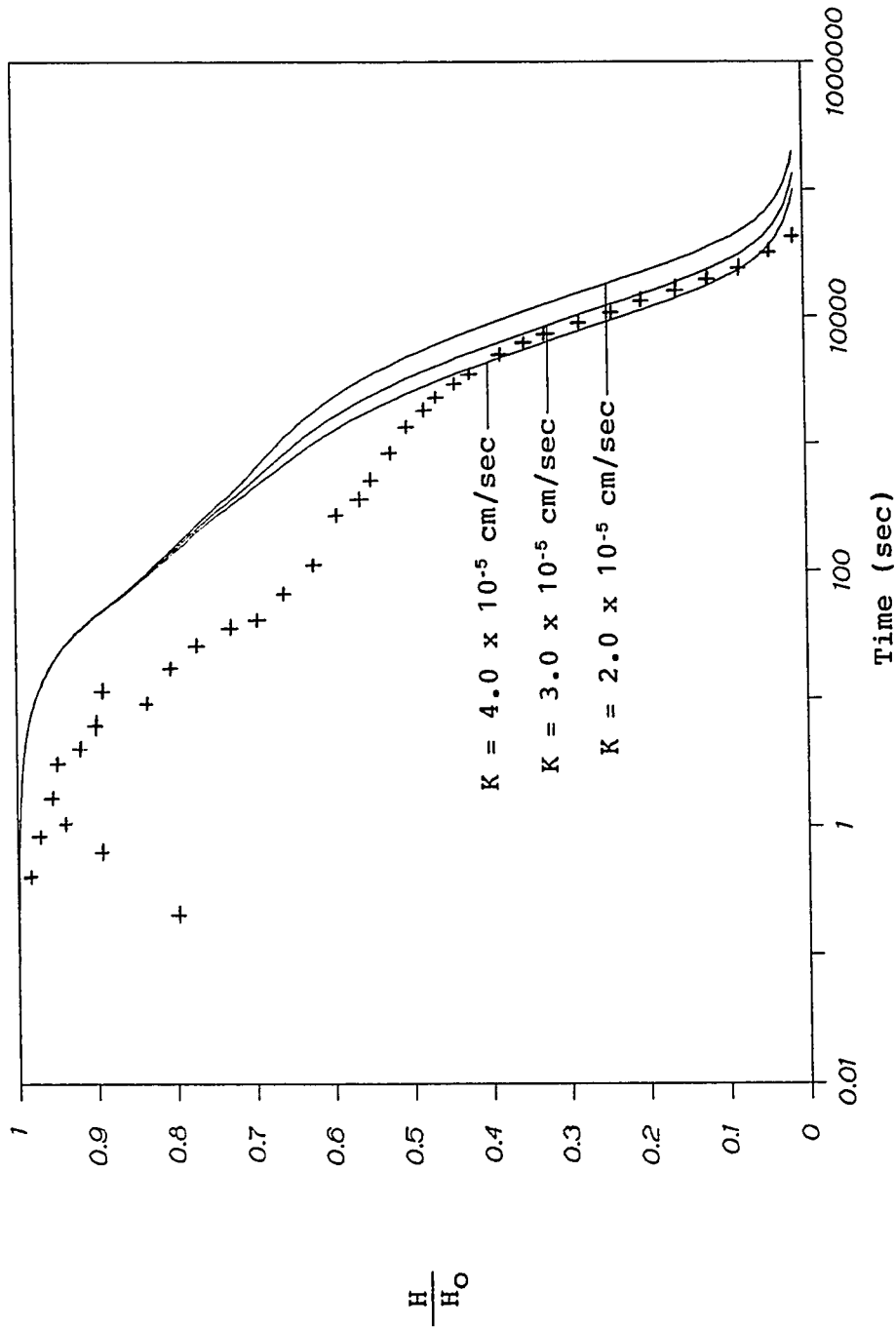
Figure 32. UNSAT2 simulation results for a bail test of Site 300 well NC7-25 shown by solid lines. Field bail test data are shown by symbols.

during the final part of recovery. The curve matching error is approximately 1.0×10^{-5} cm/sec.

A displacement tube was lowered into monitoring well NC7-25, and the water level was allowed to return to equilibrium level. The tube was then removed at the start of the bail test. The water level recovered slowly enough for the field data to define the beginning of the curve. The slug length of 123.8 cm (4.1 ft) was obtained from the field data for use in the test simulation because the initial depth of the displacement object was not available.

The first portion of the UNSAT2 curve shows a much slower recovery than the field data. This difference may be due to inaccurate representation of the unsaturated properties of the sandpack. The true unsaturated properties of the sandpack and aquifer can only be estimated because the subsurface conditions are not known in detail. The difference between the test data and the computer simulation output may also be due to the differences between the intended well geometry (used in UNSAT2 simulation input data) and the actual well geometry achieved during construction. Small differences in the well bore diameter and sandpack thickness greatly affect the initial relative recovery rate with the small dimensions of Site 300 wells.

<u>Well NC7-23</u>

Monitoring well NC7-23 is screened in clayey silt for approximately 152.4 cm (5 ft) with silty claystone in the bottom 152.4 cm (5 ft). Both a slug test and a bail test were performed on NC7-23 and modeled with UNSAT2. The program input data for UNSAT2 simulations are as follows: the saturated hydraulic conductivity of the sandpack is 0.01 cm/sec, the well diameter is 5.08 cm (2.0 in), the saturated aquifer thickness is 166.0 cm (65.4 in), the initial water displacement is 182.99 cm (72.0 in) for the slug test and 166.12 cm (65.4 in) for the bail test, the sandpack is 3.17 cm (1.25 in) thick radially, the porosity of the aquifer is 40%, the porosity of the sandpack is 30%, the unsaturated properties of the aquifer are as illustrated for siltstones and claystones on figure 12, and the unsaturated properties of the sandpack are illustrated on figure 13.

Slug Test

Figure 33 presents the output from the UNSAT2 simulation for aquifer hydraulic conductivities of 7.0×10^{-7} cm/sec, 1.0×10^{-6} cm/sec, and 2.0×10^{-6} cm/sec. The field test data are represented by symbols. The curve corresponding to 1.0×10^{-6} cm/sec
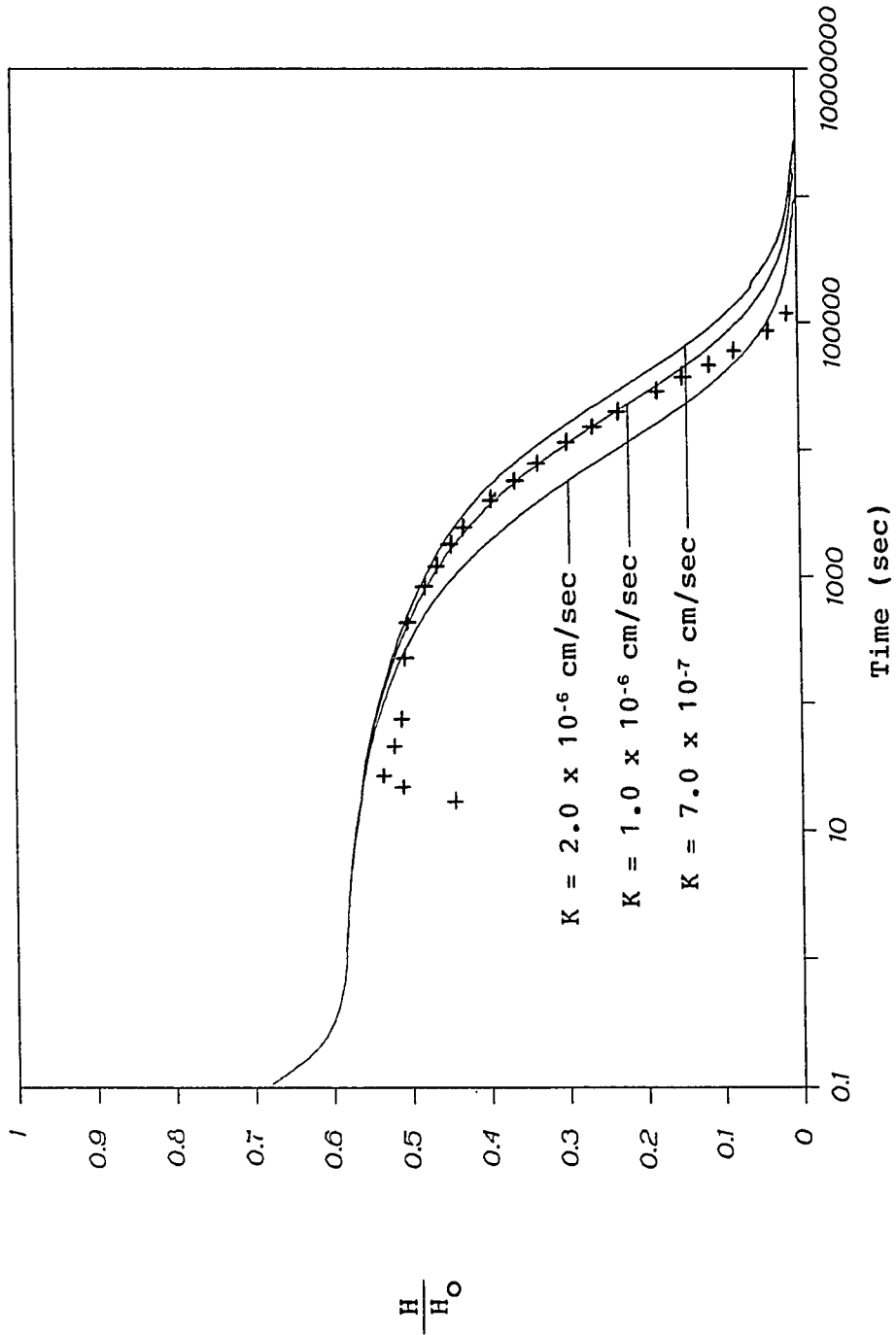
Figure 33. UNSAT2 simulation results for a slug test of Site 300 well NC7-23 shown by solid lines. Field slug test data are shown by symbols.

most closely matches the field data. The curve matching error is approximately 2.0×10^{-7} cm/sec.

Water was poured into the well to increase the water level at the start of the test. The field data show the water level in the well increasing for the first 30 seconds rather than instantaneously rising to the highest level. The injected water flows into the sandpack before the whole volume of slug water has been poured into the well, and the value of the slug length, H_0, is lost. The initial rise of the water table used for the simulation data input 182.99 cm (6 feet) was chosen so the break between the first and second portions of the curves is located at approximately the same level. The first part of the UNSAT2 curves shows a rapid sandpack response, within the first half second of testing.

Bail Test

Figure 34 presents the output from the UNSAT2 run for aquifer hydraulic conductivities of 1.0×10^{-6} cm/sec, 1.4×10^{-6} cm/sec, and 2.0×10^{-6} cm/sec. The field test data are represented by symbols. The field data overlap all three of the UNSAT2 curves, and an average of 1.5×10^{-6} cm/sec is chosen. The curve matching error is approximately 1.0×10^{-6} cm/sec.
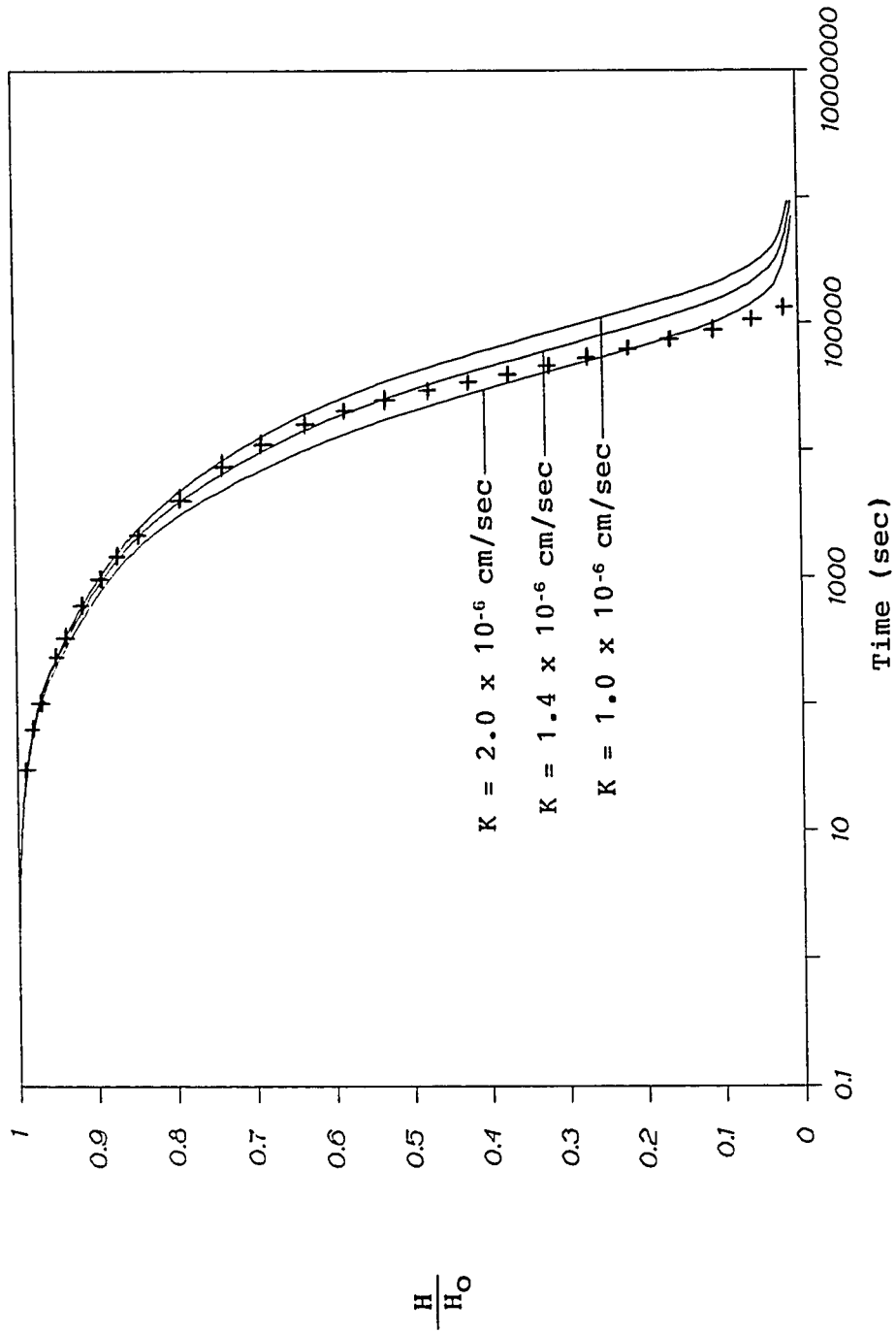
Figure 34. UNSAT2 simulation results for a bail test of Site 300 well NC7-23 shown by solid lines. Field bail test data are shown by symbols.

Well NC7-23 was manually bailed to dryness for the bail test. The sandpack was also drained during the bailing process due to the extremely fast response of the sand. The test is simulated with the initial conditions of a dry well, and a partially drained sandpack with negative pressure head values at each node equal to the elevation of the node above the datum (the bottom of the well). The aquifer is assumed to remain completely saturated during the bailing process. The sandpack response is not noticeable in either the field data or the UNSAT2 simulations because it is already drained at the starting time.

Well NC2-08

Monitoring well NC2-08 screens a zone composed of sandstone, siltstone, and claystone. Both a slug test and a bail test were performed on NC2-08 and modeled with UNSAT2. The program input data for UNSAT2 simulations are as follows: the saturated hydraulic conductivity of the sandpack is 0.01 cm/sec, the well diameter is 11.04 cm (4.35 in), the saturated aquifer thickness is 853.44 cm (336.0 in), the initial water displacement is 213.36 cm (84.0 in) for the slug test and 182.88 cm (72.0 in) for the bail test, the sandpack is 5.91 cm (2.33 in) thick radially, the porosity of the aquifer is 35%, the porosity

of the sandpack is 30%, the unsaturated properties of the
aquifer are as illustrated for sandstones on figure 12,
and the unsaturated properties of the sandpack are
illustrated on figure 13.

Slug Test

Figure 35 presents the output from the UNSAT2
simulation for aquifer hydraulic conductivities of
2.0×10^{-4} cm/sec, 3.0×10^{-4} cm/sec, 6.0×10^{-4} cm/sec,
and 1.0×10^{-3} cm/sec. The field test data are
represented by symbols. The field data overlap the curves
from 2.0×10^{-4} cm/sec to 6.0×10^{-4} cm/sec, and an
average of 4.0×10^{-4} cm/sec is chosen. The curve
matching error is approximately 2.0×10^{-4} cm/sec.

Water was poured into the well to raise the water
level at the start of the test. The water level
oscillates at the beginning of the test due to the inertia
of the water column. The field data stabilize at about
10 seconds, shortly after the break between the first and
second portions of the UNSAT2 curves. The first part of
the UNSAT2 curves show a rapid sandpack response, within
the first second of testing. The final portion of the
field test curve may recover at different rates because
the well screens a wide variety of earth material.
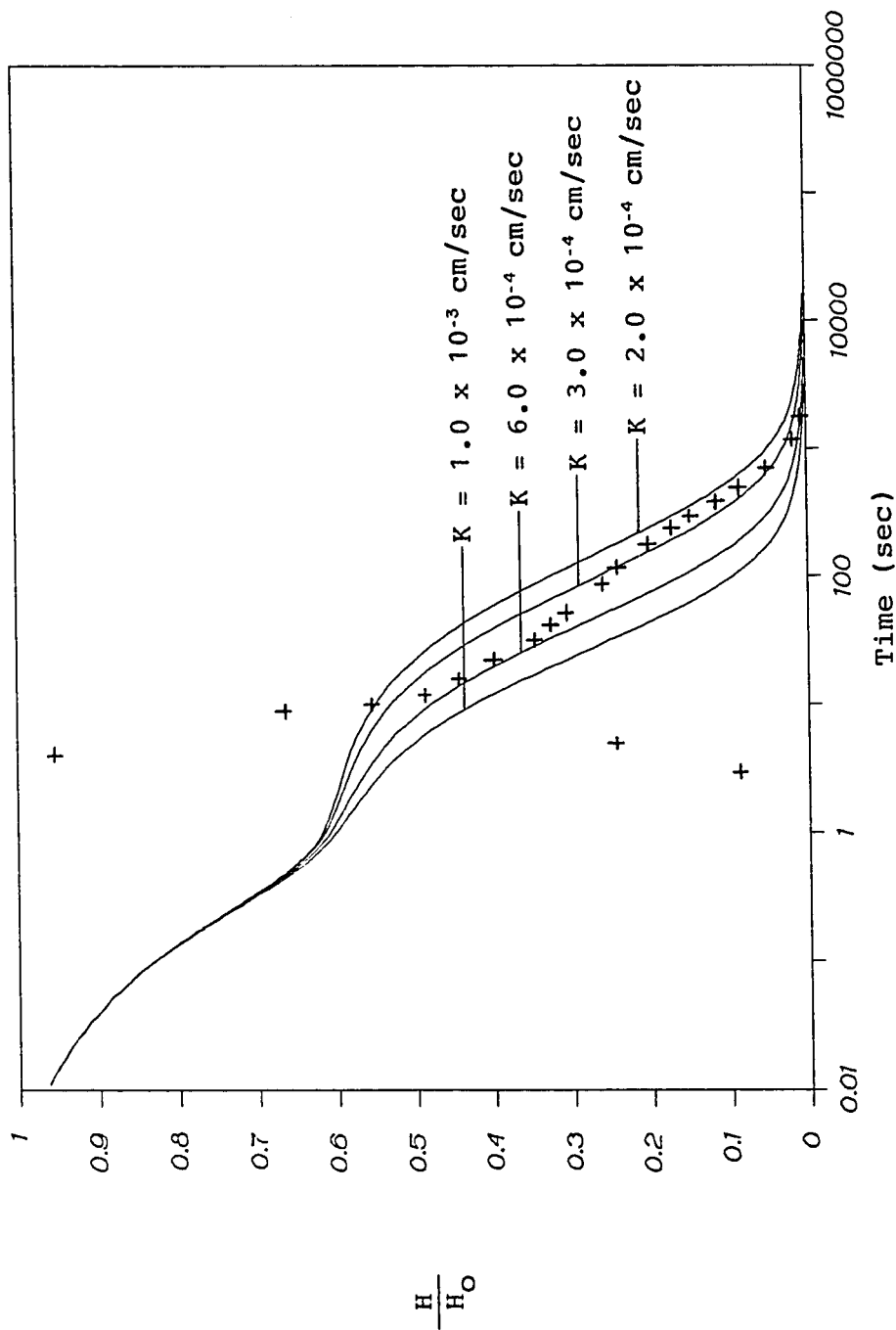
Figure 35. UNSAT2 simulation results for a slug test of Site 300 well NC2-08 shown by solid lines. Field slug test data are shown by symbols.

Bail Test

Figure 36 presents the output from the UNSAT2 run for aquifer hydraulic conductivities of 2.0 x 10^{-4} cm/sec, 3.0 x 10^{-4} cm/sec, 6.0 x 10^{-4} cm/sec, and 1.0 x 10^{-3} cm/sec. The field test data are represented by symbols. The field data overlap all four UNSAT2 curves, and an average of 5.0 x 10^{-4} cm/sec is chosen. The curve matching error is approximately 5.0 x 10^{-4} cm/sec.

Well NC2-08 was bailed manually, but not emptied. The bailing probably drained much of the sandpack before recovery data collection was started. The field data show a more defined break in the recovery curve between the initial and final portions than the UNSAT2 curves. This difference may be due to inaccurate estimation of the unsaturated properties of the sandpack for the UNSAT2 program or to the differences between the intended well geometry and the actual well geometry achieved during construction. As with the slug test for NC2-08, the final portion of the field curve may change in slope as the response of different portions of the aquifer dominate recovery.

Comparison With Analytical Methods

The results of the UNSAT2 slug and bail test simulations of Site 300 wells are compared with the
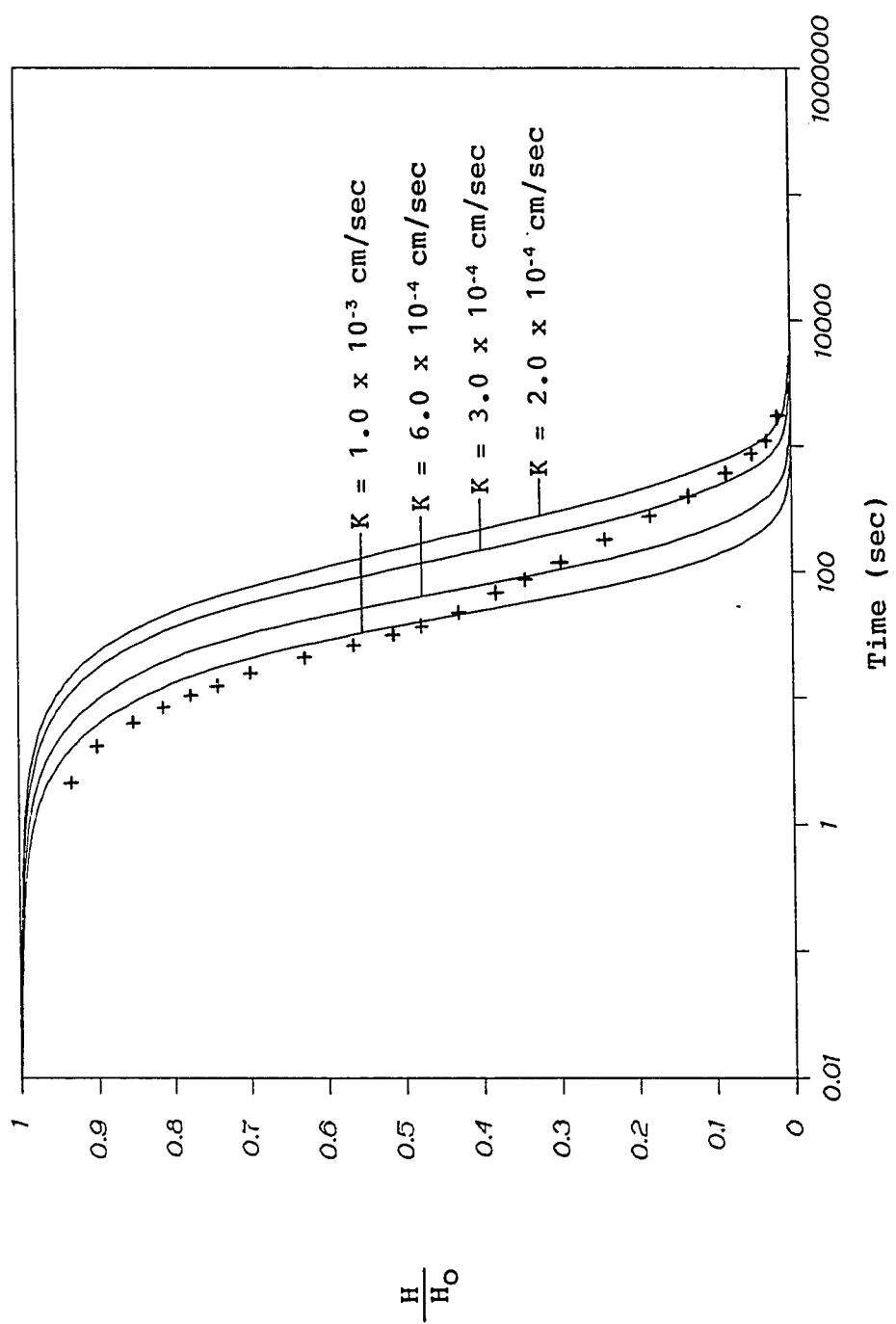
Figure 36. UNSAT2 simulation results for a bail test of Site 300 well NC2-08 shown by solid lines. Field bail test data are shown by symbols.

results of several analytical methods in table 1. The methods of Cooper et al. (1967), Hvorslev (1951), and Bouwer and Rice (1976) are included. Results from a modified version of each method are also listed, where the initial portion of the field data curves is graphically subtracted and the remaining aquifer response is rescaled. This modification uses approximately the last two thirds to half of the data and is intended to neglect the sandpack effects. The hydraulic conductivity values for the modified method of Cooper et al. (1967) are from Buddemeier et al. (1985 and 1986). The other values were calculated by the author of this paper and the variables used are listed in Appendix C. The modified well radius that accounts for the volume of pore space in the sandpack was used for all the analytical methods. The later field data points were weighted more heavily in drawing the curves for the methods of Hvorslev and Bouwer and Rice. The "Navy" method (1982) is not included because the method is based on the false assumption that the well recovery rate is constant with time, and a different hydraulic conductivity value will be calculated for each combination of data points chosen for the calculation.

The UNSAT2 results for slug and bail tests performed on the same well match closely for all three wells. The

UNSAT2 results are the same order of magnitude as two to three of the analytical results.

The results of Cooper et al. are generally higher, an order of magnitude in the most extreme case, than the hydraulic conductivities calculated by the other methods and determined by UNSAT2 curves. The Hvorslev method and the method of Bouwer and Rice result in values that generally agree with UNSAT2 simulations or that are slightly higher.

SUMMARY AND CONCLUSIONS

None of the existing analytical methods for
determining hydraulic conductivities from slug and bail
test data were developed for the specific type of well at
Site 300. The methods are modified slightly and used to
calculate hydraulic conductivities, but the results have
varied for Site 300 wells by up to two orders of magnitude
between the different methods (Buddemeier et al., 1985).
The tests were modeled using UNSAT2, a finite element
saturated-unsaturated flow computer program.

Two sample problems were simulated using UNSAT2 to
verify that the program accurately simulates well tests
for which analytical solutions are available for
comparison. The simulations include a slug test performed
in a confined aquifer, and a pump test in a confined
aquifer. The time steps between head calculations and the
dimensions of the finite element grid are verified as
sufficiently small to model slug and bail tests performed
on Site 300 wells.

A sensitivity analysis was performed by varying
different parameters, one at a time, and observing the
effect of the variations on the relative well recovery
curves generated by UNSAT2. Relative well recovery time
is indirectly proportional to the saturated hydraulic
conductivity for both the sandpack and the aquifer. The

sandpack dominated portion of the curve may be affected by the aquifer response and the aquifer dominated portion may be affected by the sandpack response. The greater the difference in hydraulic conductivity between the aquifer and sandpack, the greater these influences. This influence may lead to inaccurate aquifer hydraulic conductivity calculations.

The shape of the recovery curves varies slightly with different relative hydraulic conductivity relationships and pressure head relationships for the sandpack and aquifer. Relative well recovery time is proportional to the well diameter. Radial sandpack thickness affects the shape of the recovery curves. The early portion of the curve is more dominant for thicker sandpacks. The aquifer response is masked and shifted to the left by the sandpack response.

The well recovery time is inversely proportional to aquifer thickness. Variations in the length of the initial water level displacement in the well affect the shape of the relative recovery curves and shift the aquifer response slightly.

The results of the computer modeling were compared to the results of the analytical calculations. The UNSAT2 results generally match the results of the methods of Cooper et al. (1967), Hvorslev (1951), and Bouwer and Rice

(1976). The "Navy" method (1982) was not compared to the others because this method is based on the assumption that the well recovery rate is constant with time. The recovery rate actually decreases with time, and a different hydraulic conductivity value will be calculated for each combination of data points chosen for the calculation.

The method of Cooper et al. generally results in higher hydraulic conductivities than the other methods. The curve matching technique for the Cooper et al. curves and Site 300 data is imprecise because the field data does not form a single S-curve, but is a combination of two S-curves. Additionally, the shape of the combination curves is affected by the aquifer and sandpack parameters and well geometry. Relatively small shifts in the curve matching between Cooper et al. type curves (representing different storage coefficients) can lead to a wide range of calculated hydraulic conductivities. The choice of which type curve to use in matching the field data is difficult because of the effect of the sandpack response on the slope of the well recovery curve. It was shown in the sensitivity analysis that the presence of a sandpack can shift the portion of the recovery curve dominated by the aquifer to the left. This can lead to an artificially

small time match, and a value of hydraulic conductivity
that is too large.

There may be many reasons that the field test curves
do not match the UNSAT2 simulation curves exactly. The
assumptions that the aquifer and sandpack are homogeneous
and isotropic are not accurate, and probably contribute to
the error. Also, the wells are assumed to match the
engineered geometries when choosing input data. The
borehole is certainly not perfectly smooth, and the
sandpack is therefore not the exact engineered radial
thickness along the entire well casing. Imperfect input
data on the small scale of the well casing and sandpack
thickness may lead to relatively large errors in the
recovery curves. Other sources of uncertainty are the
unsaturated zones in the aquifer and sandpack. The
properties of these zones can not be determined by
in-place testing, so general curves from the literature
are used. Hysteresis is not considered by UNSAT2 and
average of the wetting and drying curves must be input.
The actual properties are probably variable, with average
values close to those used in UNSAT2 runs.

The analytical models provide hydraulic conductivity
values that are accurate to slightly high for the wells at
Site 300. The methods of Hvorslev and Bouwer and Rice
appear to provide the most accurate results as long as the

later field data points are weighted the most heavily when drawing recovery rate curves. The method of Cooper et al. may give artificially high hydraulic conductivity values because the effect of the sandpack on the aquifer response leads to inaccurate curve matching.

REFERENCES CITED

Bear, J., 1972, Dynamics of Fluids in Porous Media, American Elsevier Publishing Company, New York, 764 p.

Bouwer, H., 1989, The Bouwer and Rice Slug Test - An Update, Ground Water, v. 27, no. 3, p. 304-309.

Bouwer, H., and Rice, R.C., 1976, A Slug Test for Determining Hydraulic Conductivity of Unconfined Aquifers with Completely or Partially Penetrating Wells, Water Resource Research, v. 12, no. 3, p. 423-428.

Bouwer, H., and Rice, R.C., 1978, Delayed Aquifer Yield as a Phenomenon of Delayed Air Entry, Water Resource Research, v. 14, p. 1068-1074.

Brutsaert, W.F., Breitenbach, E.A., and Sunada, D.K., 1971, Computer Analysis of Free Surface Well Flow, Journal of Irrigation Division, American Society of Civil Engineers, v. 97(IR3), p. 405-420.

Buddemeier, R.W., Ruggieri, M.R., Carpenter, D.W., and Young, D.T., 1985, Investigation of Tritium in Groundwater at Site 300, Environmental Protection Investigations and Corrections Series, Lawrence Livermore National Laboratory, UCID-20600, 68 p.

Buddemeier, R.W., Ruggieri, M.R., and Oberdorder, J.A., 1986, Investigation of Tritium in Groundwater at Site 300, Environmental Protection Investigations and Corrections Series, Lawrence Livermore National Laboratory, 56 p.

Childs, E.C., 1969, An Introduction to the Physical Basis of Soil Water Phenomena, John Wiley and Sons, Ltd., New York, 493 p.

Cooley, R.L., 1971, A Finite Difference Method for Unsteady Flow in Variably Saturated Porous Media: Application to Single Pumping Well, Water Resource Research, v. 7, no. 6, p. 1607-1625.

Cooley, R.L., 1983, Some New Procedures for Numerical Solution of Variably Saturated Flow Problems, Water Resources Research, v. 19, no. 5, p. 1271-1285.

Cooper, H.H., and Jacob, C.E., 1946, A Generalized
    Graphical Method for Evaluating Formation Constants
    and Summarizing Well-Field History, Transactions,
    American Geophysical Union, v. 27, p. 526-534.

Cooper, H.H., Bredehoeft, J.D., and Papadopoulos, I.S.,
    1967, Response of a Finite-Diameter Well to an
    Instantaneous Charge of Water, Water Resources
    Research, v. 3, p. 263-269.

Davis, L.A., and Neuman, S.P., 1983, Documentation and
    User's Guide: UNSAT2 - Variably Saturated Flow Model
    (Including 4 Example Problems), Division of Waste
    Management, Office of Nuclear Material Safety and
    Safeguards, U.S. Nuclear Regulatory Commission,
    Washington, D.C., 206 p.

El-Kadi, A.I., and Brutsaert, W.F., 1986, Can Unsaturated
    Flow During Gravity Drainage be Represented by
    Boulton's Formulation, Water Resources Research,
    v. 22, no. 10, p. 1361-1366.

Fetter, C.W., 1980, Applied Hydrogeology, Charles E.
    Merrill Publishing Company, Columbus, Ohio, 488 p.

Freeze, R.A., and Cherry, J.A., 1979, Groundwater,
    Prentice-Hall, Englewood Clifts, 604 p.

Guitjens, J.C., and Luthin, J.N., 1971, Effect of Soil
    Moisture Hysteresis on the Water Table Profile Around
    a Gravity Well, Water Resources Research, v. 7,
    no. 2, p.334.

Hvorslev, M.J., 1951, Time Lag and Soil Permeability in
    Groundwater Observations, U.S.Army Corps of Engineers
    Waterways Exp. Sta., Bulletin 36, Vicksburg,
    Mississippi, 50 p.

Kirkham, D., 1945, Proposed Method for Field Measurement
    of Permeability of Soil Below the Water Table,
    Proc. Soil Science Society of America, v. 10,
    p. 58-68.

Klute, A., 1965a, Laboratory Measurement of Hydraulic
    Conductivity of Saturated Soil, Methods of Soil
    Analysis, Part 1, ed. C.A. Black, American Society of
    Agronomy, Madison, Wisconsin, p. 210-221.

Klute, A., 1965b, Water Capacity, Methods of Soil
    Analysis, Part 1, ed. C.A. Black, American Society of
    Agronomy, Madison, Wis., p. 273-278.

Klute, A., 1972, The Determination of the Hydraulic
    Conductivity and Diffusivity of Unsaturated Soils,
    Soil Science, v. 133, p. 264-276.

Luthin, J.N. and Kirkham, D., 1949, A Piezometer Method
    for Measuring Permeability of Soil in Situ Below a
    Water Table, Soil Science, v. 68, p. 349-358.

Morris, D.A. and Johnson, A.I., 1967, Summary of
    Hydrologic and Physical Properties of Rock and Soil
    Materials as Analyzed by the Hydrologic Laboratory of
    the U.S.Geological Survey 1948-1960, U.S. Geological
    Survey Water Supply Paper 1839-D.

Mualem, Y., 1967, A Catalogue of the Hydraulic Properties
    of Unsaturated Soils, Israel Institute of Technology,
    Haifa, Israel, 100 p.

Neuman, S.P., 1972, Theory of Flow in Unconfined Aquifers
    Considering Delayed Response of the Water Table,
    Water Resources Research, v. 8, no. 4, p. 1031-1045.

Neuman, S.P., 1973, Saturated-Unsaturated Seepage by
    Finite Elements, Proceedings of ASCE, Journal of
    Hydraulics Div., v. 99, no. HY12, p. 2233-2250.

Neuman, S.P., 1975a, Analysis of Pumping Test Data from
    Anisotropic Unconfined Aquifers Considering Delayed
    Gravity Response, Water Resources Research, v. 11,
    p. 329-342.

Neuman, S.P., 1975b, Galerkin Approach to Saturated-
    Unsaturated Flow in Porous Media, Ch. 10 in Finite
    Elements in Fluids, Vol. I: Viscous Flow and
    Hydrodynamics, edited by R.H. Gallagher, J.T. Oden,
    C. Taylor, and O.C. Zienkiewicz, John Wiley and Sons,
    London, p. 201-217.

Pinder, G.F. and Gray, W.G., 1977, Finite Element
    Simulation in Surface and Subsurface Hydrology,
    Academic Press, New York, 295 p.

Richards, L.A., 1965, Physical Condition of Water in Soil,
    Methods of Soil Analysis, Part 1, ed. C.A. Black,
    American Society of Agronomy, Madison, Wisconsin,
    p. 128-152.

Taylor, G.S., and Luthin, J.N., 1969, Computer Methods for Transient Analysis of Water Table Aquifers, Water Resources Research, v. 5, no. 1, p. 144-152.

Theim, G., 1906, Hydrologische Methoden, Gebhart, Leipzig, 56 p.

Theis, C.V., 1935, The Lowering of the Piezometric Surface and the Rate and Discharge of a Well Using Ground Water Storage, Transactions, American Geophysical Union, v. 16, p. 519-524.

U.S. Department of the Navy, 1982, Naval Facilities Engineering Command, Soil Mechanics Design Manual - 7.1, p. 103-108.

APPENDIX A.   INPUT AND OUTPUT FILES FOR VERIFICATION PROBLEMS

Table 2.   Input data file for slug test verification problem.

```
SLUG TEST - CONFINED AQUIFER
  205   25  191    1    1    0   30    1    0    0
    1    1   25    0   25    0    0    0    0
   13    8
    1    1
15.24     0.0       0.0       80.00     0.5
.1        100000.   1.1       100000.   0.1
1.0       0.1591549
0.01      0.01      0.35      .00164042
.028      .000001   .062      .0001     .10       .001      .15       .01
.175      0.03      0.2       .082      .225      .225      .25       .55
.275      .886      .2875     .963      .30       .992      .306      .997
.35       1.0
.028      200.0     .062      100.0     .085      80.0      .116      60.0
.178      40.0      .265      20.0      .306      10.0      .35       0.0
    1    2   15.24      0.0      80.00      0.0
   25    2   15.24     60.96     19.04      0.0
   26    0   16.51      0.0      65.00      0.0
   50    0   16.51     60.96      4.04      0.0
   51    0   17.78      0.0      65.00      0.0
   75    0   17.78     60.96      4.04      0.0
   76    0   19.68      0.0      65.00      0.0
  100    0   19.68     60.96      4.04      0.0
  101    0   22.23     ·0.0      65.00      0.0
  113    0   22.23     60.96      4.04      0.0
  114    0   26.04      0.0      65.00      0.0
  126    0   26.04     60.96      4.04      0.0
  127    0   31.75      0.0      65.00      0.0
  133    0   31.75     60.96      4.04      0.0
  134    0   40.33      0.0      65.00      0.0
  140    0   40.33     60.96      4.04      0.0
  141    0   53.19      0.0      65.00      0.0
  144    0   53.19     60.96      4.04      0.0
  145    0   72.47      0.0      65.00      0.0
  148    0   72.47     60.96      4.04      0.0
  149    0  101.40      0.0      65.00      0.0
  152    0  101.40     60.96      4.04      0.0
  153    0  144.86      0.0      65.00      0.0
  156    0  144.86     60.96      4.04      0.0
  157    0  194.35      0.0      65.00      0.0
  159    0  194.35     60.96      4.04      0.0
  160    0  243.84      0.0      65.00      0.0
  161    0  243.84     60.96      4.04      0.0
  162    0  304.80      0.0      65.00      0.0
  163    0  304.80     60.96      4.04      0.0
  164    0  441.96      0.0      65.00      0.0
  165    0  441.96     60.96      4.04      0.0
  166    0  579.12      0.0      65.00      0.0
  167    0  579.12     60.96      4.04      0.0
  168    0  784.86      0.0      65.00      0.0
  169    0  784.86     60.96      4.04      0.0
  170    0 1092.20      0.0      65.00      0.0
  171    0 1092.20     60.96      4.04      0.0
```

172	0	1554.48	0.0	65.00	0.0
173	0	1554.48	60.96	4.04	0.0
174	0	2247.90	0.0	65.00	0.0
175	0	2247.90	60.96	4.04	0.0
176	0	3286.76	0.0	65.00	0.0
177	0	3286.76	60.96	4.04	0.0
178	0	4845.05	0.0	65.00	0.0
179	0	4845.05	60.96	4.04	0.0
180	0	7180.58	0.0	65.00	0.0
181	0	7180.58	60.96	4.04	0.0
182	0	10681.97	0.0	65.00	0.0
183	0	10681.97	60.96	4.04	0.0
184	0	15932.15	0.0	65.00	0.0
185	0	15932.15	60.96	4.04	0.0
186	0	23807.42	0.0	65.00	0.0
187	0	23807.42	60.96	4.04	0.0
188	0	35618.42	0.0	65.00	0.0
189	0	35618.42	60.96	4.04	0.0
190	0	53334.92	0.0	65.00	0.0
191	0	53334.92	60.96	4.04	0.0
192	0	79909.67	0.0	65.00	0.0
193	0	79909.67	60.96	4.04	0.0
194	0	119769.89	0.0	65.00	0.0
195	0	119769.89	60.96	4.04	0.0
196	0	179560.22	0.0	65.00	0.0
197	0	179560.22	60.96	4.04	0.0
198	0	269243.81	0.0	65.00	0.0
199	0	269243.81	60.96	4.04	0.0
200	0	403767.29	0.0	65.00	0.0
201	0	403767.29	60.96	4.04	0.0
202	0	605552.51	0.0	65.00	0.0
203	0	605552.51	60.96	4.04	0.0
204	1	908230.34	0.0	65.00	0.0
205	1	908230.34	60.96	4.04	0.0

1	1	26	27	2	1	0.0
24	24	49	50	25	1	0.0
25	26	51	52	27	1	0.0
48	49	74	75	50	1	0.0
49	51	76	77	52	1	0.0
72	74	99	100	75	1	0.0
73	76	101	77	77	1	0.0
74	77	101	102	102	1	0.0
75	77	102	78	78	1	0.0
76	78	102	79	79	1	0.0
77	79	102	103	103	1	0.0
78	79	103	80	80	1	0.0
79	80	103	81	81	1	0.0
80	81	103	104	104	1	0.0
81	81	104	82	82	1	0.0
82	82	104	83	83	1	0.0
83	83	104	105	105	1	0.0
84	83	105	84	84	1	0.0
85	84	105	85	85	1	0.0
86	85	105	106	106	1	0.0
87	85	106	86	86	1	0.0
88	86	106	87	87	1	0.0
89	87	106	107	107	1	0.0
90	87	107	88	88	1	0.0
91	88	107	89	89	1	0.0
92	89	107	108	108	1	0.0
93	89	108	90	90	1	0.0
94	90	108	91	91	1	0.0
95	91	108	109	109	1	0.0
96	91	109	92	92	1	0.0
97	92	109	93	93	1	0.0

98	93	109	110	110	1	0.0
99	93	110	94	94	1	0.0
100	94	110	95	95	1	0.0
101	95	110	111	111	1	0.0
102	95	111	96	96	1	0.0
103	96	111	97	97	1	0.0
104	97	111	112	112	1	0.0
105	97	112	98	98	1	0.0
106	98	112	99	99	1	0.0
107	99	112	113	113	1	0.0
108	99	113	100	100	1	0.0
109	101	114	115	102	1	0.0
120	112	125	126	113	1	0.0
121	114	127	115	115	1	0.0
122	115	127	128	128	1	0.0
123	115	128	116	116	1	0.0
124	116	128	117	117	1	0.0
125	117	128	129	129	1	0.0
126	117	129	118	118	1	0.0
127	118	129	119	119	1	0.0
128	119	129	130	130	1	0.0
129	119	130	120	120	1	0.0
130	120	130	121	121	1	0.0
131	121	130	131	131	1	0.0
132	121	131	122	122	1	0.0
133	122	131	123	123	1	0.0
134	123	131	132	132	1	0.0
135	123	132	124	124	1	0.0
136	124	132	125	125	1	0.0
137	125	132	133	133	1	0.0
138	125	133	126	126	1	0.0
139	127	134	135	128	1	0.0
144	132	139	140	133	1	0.0
145	134	141	135	135	1	0.0
146	135	141	142	142	1	0.0
147	135	142	136	136	1	0.0
148	136	142	137	137	1	0.0
149	137	142	143	143	1	0.0
150	137	143	138	138	1	0.0
151	138	143	139	139	1	0.0
152	139	143	144	144	1	0.0
153	139	144	140	140	1	0.0
154	141	145	146	142	1	0.0
156	143	147	148	144	1	0.0
157	145	149	150	146	1	0.0
159	147	151	152	148	1	0.0
160	149	153	154	150	1	0.0
162	151	155	156	152	1	0.0
163	153	157	158	154	1	0.0
164	154	158	155	155	1	0.0
165	155	158	159	159	1	0.0
166	155	159	156	156	1	0.0
167	157	160	158	158	1	0.0
168	158	160	161	161	1	0.0
169	158	161	159	159	1	0.0
170	160	162	163	161	1	0.0
171	162	164	165	163	1	0.0
172	164	166	167	165	1	0.0
173	166	168	169	167	1	0.0
174	168	170	171	169	1	0.0
175	170	172	173	171	1	0.0
176	172	174	175	173	1	0.0
177	174	176	177	175	1	0.0
178	176	178	179	177	1	0.0
179	178	180	181	179	1	0.0

```
180  180  182  183  181    1      0.0
181  182  184  185  183    1      0.0
182  184  186  187  185    1      0.0
183  186  188  189  187    1      0.0
184  188  190  191  189    1      0.0
185  190  192  193  191    1      0.0
186  192  194  195  193    1      0.0
187  194  196  197  195    1      0.0
188  196  198  199  197    1      0.0
189  198  200  201  199    1      0.0
190  200  202  203  201    1      0.0
191  202  204  205  203    1      0.0
END
```

Table 3. Output from UNSAT2 for slug test verification problem, for time step = 10, 50, and 75.

TIME =   .15937E+01   TIME STEP = 10

MAX CHANGE IN PRESS HEAD DURING ITERATION 2 WAS   .67141E-02 AT NODE   25

CUMULATIVE INFLOW INTO SYSTEM IS =   .44989E+03
DISCHARGE FROM WELL = 0.
WATER LEVEL IN WELL =   .79462E+02

O NODE	HEAD	PRESS HEAD	DISCHARGE	NODE	HEAD	PRESS HEAD	DISCHARGE
1	.795E+02	.795E+02	.387E+01	2	.795E+02	.769E+02	.767E+01
3	.795E+02	.744E+02	.763E+01	4	.795E+02	.718E+02	.766E+01
5	.795E+02	.693E+02	.763E+01	6	.795E+02	.668E+02	.766E+01
7	.795E+02	.642E+02	.763E+01	8	.795E+02	.617E+02	.766E+01
9	.795E+02	.591E+02	.763E+01	10	.795E+02	.566E+02	.766E+01
11	.795E+02	.541E+02	.763E+01	12	.795E+02	.515E+02	.766E+01
13	.795E+02	.490E+02	.763E+01	14	.795E+02	.464E+02	.766E+01
15	.795E+02	.439E+02	.763E+01	16	.795E+02	.414E+02	.766E+01
17	.795E+02	.388E+02	.763E+01	18	.795E+02	.363E+02	.766E+01
19	.795E+02	.337E+02	.763E+01	20	.795E+02	.312E+02	.766E+01
21	.795E+02	.287E+02	.763E+01	22	.795E+02	.261E+02	.766E+01
23	.795E+02	.236E+02	.762E+01	24	.795E+02	.210E+02	.765E+01
25	.795E+02	.185E+02	.376E+01	26	.756E+02	.756E+02	0.
27	.756E+02	.731E+02	0.	28	.756E+02	.706E+02	0.
29	.756E+02	.680E+02	0.	30	.756E+02	.655E+02	0.
31	.756E+02	.629E+02	0.	32	.756E+02	.604E+02	0.
33	.756E+02	.578E+02	0.	34	.756E+02	.553E+02	0.
35	.756E+02	.528E+02	0.	36	.756E+02	.502E+02	0.
37	.756E+02	.477E+02	0.	38	.756E+02	.452E+02	0.
39	.756E+02	.426E+02	0.	40	.756E+02	.401E+02	0.
41	.756E+02	.375E+02	0.	42	.756E+02	.350E+02	0.
43	.756E+02	.324E+02	0.	44	.756E+02	.299E+02	0.
45	.756E+02	.274E+02	0.	46	.756E+02	.248E+02	0.
47	.756E+02	.223E+02	0.	48	.756E+02	.198E+02	0.
49	.756E+02	.172E+02	0.	50	.756E+02	.147E+02	0.
51	.724E+02	.724E+02	0.	52	.723E+02	.698E+02	0.
53	.724E+02	.673E+02	0.	54	.723E+02	.647E+02	0.
55	.724E+02	.622E+02	0.	56	.723E+02	.596E+02	0.
57	.724E+02	.571E+02	0.	58	.723E+02	.545E+02	0.
59	.724E+02	.520E+02	0.	60	.723E+02	.495E+02	0.
61	.724E+02	.470E+02	0.	62	.723E+02	.444E+02	0.
63	.724E+02	.419E+02	0.	64	.723E+02	.393E+02	0.
65	.724E+02	.368E+02	0.	66	.723E+02	.342E+02	0.
67	.724E+02	.317E+02	0.	68	.723E+02	.291E+02	0.
69	.724E+02	.266E+02	0.	70	.723E+02	.241E+02	0.
71	.724E+02	.216E+02	0.	72	.723E+02	.190E+02	0.
73	.724E+02	.165E+02	0.	74	.723E+02	.139E+02	0.
75	.724E+02	.114E+02	0.	76	.689E+02	.689E+02	0.
77	.687E+02	.661E+02	0.	78	.688E+02	.638E+02	0.
79	.687E+02	.610E+02	0.	80	.688E+02	.587E+02	0.
81	.687E+02	.560E+02	0.	82	.688E+02	.536E+02	0.
83	.687E+02	.509E+02	0.	84	.688E+02	.485E+02	0.
85	.687E+02	.458E+02	0.	86	.688E+02	.434E+02	0.
87	.687E+02	.407E+02	0.	88	.688E+02	.384E+02	0.
89	.687E+02	.356E+02	0.	90	.688E+02	.333E+02	0.
91	.687E+02	.306E+02	0.	92	.688E+02	.282E+02	0.
93	.687E+02	.255E+02	0.	94	.688E+02	.231E+02	0.

95	.687E+02	.204E+02	0.	96	.688E+02	.180E+02	0.
97	.687E+02	.153E+02	0.	98	.688E+02	.130E+02	0.
99	.687E+02	.102E+02	0.	100	.688E+02	.783E+01	0.
101	.661E+02	.661E+02	0.	102	.662E+02	.612E+02	0.
103	.663E+02	.561E+02	0.	104	.662E+02	.510E+02	0.
105	.663E+02	.459E+02	0.	106	.662E+02	.408E+02	0.
107	.663E+02	.358E+02	0.	108	.662E+02	.307E+02	0.
109	.663E+02	.256E+02	0.	110	.662E+02	.205E+02	0.
111	.663E+02	.155E+02	0.	112	.663E+02	.104E+02	0.
113	.664E+02	.542E+01	0.	114	.652E+02	.652E+02	0.
115	.652E+02	.601E+02	0.	116	.652E+02	.551E+02	0.
117	.652E+02	.499E+02	0.	118	.652E+02	.449E+02	0.
119	.652E+02	.398E+02	0.	120	.652E+02	.347E+02	0.
121	.652E+02	.296E+02	0.	122	.652E+02	.246E+02	0.
123	.652E+02	.195E+02	0.	124	.652E+02	.144E+02	0.
125	.652E+02	.930E+01	0.	126	.652E+02	.426E+01	0.
127	.650E+02	.650E+02	0.	128	.650E+02	.549E+02	0.
129	.650E+02	.447E+02	0.	130	.650E+02	.345E+02	0.
131	.650E+02	.244E+02	0.	132	.650E+02	.142E+02	0.
133	.650E+02	.406E+01	0.	134	.650E+02	.650E+02	0.
135	.650E+02	.548E+02	0.	136	.650E+02	.447E+02	0.
137	.650E+02	.345E+02	0.	138	.650E+02	.244E+02	0.
139	.650E+02	.142E+02	0.	140	.650E+02	.404E+01	0.
141	.650E+02	.650E+02	0.	142	.650E+02	.447E+02	0.
143	.650E+02	.244E+02	0.	144	.650E+02	.404E+01	0.
145	.650E+02	.650E+02	0.	146	.650E+02	.447E+02	0.
147	.650E+02	.244E+02	0.	148	.650E+02	.404E+01	0.
149	.650E+02	.650E+02	0.	150	.650E+02	.447E+02	0.
151	.650E+02	.244E+02	0.	152	.650E+02	.404E+01	0.
153	.650E+02	.650E+02	0.	154	.650E+02	.447E+02	0.
155	.650E+02	.244E+02	0.	156	.650E+02	.404E+01	0.
157	.650E+02	.650E+02	0.	158	.650E+02	.345E+02	0.
159	.650E+02	.404E+01	0.	160	.650E+02	.650E+02	0.
161	.650E+02	.404E+01	0.	162	.650E+02	.650E+02	0.
163	.650E+02	.404E+01	0.	164	.650E+02	.650E+02	0.
165	.650E+02	.404E+01	0.	166	.650E+02	.650E+02	0.
167	.650E+02	.404E+01	0.	168	.650E+02	.650E+02	0.
169	.650E+02	.404E+01	0.	170	.650E+02	.650E+02	0.
171	.650E+02	.404E+01	0.	172	.650E+02	.650E+02	0.
173	.650E+02	.404E+01	0.	174	.650E+02	.650E+02	0.
175	.650E+02	.404E+01	0.	176	.650E+02	.650E+02	0.
177	.650E+02	.404E+01	0.	178	.650E+02	.650E+02	0.
179	.650E+02	.404E+01	0.	180	.650E+02	.650E+02	0.
181	.650E+02	.404E+01	0.	182	.650E+02	.650E+02	0.
183	.650E+02	.404E+01	0.	184	.650E+02	.650E+02	0.
185	.650E+02	.404E+01	0.	186	.650E+02	.650E+02	0.
187	.650E+02	.404E+01	0.	188	.650E+02	.650E+02	0.
189	.650E+02	.404E+01	0.	190	.650E+02	.650E+02	0.
191	.650E+02	.404E+01	0.	192	.650E+02	.650E+02	0.
193	.650E+02	.404E+01	0.	194	.650E+02	.650E+02	0.
195	.650E+02	.404E+01	0.	196	.650E+02	.650E+02	0.
197	.650E+02	.404E+01	0.	198	.650E+02	.650E+02	0.
199	.650E+02	.404E+01	0.	200	.650E+02	.650E+02	0.
201	.650E+02	.404E+01	0.	202	.650E+02	.650E+02	0.
203	.650E+02	.404E+01	0.	204	.650E+02	.650E+02	-.111E-03
205	.650E+02	.404E+01	.321E-04	0	0.	0.	0.

MOISTURE CONTENT AT UNSATURATED NODES CORRESPONDING TO MATERIAL   1

    0 0.   0 0.   0 0.

TIME = .11639E+03   TIME STEP = 50

MAX CHANGE IN PRESS HEAD DURING ITERATION 2 WAS   .63989E-01 AT NODE   50

CUMULATIVE INFLOW INTO SYSTEM IS =   .49353E+04
DISCHARGE FROM WELL = 0.
WATER LEVEL IN WELL =   .73897E+02

O NODE	HEAD	PRESS HEAD	DISCHARGE	NODE	HEAD	PRESS HEAD	DISCHARGE
1	.739E+02	.739E+02	.437E+00	2	.739E+02	.714E+02	.865E+00
3	.739E+02	.688E+02	.864E+00	4	.739E+02	.663E+02	.864E+00
5	.739E+02	.637E+02	.862E+00	6	.739E+02	.612E+02	.862E+00
7	.739E+02	.587E+02	.861E+00	8	.739E+02	.561E+02	.861E+00
9	.739E+02	.536E+02	.859E+00	10	.739E+02	.510E+02	.859E+00
11	.739E+02	.485E+02	.858E+00	12	.739E+02	.460E+02	.858E+00
13	.739E+02	.434E+02	.857E+00	14	.739E+02	.409E+02	.857E+00
15	.739E+02	.383E+02	.855E+00	16	.739E+02	.358E+02	.855E+00
17	.739E+02	.333E+02	.854E+00	18	.739E+02	.307E+02	.854E+00
19	.739E+02	.282E+02	.853E+00	20	.739E+02	.256E+02	.853E+00
21	.739E+02	.231E+02	.851E+00	22	.739E+02	.206E+02	.851E+00
23	.739E+02	.180E+02	.850E+00	24	.739E+02	.155E+02	.850E+00
25	.739E+02	.129E+02	.419E+00	26	.735E+02	.735E+02	0.
27	.735E+02	.710E+02	0.	28	.735E+02	.684E+02	0.
29	.735E+02	.659E+02	0.	30	.735E+02	.633E+02	0.
31	.735E+02	.608E+02	0.	32	.735E+02	.583E+02	0.
33	.735E+02	.557E+02	0.	34	.735E+02	.532E+02	0.
35	.735E+02	.506E+02	0.	36	.735E+02	.481E+02	0.
37	.735E+02	.456E+02	0.	38	.735E+02	.430E+02	0.
39	.735E+02	.405E+02	0.	40	.735E+02	.379E+02	0.
41	.735E+02	.354E+02	0.	42	.735E+02	.329E+02	0.
43	.735E+02	.303E+02	0.	44	.735E+02	.278E+02	0.
45	.735E+02	.252E+02	0.	46	.735E+02	.227E+02	0.
47	.735E+02	.202E+02	0.	48	.735E+02	.176E+02	0.
49	.735E+02	.151E+02	0.	50	.735E+02	.125E+02	0.
51	.731E+02	.731E+02	0.	52	.731E+02	.705E+02	0.
53	.731E+02	.680E+02	0.	54	.731E+02	.655E+02	0.
55	.731E+02	.629E+02	0.	56	.731E+02	.604E+02	0.
57	.731E+02	.579E+02	0.	58	.731E+02	.553E+02	0.
59	.731E+02	.528E+02	0.	60	.731E+02	.502E+02	0.
61	.731E+02	.477E+02	0.	62	.731E+02	.452E+02	0.
63	.731E+02	.426E+02	0.	64	.731E+02	.401E+02	0.
65	.731E+02	.375E+02	0.	66	.731E+02	.350E+02	0.
67	.731E+02	.325E+02	0.	68	.731E+02	.299E+02	0.
69	.731E+02	.274E+02	0.	70	.731E+02	.248E+02	0.
71	.731E+02	.223E+02	0.	72	.731E+02	.198E+02	0.
73	.731E+02	.172E+02	0.	74	.731E+02	.147E+02	0.
75	.731E+02	.121E+02	0.	76	.725E+02	.725E+02	0.
77	.725E+02	.700E+02	0.	78	.725E+02	.674E+02	0.
79	.725E+02	.649E+02	0.	80	.725E+02	.624E+02	0.
81	.725E+02	.598E+02	0.	82	.725E+02	.573E+02	0.
83	.725E+02	.547E+02	0.	84	.725E+02	.522E+02	0.
85	.725E+02	.497E+02	0.	86	.725E+02	.471E+02	0.
87	.725E+02	.446E+02	0.	88	.725E+02	.421E+02	0.
89	.725E+02	.395E+02	0.	90	.725E+02	.370E+02	0.
91	.725E+02	.344E+02	0.	92	.725E+02	.319E+02	0.
93	.725E+02	.294E+02	0.	94	.725E+02	.268E+02	0.
95	.725E+02	.243E+02	0.	96	.725E+02	.217E+02	0.
97	.725E+02	.192E+02	0.	98	.725E+02	.167E+02	0.
99	.725E+02	.141E+02	0.	100	.725E+02	.116E+02	0.
101	.718E+02	.718E+02	0.	102	.718E+02	.667E+02	0.
103	.718E+02	.617E+02	0.	104	.718E+02	.566E+02	0.
105	.718E+02	.515E+02	0.	106	.718E+02	.464E+02	0.
107	.718E+02	.414E+02	0.	108	.718E+02	.363E+02	0.

109	.719E+02	.312E+02	0.	110	.718E+02	.261E+02	0.
111	.719E+02	.211E+02	0.	112	.719E+02	.160E+02	0.
113	.719E+02	.109E+02	0.	114	.709E+02	.709E+02	0.
115	.709E+02	.658E+02	0.	116	.709E+02	.607E+02	0.
117	.709E+02	.557E+02	0.	118	.709E+02	.506E+02	0.
119	.709E+02	.455E+02	0.	120	.709E+02	.404E+02	0.
121	.709E+02	.354E+02	0.	122	.709E+02	.303E+02	0.
123	.709E+02	.252E+02	0.	124	.709E+02	.201E+02	0.
125	.709E+02	.151E+02	0.	126	.710E+02	.999E+01	0.
127	.697E+02	.697E+02	0.	128	.697E+02	.596E+02	0.
129	.697E+02	.494E+02	0.	130	.697E+02	.393E+02	0.
131	.698E+02	.291E+02	0.	132	.698E+02	.190E+02	0.
133	.698E+02	.883E+01	0.	134	.683E+02	.683E+02	0.
135	.683E+02	.581E+02	0.	136	.683E+02	.480E+02	0.
137	.683E+02	.378E+02	0.	138	.684E+02	.277E+02	0.
139	.683E+02	.175E+02	0.	140	.684E+02	.741E+01	0.
141	.667E+02	.667E+02	0.	142	.668E+02	.465E+02	0.
143	.668E+02	.262E+02	0.	144	.669E+02	.595E+01	0.
145	.656E+02	.656E+02	0.	146	.656E+02	.453E+02	0.
147	.656E+02	.250E+02	0.	148	.657E+02	.471E+01	0.
149	.651E+02	.651E+02	0.	150	.651E+02	.448E+02	0.
151	.651E+02	.245E+02	0.	152	.651E+02	.415E+01	0.
153	.650E+02	.650E+02	0.	154	.650E+02	.447E+02	0.
155	.650E+02	.244E+02	0.	156	.650E+02	.405E+01	0.
157	.650E+02	.650E+02	0.	158	.650E+02	.345E+02	0.
159	.650E+02	.404E+01	0.	160	.650E+02	.650E+02	0.
161	.650E+02	.404E+01	0.	162	.650E+02	.650E+02	0.
163	.650E+02	.404E+01	0.	164	.650E+02	.650E+02	0.
165	.650E+02	.404E+01	0.	166	.650E+02	.650E+02	0.
167	.650E+02	.404E+01	0.	168	.650E+02	.650E+02	0.
169	.650E+02	.404E+01	0.	170	.650E+02	.650E+02	0.
171	.650E+02	.404E+01	0.	172	.650E+02	.650E+02	0.
173	.650E+02	.404E+01	0.	174	.650E+02	.650E+02	0.
175	.650E+02	.404E+01	0.	176	.650E+02	.650E+02	0.
177	.650E+02	.404E+01	0.	178	.650E+02	.650E+02	0.
179	.650E+02	.404E+01	0.	180	.650E+02	.650E+02	0.
181	.650E+02	.404E+01	0.	182	.650E+02	.650E+02	0.
183	.650E+02	.404E+01	0.	184	.650E+02	.650E+02	0.
185	.650E+02	.404E+01	0.	186	.650E+02	.650E+02	0.
187	.650E+02	.404E+01	0.	188	.650E+02	.650E+02	0.
189	.650E+02	.404E+01	0.	190	.650E+02	.650E+02	0.
191	.650E+02	.404E+01	0.	192	.650E+02	.650E+02	0.
193	.650E+02	.404E+01	0.	194	.650E+02	.650E+02	0.
195	.650E+02	.404E+01	0.	196	.650E+02	.650E+02	0.
197	.650E+02	.404E+01	0.	198	.650E+02	.650E+02	0.
199	.650E+02	.404E+01	0.	200	.650E+02	.650E+02	0.
201	.650E+02	.404E+01	0.	202	.650E+02	.650E+02	0.
203	.650E+02	.404E+01	0.	204	.650E+02	.650E+02	-.111E-03
205	.650E+02	.404E+01	.321E-04	0	0.	0.	0.

MOISTURE CONTENT AT UNSATURATED NODES CORRESPONDING TO MATERIAL 1

　　0　0.　　　　　　0　0.　　　　　　0　0.

TIME = .12709E+04　　TIME STEP = 75

MAX CHANGE IN PRESS HEAD DURING ITERATION 2 WAS .49665E-01 AT NODE 50

CUMULATIVE INFLOW INTO SYSTEM IS = .10413E+05
DISCHARGE FROM WELL = 0.
WATER LEVEL IN WELL = .66759E+02

O NODE	HEAD	PRESS HEAD	DISCHARGE	NODE	HEAD	PRESS HEAD	DISCHARGE
1	.668E+02	.668E+02	.243E-01	2	.668E+02	.642E+02	.481E-01
3	.668E+02	.617E+02	.481E-01	4	.668E+02	.591E+02	.481E-01
5	.668E+02	.566E+02	.481E-01	6	.668E+02	.541E+02	.481E-01
7	.668E+02	.515E+02	.481E-01	8	.668E+02	.490E+02	.481E-01
9	.668E+02	.464E+02	.481E-01	10	.668E+02	.439E+02	.481E-01
11	.668E+02	.414E+02	.481E-01	12	.668E+02	.388E+02	.481E-01
13	.668E+02	.363E+02	.481E-01	14	.668E+02	.337E+02	.481E-01
15	.668E+02	.312E+02	.481E-01	16	.668E+02	.287E+02	.481E-01
17	.668E+02	.261E+02	.481E-01	18	.668E+02	.236E+02	.481E-01
19	.668E+02	.210E+02	.481E-01	20	.668E+02	.185E+02	.481E-01
21	.668E+02	.160E+02	.481E-01	22	.668E+02	.134E+02	.481E-01
23	.668E+02	.109E+02	.481E-01	24	.668E+02	.834E+01	.481E-01
25	.668E+02	.580E+01	.237E-01	26	.668E+02	.668E+02	0.
27	.668E+02	.642E+02	0.	28	.668E+02	.617E+02	0.
29	.668E+02	.591E+02	0.	30	.668E+02	.566E+02	0.
31	.668E+02	.541E+02	0.	32	.668E+02	.515E+02	0.
33	.668E+02	.490E+02	0.	34	.668E+02	.464E+02	0.
35	.668E+02	.439E+02	0.	36	.668E+02	.414E+02	0.
37	.668E+02	.388E+02	0.	38	.668E+02	.363E+02	0.
39	.668E+02	.337E+02	0.	40	.668E+02	.312E+02	0.
41	.668E+02	.287E+02	0.	42	.668E+02	.261E+02	0.
43	.668E+02	.236E+02	0.	44	.668E+02	.210E+02	0.
45	.668E+02	.185E+02	0.	46	.668E+02	.160E+02	0.
47	.668E+02	.134E+02	0.	48	.668E+02	.109E+02	0.
49	.668E+02	.833E+01	0.	50	.668E+02	.579E+01	0.
51	.667E+02	.667E+02	0.	52	.667E+02	.642E+02	0.
53	.667E+02	.616E+02	0.	54	.667E+02	.591E+02	0.
55	.667E+02	.566E+02	0.	56	.667E+02	.540E+02	0.
57	.667E+02	.515E+02	0.	58	.667E+02	.489E+02	0.
59	.667E+02	.464E+02	0.	60	.667E+02	.439E+02	0.
61	.667E+02	.413E+02	0.	62	.667E+02	.388E+02	0.
63	.667E+02	.362E+02	0.	64	.667E+02	.337E+02	0.
65	.667E+02	.312E+02	0.	66	.667E+02	.286E+02	0.
67	.667E+02	.261E+02	0.	68	.667E+02	.235E+02	0.
69	.667E+02	.210E+02	0.	70	.667E+02	.185E+02	0.
71	.667E+02	.159E+02	0.	72	.667E+02	.134E+02	0.
73	.667E+02	.108E+02	0.	74	.667E+02	.831E+01	0.
75	.667E+02	.577E+01	0.	76	.667E+02	.667E+02	0.
77	.667E+02	.642E+02	0.	78	.667E+02	.616E+02	0.
79	.667E+02	.591E+02	0.	80	.667E+02	.565E+02	0.
81	.667E+02	.540E+02	0.	82	.667E+02	.515E+02	0.
83	.667E+02	.489E+02	0.	84	.667E+02	.464E+02	0.
85	.667E+02	.438E+02	0.	86	.667E+02	.413E+02	0.
87	.667E+02	.388E+02	0.	88	.667E+02	.362E+02	0.
89	.667E+02	.337E+02	0.	90	.667E+02	.311E+02	0.
91	.667E+02	.286E+02	0.	92	.667E+02	.261E+02	0.
93	.667E+02	.235E+02	0.	94	.667E+02	.210E+02	0.
95	.667E+02	.184E+02	0.	96	.667E+02	.159E+02	0.
97	.667E+02	.134E+02	0.	98	.667E+02	.108E+02	0.
99	.667E+02	.828E+01	0.	100	.667E+02	.574E+01	0.
101	.667E+02	.667E+02	0.	102	.667E+02	.616E+02	0.
103	.667E+02	.565E+02	0.	104	.667E+02	.514E+02	0.
105	.667E+02	.463E+02	0.	106	.667E+02	.413E+02	0.
107	.667E+02	.362E+02	0.	108	.667E+02	.311E+02	0.
109	.667E+02	.260E+02	0.	110	.667E+02	.209E+02	0.
111	.667E+02	.159E+02	0.	112	.667E+02	.108E+02	0.
113	.667E+02	.570E+01	0.	114	.666E+02	.666E+02	0.
115	.666E+02	.615E+02	0.	116	.666E+02	.564E+02	0.
117	.666E+02	.514E+02	0.	118	.666E+02	.463E+02	0.
119	.666E+02	.412E+02	0.	120	.666E+02	.361E+02	0.
121	.666E+02	.310E+02	0.	122	.666E+02	.260E+02	0.
123	.666E+02	.209E+02	0.	124	.666E+02	.158E+02	0.
125	.666E+02	.107E+02	0.	126	.666E+02	.564E+01	0.

127	.665E+02	.665E+02	0.	128	.665E+02	.564E+02	0.
129	.665E+02	.462E+02	0.	130	.665E+02	.361E+02	0.
131	.665E+02	.259E+02	0.	132	.665E+02	.157E+02	0.
133	.665E+02	.557E+01	0.	134	.664E+02	.664E+02	0.
135	.664E+02	.563E+02	0.	136	.664E+02	.461E+02	0.
137	.664E+02	.360E+02	0.	138	.664E+02	.258E+02	0.
139	.664E+02	.156E+02	0.	140	.664E+02	.547E+01	0.
141	.663E+02	.663E+02	0.	142	.663E+02	.460E+02	0.
143	.663E+02	.257E+02	0.	144	.663E+02	.533E+01	0.
145	.661E+02	.661E+02	0.	146	.661E+02	.458E+02	0.
147	.661E+02	.255E+02	0.	148	.661E+02	.514E+01	0.
149	.658E+02	.658E+02	0.	150	.658E+02	.455E+02	0.
151	.658E+02	.252E+02	0.	152	.658E+02	.488E+01	0.
153	.655E+02	.655E+02	0.	154	.655E+02	.452E+02	0.
155	.655E+02	.249E+02	0.	156	.655E+02	.455E+01	0.
157	.653E+02	.653E+02	0.	158	.653E+02	.348E+02	0.
159	.653E+02	.430E+01	0.	160	.651E+02	.651E+02	0.
161	.651E+02	.415E+01	0.	162	.650E+02	.650E+02	0.
163	.650E+02	.407E+01	0.	164	.650E+02	.650E+02	0.
165	.650E+02	.404E+01	0.	166	.650E+02	.650E+02	0.
167	.650E+02	.404E+01	0.	168	.650E+02	.650E+02	0.
169	.650E+02	.404E+01	0.	170	.650E+02	.650E+02	0.
171	.650E+02	.404E+01	0.	172	.650E+02	.650E+02	0.
173	.650E+02	.404E+01	0.	174	.650E+02	.650E+02	0.
175	.650E+02	.404E+01	0.	176	.650E+02	.650E+02	0.
177	.650E+02	.404E+01	0.	178	.650E+02	.650E+02	0.
179	.650E+02	.404E+01	0.	180	.650E+02	.650E+02	0.
181	.650E+02	.404E+01	0.	182	.650E+02	.650E+02	0.
183	.650E+02	.404E+01	0.	184	.650E+02	.650E+02	0.
185	.650E+02	.404E+01	0.	186	.650E+02	.650E+02	0.
187	.650E+02	.404E+01	0.	188	.650E+02	.650E+02	0.
189	.650E+02	.404E+01	0.	190	.650E+02	.650E+02	0.
191	.650E+02	.404E+01	0.	192	.650E+02	.650E+02	0.
193	.650E+02	.404E+01	0.	194	.650E+02	.650E+02	0.
195	.650E+02	.404E+01	0.	196	.650E+02	.650E+02	0.
197	.650E+02	.404E+01	0.	198	.650E+02	.650E+02	0.
199	.650E+02	.404E+01	0.	200	.650E+02	.650E+02	0.
201	.650E+02	.404E+01	0.	202	.650E+02	.650E+02	0.
203	.650E+02	.404E+01	0.	204	.650E+02	.650E+02	-.111E-03
205	.650E+02	.404E+01	.321E-04	0	0.	0.	0.

MOISTURE CONTENT AT UNSATURATED NODES CORRESPONDING TO MATERIAL 1

    0 0.   0 0.   0 0.

Table 4.   Input data file for pump test verification problem.

```
PUMPC  -  .1 CM  RADIUS  WELL
  205    25  191    1    1    0   30    1    1   25
    1     1   25    1   25    0    0    0    0
    4     3
   25    -1
    1     2    3    4    5    6    7    8    9   10   11   12   13   14   15   16
   17    18   19   20   21   22   23   24   25
    1     1
 .1       0.0       5.0        90.00      0.5
 .01      100.      1.001      100.       0.1
1.0       0.1591549
0.01      0.01      0.35        .16404E-04
 .01       .000001   .20        .05         .257      .95       .35      1.0
 .01      340.       .18       170.         .35       0.
    1     2      .10        0.0      90.00      0.0
   25     2      .10       60.96     29.04      0.0
   26     0     1.37        0.0      90.00      0.0
   50     0     1.37       60.96     29.04      0.0
   51     0     2.64        0.0      90.00      0.0
   75     0     2.64       60.96     29.04      0.0
   76     0     4.55        0.0      90.00      0.0
  100     0     4.55       60.96     29.04      0.0
  101     0     7.09        0.0      90.00      0.0
  113     0     7.09       60.96     29.04      0.0
  114     0    10.90        0.0      90.00      0.0
  126     0    10.90       60.96     29.04      0.0
  127     0    16.61        0.0      90.00      0.0
  133     0    16.61       60.96     29.04      0.0
  134     0    25.18        0.0      90.00      0.0
  140     0    25.18       60.96     29.04      0.0
  141     0    38.04        0.0      90.00      0.0
  144     0    38.04       60.96     29.04      0.0
  145     0    57.34        0.0      90.00      0.0
  148     0    57.34       60.96     29.04      0.0
  149     0    86.30        0.0      90.00      0.0
  152     0    86.30       60.96     29.04      0.0
  153     0   129.48        0.0      90.00      0.0
  156     0   129.48       60.96     29.04      0.0
  157     0   193.45        0.0      90.00      0.0
  159     0   193.45       60.96     29.04      0.0
  160     0   243.34        0.0      90.00      0.0
  161     0   243.34       60.96     29.04      0.0
  162     0   304.50        0.0      90.00      0.0
  163     0   304.50       60.96     29.04      0.0
  164     0   441.96        0.0      90.00      0.0
  165     0   441.96       60.96     29.04      0.0
  166     0   579.12        0.0      90.00      0.0
  167     0   579.12       60.96     29.04      0.0
  168     0   784.86        0.0      90.00      0.0
  169     0   784.86       60.96     29.04      0.0
  170     0  1092.20        0.0      90.00      0.0
  171     0  1092.20       60.96     29.04      0.0
  172     0  1554.48        0.0      90.00      0.0
  173     0  1554.48       60.96     29.04      0.0
  174     0  2247.90        0.0      90.00      0.0
  175     0  2247.90       60.96     29.04      0.0
  176     0  3286.76        0.0      90.00      0.0
  177     0  3286.76       60.96     29.04      0.0
```

178	0	4845.05	0.0	90.00	0.0
179	0	4845.05	60.96	29.04	0.0
180	0	7180.58	0.0	90.00	0.0
181	0	7180.58	60.96	29.04	0.0
182	0	10681.97	0.0	90.00	0.0
183	0	10681.97	60.96	29.04	0.0
184	0	15932.15	0.0	90.00	0.0
185	0	15932.15	60.96	29.04	0.0
186	0	23807.42	0.0	90.00	0.0
187	0	23807.42	60.96	29.04	0.0
188	0	35618.42	0.0	90.00	0.0
189	0	35618.42	60.96	29.04	0.0
190	0	53334.92	0.0	90.00	0.0
191	0	53334.92	60.96	29.04	0.0
192	0	79909.67	0.0	90.00	0.0
193	0	79909.67	60.96	29.04	0.0
194	0	119769.89	0.0	90.00	0.0
195	0	119769.89	60.96	29.04	0.0
196	0	179560.22	0.0	90.00	0.0
197	0	179560.22	60.96	29.04	0.0
198	0	269243.81	0.0	90.00	0.0
199	0	269243.81	60.96	29.04	0.0
200	0	403767.29	0.0	90.00	0.0
201	0	403767.29	60.96	29.04	0.0
202	0	605552.51	0.0	90.00	0.0
203	0	605552.51	60.96	29.04	0.0
204	1	908230.34	0.0	90.00	0.0
205	1	908230.34	60.96	29.04	0.0

1	1	26	27	2	1	0.0
24	24	49	50	25	1	0.0
25	26	51	52	27	1	0.0
48	49	74	75	50	1	0.0
49	51	76	77	52	1	0.0
72	74	99	100	75	1	0.0
73	76	101	77	77	1	0.0
74	77	101	102	102	1	0.0
75	77	102	78	78	1	0.0
76	78	102	79	79	1	0.0
77	79	102	103	103	1	0.0
78	79	103	80	80	1	0.0
79	80	103	81	81	1	0.0
80	81	103	104	104	1	0.0
81	81	104	82	82	1	0.0
82	82	104	83	83	1	0.0
83	83	104	105	105	1	0.0
84	83	105	84	84	1	0.0
85	84	105	85	85	1	0.0
86	85	105	106	106	1	0.0
87	85	106	86	86	1	0.0
88	86	106	87	87	1	0.0
89	87	106	107	107	1	0.0
90	87	107	88	88	1	0.0
91	88	107	89	89	1	0.0
92	89	107	108	108	1	0.0
93	89	108	90	90	1	0.0
94	90	108	91	91	1	0.0
95	91	108	109	109	1	0.0
96	91	109	92	92	1	0.0
97	92	109	93	93	1	0.0
98	93	109	110	110	1	0.0
99	93	110	94	94	1	0.0
100	94	110	95	95	1	0.0
101	95	110	111	111	1	0.0
102	95	111	96	96	1	0.0
103	96	111	97	97	1	0.0

104	97	111	112	112	1	0.0
105	97	112	98	98	1	0.0
106	98	112	99	99	1	0.0
107	99	112	113	113	1	0.0
108	99	113	100	100	1	0.0
109	101	114	115	102	1	0.0
120	112	125	126	113	1	0.0
121	114	127	115	115	1	0.0
122	115	127	128	128	1	0.0
123	115	128	116	116	1	0.0
124	116	128	117	117	1	0.0
125	117	128	129	129	1	0.0
126	117	129	118	118	1	0.0
127	118	129	119	119	1	0.0
128	119	129	130	130	1	0.0
129	119	130	120	120	1	0.0
130	120	130	121	121	1	0.0
131	121	130	131	131	1	0.0
132	121	131	122	122	1	0.0
133	122	131	123	123	1	0.0
134	123	131	132	132	1	0.0
135	123	132	124	124	1	0.0
136	124	132	125	125	1	0.0
137	125	132	133	133	1	0.0
138	125	133	126	126	1	0.0
139	127	134	135	128	1	0.0
144	132	139	140	133	1	0.0
145	134	141	135	135	1	0.0
146	135	141	142	142	1	0.0
147	135	142	136	136	1	0.0
148	136	142	137	137	1	0.0
149	137	142	143	143	1	0.0
150	137	143	138	138	1	0.0
151	138	143	139	139	1	0.0
152	139	143	144	144	1	0.0
153	139	144	140	140	1	0.0
154	141	145	146	142	1	0.0
156	143	147	148	144	1	0.0
157	145	149	150	146	1	0.0
159	147	151	152	148	1	0.0
160	149	153	154	150	1	0.0
162	151	155	156	152	1	0.0
163	153	157	158	154	1	0.0
164	154	158	155	155	1	0.0
165	155	158	159	159	1	0.0
166	155	159	156	156	1	0.0
167	157	160	158	158	1	0.0
168	158	160	161	161	1	0.0
169	158	161	159	159	1	0.0
170	160	162	163	161	1	0.0
171	162	164	165	163	1	0.0
172	164	166	167	165	1	0.0
173	166	168	169	167	1	0.0
174	168	170	171	169	1	0.0
175	170	172	173	171	1	0.0
176	172	174	175	173	1	0.0
177	174	176	177	175	1	0.0
178	176	178	179	177	1	0.0
179	178	180	181	179	1	0.0
180	180	182	183	181	1	0.0
181	182	184	185	183	1	0.0
182	184	186	187	185	1	0.0
183	186	188	189	187	1	0.0
184	188	190	191	189	1	0.0
185	190	192	193	191	1	0.0

```
186  192  194  195  193    1      0.0
187  194  196  197  195    1      0.0
188  196  198  199  197    1      0.0
189  198  200  201  199    1      0.0
190  200  202  203  201    1      0.0
191  202  204  205  203    1      0.0
END
```

Table 5. Output from UNSAT2 for pump test verification problem, for time step = 10, 100, and 1000.

TIME = .10045E+00   TIME STEP = 10

MAX CHANGE IN PRESS HEAD DURING ITERATION 2 WAS   .14203E-01 AT NODE   26

CUMULATIVE INFLOW INTO SYSTEM IS = -.37483E+00
DISCHARGE FROM WELL =   .50000E+01
WATER LEVEL IN WELL =   .85649E+02

O NODE	HEAD	PRESS HEAD	DISCHARGE	NODE	HEAD	PRESS HEAD	DISCHARGE
1	.856E+02	.856E+02	-.116E+00	2	.856E+02	.831E+02	-.188E+00
3	.856E+02	.806E+02	-.190E+00	4	.856E+02	.780E+02	-.190E+00
5	.856E+02	.755E+02	-.190E+00	6	.856E+02	.729E+02	-.191E+00
7	.856E+02	.704E+02	-.190E+00	8	.856E+02	.679E+02	-.191E+00
9	.856E+02	.653E+02	-.190E+00	10	.856E+02	.628E+02	-.191E+00
11	.856E+02	.602E+02	-.190E+00	12	.856E+02	.577E+02	-.191E+00
13	.856E+02	.552E+02	-.190E+00	14	.856E+02	.526E+02	-.191E+00
15	.856E+02	.501E+02	-.190E+00	16	.856E+02	.475E+02	-.191E+00
17	.856E+02	.450E+02	-.190E+00	18	.856E+02	.425E+02	-.191E+00
19	.856E+02	.399E+02	-.190E+00	20	.856E+02	.374E+02	-.191E+00
21	.856E+02	.348E+02	-.191E+00	22	.856E+02	.323E+02	-.191E+00
23	.856E+02	.298E+02	-.191E+00	24	.856E+02	.272E+02	-.194E+00
25	.856E+02	.247E+02	-.723E-01	26	.876E+02	.876E+02	0.
27	.877E+02	.852E+02	0.	28	.877E+02	.826E+02	0.
29	.877E+02	.801E+02	0.	30	.877E+02	.776E+02	0.
31	.877E+02	.750E+02	0.	32	.877E+02	.725E+02	0.
33	.877E+02	.699E+02	0.	34	.877E+02	.674E+02	0.
35	.877E+02	.649E+02	0.	36	.877E+02	.623E+02	0.
37	.877E+02	.598E+02	0.	38	.877E+02	.572E+02	0.
39	.877E+02	.547E+02	0.	40	.877E+02	.522E+02	0.
41	.877E+02	.496E+02	0.	42	.877E+02	.471E+02	0.
43	.877E+02	.445E+02	0.	44	.877E+02	.420E+02	0.
45	.877E+02	.395E+02	0.	46	.877E+02	.369E+02	0.
47	.877E+02	.344E+02	0.	48	.877E+02	.318E+02	0.
49	.878E+02	.293E+02	0.	50	.879E+02	.269E+02	0.
51	.884E+02	.884E+02	0.	52	.884E+02	.859E+02	0.
53	.884E+02	.834E+02	0.	54	.885E+02	.808E+02	0.
55	.885E+02	.783E+02	0.	56	.885E+02	.758E+02	0.
57	.885E+02	.732E+02	0.	58	.885E+02	.707E+02	0.
59	.885E+02	.681E+02	0.	60	.885E+02	.656E+02	0.
61	.885E+02	.631E+02	0.	62	.885E+02	.605E+02	0.
63	.885E+02	.580E+02	0.	64	.885E+02	.554E+02	0.
65	.885E+02	.529E+02	0.	66	.885E+02	.504E+02	0.
67	.885E+02	.478E+02	0.	68	.885E+02	.453E+02	0.
69	.885E+02	.427E+02	0.	70	.885E+02	.402E+02	0.
71	.885E+02	.377E+02	0.	72	.885E+02	.351E+02	0.
73	.885E+02	.326E+02	0.	74	.885E+02	.301E+02	0.
75	.885E+02	.276E+02	0.	76	.890E+02	.890E+02	0.
77	.890E+02	.865E+02	0.	78	.890E+02	.839E+02	0.
79	.890E+02	.814E+02	0.	80	.890E+02	.789E+02	0.
81	.890E+02	.763E+02	0.	82	.890E+02	.738E+02	0.
83	.890E+02	.713E+02	0.	84	.890E+02	.687E+02	0.
85	.890E+02	.662E+02	0.	86	.890E+02	.636E+02	0.
87	.890E+02	.611E+02	0.	88	.890E+02	.585E+02	0.
89	.890E+02	.560E+02	0.	90	.890E+02	.535E+02	0.
91	.890E+02	.509E+02	0.	92	.890E+02	.484E+02	0.
93	.890E+02	.459E+02	0.	94	.890E+02	.433E+02	0.

95	.890E+02	.408E+02	0.	96	.890E+02	.382E+02	0.
97	.891E+02	.357E+02	0.	98	.890E+02	.332E+02	0.
99	.891E+02	.306E+02	0.	100	.891E+02	.281E+02	0.
101	.895E+02	.895E+02	0.	102	.895E+02	.844E+02	0.
103	.895E+02	.793E+02	0.	104	.895E+02	.742E+02	0.
105	.895E+02	.691E+02	0.	106	.895E+02	.641E+02	0.
107	.895E+02	.590E+02	0.	108	.895E+02	.539E+02	0.
109	.895E+02	.488E+02	0.	110	.895E+02	.437E+02	0.
111	.895E+02	.387E+02	0.	112	.895E+02	.336E+02	0.
113	.894E+02	.285E+02	0.	114	.897E+02	.897E+02	0.
115	.898E+02	.847E+02	0.	116	.898E+02	.796E+02	0.
117	.898E+02	.745E+02	0.	118	.898E+02	.694E+02	0.
119	.898E+02	.644E+02	0.	120	.898E+02	.593E+02	0.
121	.898E+02	.542E+02	0.	122	.898E+02	.491E+02	0.
123	.898E+02	.441E+02	0.	124	.898E+02	.390E+02	0.
125	.898E+02	.339E+02	0.	126	.898E+02	.288E+02	0.
127	.899E+02	.899E+02	0.	128	.899E+02	.798E+02	0.
129	.899E+02	.696E+02	0.	130	.899E+02	.595E+02	0.
131	.899E+02	.493E+02	0.	132	.899E+02	.391E+02	0.
133	.899E+02	.290E+02	0.	134	.900E+02	.900E+02	0.
135	.900E+02	.798E+02	0.	136	.900E+02	.697E+02	0.
137	.900E+02	.595E+02	0.	138	.900E+02	.493E+02	0.
139	.900E+02	.392E+02	0.	140	.900E+02	.290E+02	0.
141	.900E+02	.900E+02	0.	142	.900E+02	.697E+02	0.
143	.900E+02	.494E+02	0.	144	.900E+02	.290E+02	0.
145	.900E+02	.900E+02	0.	146	.900E+02	.697E+02	0.
147	.900E+02	.494E+02	0.	148	.900E+02	.290E+02	0.
149	.900E+02	.900E+02	0.	150	.900E+02	.697E+02	0.
151	.900E+02	.494E+02	0.	152	.900E+02	.290E+02	0.
153	.900E+02	.900E+02	0.	154	.900E+02	.697E+02	0.
155	.900E+02	.494E+02	0.	156	.900E+02	.290E+02	0.
157	.900E+02	.900E+02	0.	158	.900E+02	.595E+02	0.
159	.900E+02	.290E+02	0.	160	.900E+02	.900E+02	0.
161	.900E+02	.290E+02	0.	162	.900E+02	.900E+02	0.
163	.900E+02	.290E+02	0.	164	.900E+02	.900E+02	0.
165	.900E+02	.290E+02	0.	166	.900E+02	.900E+02	0.
167	.900E+02	.290E+02	0.	168	.900E+02	.900E+02	0.
169	.900E+02	.290E+02	0.	170	.900E+02	.900E+02	0.
171	.900E+02	.290E+02	0.	172	.900E+02	.900E+02	0.
173	.900E+02	.290E+02	0.	174	.900E+02	.900E+02	0.
175	.900E+02	.290E+02	0.	176	.900E+02	.900E+02	0.
177	.900E+02	.290E+02	0.	178	.900E+02	.900E+02	0.
179	.900E+02	.290E+02	0.	180	.900E+02	.900E+02	0.
181	.900E+02	.290E+02	0.	182	.900E+02	.900E+02	0.
183	.900E+02	.290E+02	0.	184	.900E+02	.900E+02	0.
185	.900E+02	.290E+02	0.	186	.900E+02	.900E+02	0.
187	.900E+02	.290E+02	0.	188	.900E+02	.900E+02	0.
189	.900E+02	.290E+02	0.	190	.900E+02	.900E+02	0.
191	.900E+02	.290E+02	0.	192	.900E+02	.900E+02	0.
193	.900E+02	.290E+02	0.	194	.900E+02	.900E+02	0.
195	.900E+02	.290E+02	0.	196	.900E+02	.900E+02	0.
197	.900E+02	.290E+02	0.	198	.900E+02	.900E+02	0.
199	.900E+02	.290E+02	0.	200	.900E+02	.900E+02	0.
201	.900E+02	.290E+02	0.	202	.900E+02	.900E+02	0.
203	.900E+02	.290E+02	0.	204	.900E+02	.900E+02	-.893E-04
205	.900E+02	.290E+02	.455E-04	0	0.	0.	0.

MOISTURE CONTENT AT UNSATURATED NODES CORRESPONDING TO MATERIAL 1

0 0.   0 0.   0 0.

TIME = .10512E+01   TIME STEP = 100

MAX CHANGE IN PRESS HEAD DURING ITERATION 2 WAS   .94602E-03 AT NODE   25

CUMULATIVE INFLOW INTO SYSTEM IS = -.50607E+01
DISCHARGE FROM WELL =   .50000E+01
WATER LEVEL IN WELL =   .83597E+02

O NODE	HEAD	PRESS HEAD	DISCHARGE	NODE	HEAD	PRESS HEAD	DISCHARGE
1	.836E+02	.836E+02	-.126E+00	2	.836E+02	.811E+02	-.205E+00
3	.836E+02	.785E+02	-.206E+00	4	.836E+02	.760E+02	-.207E+00
5	.836E+02	.734E+02	-.207E+00	6	.836E+02	.709E+02	-.208E+00
7	.836E+02	.684E+02	-.207E+00	8	.836E+02	.658E+02	-.208E+00
9	.836E+02	.633E+02	-.207E+00	10	.836E+02	.607E+02	-.208E+00
11	.836E+02	.582E+02	-.207E+00	12	.836E+02	.557E+02	-.208E+00
13	.836E+02	.531E+02	-.207E+00	14	.836E+02	.506E+02	-.208E+00
15	.836E+02	.480E+02	-.207E+00	16	.836E+02	.455E+02	-.208E+00
17	.836E+02	.430E+02	-.207E+00	18	.836E+02	.404E+02	-.208E+00
19	.836E+02	.379E+02	-.207E+00	20	.836E+02	.353E+02	-.208E+00
21	.836E+02	.328E+02	-.207E+00	22	.836E+02	.303E+02	-.208E+00
23	.836E+02	.277E+02	-.208E+00	24	.836E+02	.252E+02	-.211E+00
25	.836E+02	.226E+02	-.790E-01	26	.857E+02	.857E+02	0.
27	.858E+02	.833E+02	0.	28	.858E+02	.808E+02	0.
29	.858E+02	.782E+02	0.	30	.858E+02	.757E+02	0.
31	.858E+02	.731E+02	0.	32	.858E+02	.706E+02	0.
33	.858E+02	.681E+02	0.	34	.858E+02	.655E+02	0.
35	.858E+02	.630E+02	0.	36	.858E+02	.604E+02	0.
37	.858E+02	.579E+02	0.	38	.858E+02	.554E+02	0.
39	.858E+02	.528E+02	0.	40	.858E+02	.503E+02	0.
41	.858E+02	.477E+02	0.	42	.858E+02	.452E+02	0.
43	.858E+02	.427E+02	0.	44	.858E+02	.401E+02	0.
45	.858E+02	.376E+02	0.	46	.858E+02	.350E+02	0.
47	.859E+02	.325E+02	0.	48	.859E+02	.300E+02	0.
49	.859E+02	.275E+02	0.	50	.860E+02	.250E+02	0.
51	.866E+02	.866E+02	0.	52	.866E+02	.841E+02	0.
53	.867E+02	.816E+02	0.	54	.867E+02	.790E+02	0.
55	.867E+02	.765E+02	0.	56	.867E+02	.740E+02	0.
57	.867E+02	.714E+02	0.	58	.867E+02	.689E+02	0.
59	.867E+02	.663E+02	0.	60	.867E+02	.638E+02	0.
61	.867E+02	.613E+02	0.	62	.867E+02	.587E+02	0.
63	.867E+02	.562E+02	0.	64	.867E+02	.536E+02	0.
65	.867E+02	.511E+02	0.	66	.867E+02	.486E+02	0.
67	.867E+02	.460E+02	0.	68	.867E+02	.435E+02	0.
69	.867E+02	.409E+02	0.	70	.867E+02	.384E+02	0.
71	.867E+02	.359E+02	0.	72	.867E+02	.333E+02	0.
73	.867E+02	.308E+02	0.	74	.867E+02	.283E+02	0.
75	.867E+02	.258E+02	0.	76	.873E+02	.873E+02	0.
77	.873E+02	.848E+02	0.	78	.873E+02	.823E+02	0.
79	.874E+02	.797E+02	0.	80	.873E+02	.772E+02	0.
81	.874E+02	.747E+02	0.	82	.873E+02	.721E+02	0.
83	.874E+02	.696E+02	0.	84	.873E+02	.670E+02	0.
85	.874E+02	.645E+02	0.	86	.873E+02	.619E+02	0.
87	.874E+02	.594E+02	0.	88	.873E+02	.569E+02	0.
89	.874E+02	.543E+02	0.	90	.873E+02	.518E+02	0.
91	.874E+02	.493E+02	0.	92	.873E+02	.467E+02	0.
93	.874E+02	.442E+02	0.	94	.873E+02	.416E+02	0.
95	.874E+02	.391E+02	0.	96	.873E+02	.365E+02	0.
97	.874E+02	.340E+02	0.	98	.874E+02	.315E+02	0.
99	.874E+02	.290E+02	0.	100	.874E+02	.264E+02	0.
101	.879E+02	.879E+02	0.	102	.879E+02	.828E+02	0.
103	.879E+02	.777E+02	0.	104	.879E+02	.727E+02	0.
105	.879E+02	.676E+02	0.	106	.879E+02	.625E+02	0.
107	.879E+02	.574E+02	0.	108	.879E+02	.524E+02	0.

```
109   .879E+02    .473E+02  0.        110   .879E+02    .422E+02  0.
111   .879E+02    .371E+02  0.        112   .879E+02    .320E+02  0.
113   .879E+02    .269E+02  0.        114   .884E+02    .884E+02  0.
115   .885E+02    .834E+02  0.        116   .884E+02    .783E+02  0.
117   .885E+02    .732E+02  0.        118   .884E+02    .681E+02  0.
119   .885E+02    .631E+02  0.        120   .884E+02    .580E+02  0.
121   .885E+02    .529E+02  0.        122   .884E+02    .478E+02  0.
123   .885E+02    .427E+02  0.        124   .884E+02    .376E+02  0.
125   .885E+02    .326E+02  0.        126   .884E+02    .275E+02  0.
127   .890E+02    .890E+02  0.        128   .890E+02    .788E+02  0.
129   .889E+02    .686E+02  0.        130   .889E+02    .585E+02  0.
131   .889E+02    .483E+02  0.        132   .889E+02    .381E+02  0.
133   .889E+02    .280E+02  0.        134   .894E+02    .894E+02  0.
135   .894E+02    .792E+02  0.        136   .894E+02    .691E+02  0.
137   .894E+02    .589E+02  0.        138   .894E+02    .487E+02  0.
139   .894E+02    .386E+02  0.        140   .894E+02    .284E+02  0.
141   .898E+02    .898E+02  0.        142   .897E+02    .694E+02  0.
143   .897E+02    .491E+02  0.        144   .897E+02    .288E+02  0.
145   .899E+02    .899E+02  0.        146   .899E+02    .696E+02  0.
147   .899E+02    .493E+02  0.        148   .899E+02    .290E+02  0.
149   .900E+02    .900E+02  0.        150   .900E+02    .697E+02  0.
151   .900E+02    .494E+02  0.        152   .900E+02    .290E+02  0.
153   .900E+02    .900E+02  0.        154   .900E+02    .697E+02  0.
155   .900E+02    .494E+02  0.        156   .900E+02    .290E+02  0.
157   .900E+02    .900E+02  0.        158   .900E+02    .595E+02  0.
159   .900E+02    .290E+02  0.        160   .900E+02    .900E+02  0.
161   .900E+02    .290E+02  0.        162   .900E+02    .900E+02  0.
163   .900E+02    .290E+02  0.        164   .900E+02    .900E+02  0.
165   .900E+02    .290E+02  0.        166   .900E+02    .900E+02  0.
167   .900E+02    .290E+02  0.        168   .900E+02    .900E+02  0.
169   .900E+02    .290E+02  0.        170   .900E+02    .900E+02  0.
171   .900E+02    .290E+02  0.        172   .900E+02    .900E+02  0.
173   .900E+02    .290E+02  0.        174   .900E+02    .900E+02  0.
175   .900E+02    .290E+02  0.        176   .900E+02    .900E+02  0.
177   .900E+02    .290E+02  0.        178   .900E+02    .900E+02  0.
179   .900E+02    .290E+02  0.        180   .900E+02    .900E+02  0.
181   .900E+02    .290E+02  0.        182   .900E+02    .900E+02  0.
183   .900E+02    .290E+02  0.        184   .900E+02    .900E+02  0.
185   .900E+02    .290E+02  0.        186   .900E+02    .900E+02  0.
187   .900E+02    .290E+02  0.        188   .900E+02    .900E+02  0.
189   .900E+02    .290E+02  0.        190   .900E+02    .900E+02  0.
191   .900E+02    .290E+02  0.        192   .900E+02    .900E+02  0.
193   .900E+02    .290E+02  0.        194   .900E+02    .900E+02  0.
195   .900E+02    .290E+02  0.        196   .900E+02    .900E+02  0.
197   .900E+02    .290E+02  0.        198   .900E+02    .900E+02  0.
199   .900E+02    .290E+02  0.        200   .900E+02    .900E+02  0.
201   .900E+02    .290E+02  0.        202   .900E+02    .900E+02  0.
203   .900E+02    .290E+02  0.        204   .900E+02    .900E+02  -.893E-04
205   .900E+02    .290E+02  .455E-04    0   0.          0.        0.
```

MOISTURE CONTENT AT UNSATURATED NODES CORRESPONDING TO MATERIAL   1

```
    0  0.              0  0.              0  0.
```


```
            TIME =   .17169E+02     TIME STEP =1000
```

MAX CHANGE IN PRESS HEAD DURING ITERATION 2 WAS   .16519E-03 AT NODE   26

CUMULATIVE INFLOW INTO SYSTEM IS = -.85591E+02
DISCHARGE FROM WELL =   .50000E+01
WATER LEVEL IN WELL =   .81742E+02

O NODE	HEAD	PRESS HEAD	DISCHARGE	NODE	HEAD	PRESS HEAD	DISCHARGE
1	.817E+02	.817E+02	-.127E+00	2	.817E+02	.792E+02	-.206E+00
3	.817E+02	.767E+02	-.207E+00	4	.817E+02	.741E+02	-.208E+00
5	.817E+02	.716E+02	-.208E+00	6	.817E+02	.690E+02	-.208E+00
7	.817E+02	.665E+02	-.208E+00	8	.817E+02	.640E+02	-.208E+00
9	.817E+02	.614E+02	-.208E+00	10	.817E+02	.589E+02	-.208E+00
11	.817E+02	.563E+02	-.208E+00	12	.817E+02	.538E+02	-.208E+00
13	.817E+02	.513E+02	-.208E+00	14	.817E+02	.487E+02	-.208E+00
15	.817E+02	.462E+02	-.208E+00	16	.817E+02	.436E+02	-.208E+00
17	.817E+02	.411E+02	-.208E+00	18	.817E+02	.386E+02	-.208E+00
19	.817E+02	.360E+02	-.208E+00	20	.817E+02	.335E+02	-.209E+00
21	.817E+02	.309E+02	-.208E+00	22	.817E+02	.284E+02	-.209E+00
23	.817E+02	.259E+02	-.209E+00	24	.817E+02	.233E+02	-.212E+00
25	.817E+02	.208E+02	-.794E-01	26	.839E+02	.839E+02	0.
27	.840E+02	.814E+02	0.	28	.840E+02	.789E+02	0.
29	.840E+02	.764E+02	0.	30	.840E+02	.738E+02	0.
31	.840E+02	.713E+02	0.	32	.840E+02	.688E+02	0.
33	.840E+02	.662E+02	0.	34	.840E+02	.637E+02	0.
35	.840E+02	.611E+02	0.	36	.840E+02	.586E+02	0.
37	.840E+02	.561E+02	0.	38	.840E+02	.535E+02	0.
39	.840E+02	.510E+02	0.	40	.840E+02	.484E+02	0.
41	.840E+02	.459E+02	0.	42	.840E+02	.434E+02	0.
43	.840E+02	.408E+02	0.	44	.840E+02	.383E+02	0.
45	.840E+02	.357E+02	0.	46	.840E+02	.332E+02	0.
47	.840E+02	.307E+02	0.	48	.840E+02	.281E+02	0.
49	.840E+02	.256E+02	0.	50	.842E+02	.232E+02	0.
51	.847E+02	.847E+02	0.	52	.848E+02	.823E+02	0.
53	.848E+02	.797E+02	0.	54	.848E+02	.772E+02	0.
55	.848E+02	.747E+02	0.	56	.848E+02	.721E+02	0.
57	.848E+02	.696E+02	0.	58	.848E+02	.670E+02	0.
59	.848E+02	.645E+02	0.	60	.848E+02	.620E+02	0.
61	.848E+02	.594E+02	0.	62	.848E+02	.569E+02	0.
63	.848E+02	.543E+02	0.	64	.848E+02	.518E+02	0.
65	.848E+02	.493E+02	0.	66	.848E+02	.467E+02	0.
67	.848E+02	.442E+02	0.	68	.848E+02	.416E+02	0.
69	.848E+02	.391E+02	0.	70	.848E+02	.366E+02	0.
71	.848E+02	.340E+02	0.	72	.848E+02	.315E+02	0.
73	.848E+02	.290E+02	0.	74	.849E+02	.264E+02	0.
75	.849E+02	.239E+02	0.	76	.855E+02	.855E+02	0.
77	.855E+02	.830E+02	0.	78	.855E+02	.804E+02	0.
79	.855E+02	.779E+02	0.	80	.855E+02	.753E+02	0.
81	.855E+02	.728E+02	0.	82	.855E+02	.703E+02	0.
83	.855E+02	.677E+02	0.	84	.855E+02	.652E+02	0.
85	.855E+02	.627E+02	0.	86	.855E+02	.601E+02	0.
87	.855E+02	.576E+02	0.	88	.855E+02	.550E+02	0.
89	.855E+02	.525E+02	0.	90	.855E+02	.499E+02	0.
91	.855E+02	.474E+02	0.	92	.855E+02	.449E+02	0.
93	.855E+02	.423E+02	0.	94	.855E+02	.398E+02	0.
95	.855E+02	.373E+02	0.	96	.855E+02	.347E+02	0.
97	.855E+02	.322E+02	0.	98	.855E+02	.296E+02	0.
99	.856E+02	.271E+02	0.	100	.856E+02	.246E+02	0.
101	.861E+02	.861E+02	0.	102	.861E+02	.810E+02	0.
103	.861E+02	.759E+02	0.	104	.861E+02	.709E+02	0.
105	.861E+02	.658E+02	0.	106	.861E+02	.607E+02	0.
107	.861E+02	.556E+02	0.	108	.861E+02	.505E+02	0.
109	.861E+02	.454E+02	0.	110	.861E+02	.404E+02	0.
111	.861E+02	.353E+02	0.	112	.861E+02	.302E+02	0.
113	.861E+02	.251E+02	0.	114	.866E+02	.866E+02	0.
115	.866E+02	.816E+02	0.	116	.866E+02	.765E+02	0.
117	.866E+02	.714E+02	0.	118	.866E+02	.663E+02	0.
119	.866E+02	.612E+02	0.	120	.866E+02	.562E+02	0.
121	.866E+02	.511E+02	0.	122	.866E+02	.460E+02	0.
123	.866E+02	.409E+02	0.	124	.866E+02	.358E+02	0.
125	.866E+02	.308E+02	0.	126	.866E+02	.257E+02	0.

127	.872E+02	.872E+02	0.	128	.872E+02	.770E+02	0.
129	.872E+02	.669E+02	0.	130	.872E+02	.567E+02	0.
131	.872E+02	.465E+02	0.	132	.872E+02	.364E+02	0.
133	.872E+02	.262E+02	0.	134	.877E+02	.877E+02	0.
135	.877E+02	.776E+02	0.	136	.877E+02	.674E+02	0.
137	.877E+02	.572E+02	0.	138	.877E+02	.471E+02	0.
139	.877E+02	.369E+02	0.	140	.877E+02	.267E+02	0.
141	.882E+02	.882E+02	0.	142	.882E+02	.679E+02	0.
143	.882E+02	.476E+02	0.	144	.882E+02	.273E+02	0.
145	.887E+02	.887E+02	0.	146	.887E+02	.684E+02	0.
147	.887E+02	.481E+02	0.	148	.887E+02	.278E+02	0.
149	.892E+02	.892E+02	0.	150	.892E+02	.689E+02	0.
151	.892E+02	.485E+02	0.	152	.892E+02	.282E+02	0.
153	.896E+02	.896E+02	0.	154	.896E+02	.693E+02	0.
155	.896E+02	.489E+02	0.	156	.896E+02	.286E+02	0.
157	.898E+02	.898E+02	0.	158	.898E+02	.594E+02	0.
159	.898E+02	.289E+02	0.	160	.899E+02	.899E+02	0.
161	.899E+02	.290E+02	0.	162	.900E+02	.900E+02	0.
163	.900E+02	.290E+02	0.	164	.900E+02	.900E+02	0.
165	.900E+02	.290E+02	0.	166	.900E+02	.900E+02	0.
167	.900E+02	.290E+02	0.	168	.900E+02	.900E+02	0.
169	.900E+02	.290E+02	0.	170	.900E+02	.900E+02	0.
171	.900E+02	.290E+02	0.	172	.900E+02	.900E+02	0.
173	.900E+02	.290E+02	0.	174	.900E+02	.900E+02	0.
175	.900E+02	.290E+02	0.	176	.900E+02	.900E+02	0.
177	.900E+02	.290E+02	0.	178	.900E+02	.900E+02	0.
179	.900E+02	.290E+02	0.	180	.900E+02	.900E+02	0.
181	.900E+02	.290E+02	0.	182	.900E+02	.900E+02	0.
183	.900E+02	.290E+02	0.	184	.900E+02	.900E+02	0.
185	.900E+02	.290E+02	0.	186	.900E+02	.900E+02	0.
187	.900E+02	.290E+02	0.	188	.900E+02	.900E+02	0.
189	.900E+02	.290E+02	0.	190	.900E+02	.900E+02	0.
191	.900E+02	.290E+02	0.	192	.900E+02	.900E+02	0.
193	.900E+02	.290E+02	0.	194	.900E+02	.900E+02	0.
195	.900E+02	.290E+02	0.	196	.900E+02	.900E+02	0.
197	.900E+02	.290E+02	0.	198	.900E+02	.900E+02	0.
199	.900E+02	.290E+02	0.	200	.900E+02	.900E+02	0.
201	.900E+02	.290E+02	0.	202	.900E+02	.900E+02	0.
203	.900E+02	.290E+02	0.	204	.900E+02	.900E+02	-.893E-04
205	.900E+02	.290E+02	.455E-04	0	0.	0.	0.

MOISTURE CONTENT AT UNSATURATED NODES CORRESPONDING TO MATERIAL 1

0 0.   0 0.   0 0.

APPENDIX B. INPUT AND OUTPUT DATA FILES FOR WELL
NC7-25

Table 6. Input data file for a slug test for well
NC7-25.


```
NC7-25  SLUG TEST
   205   25  191    1    2    0   30    1    0    0
     1    1   25    0   25    0    0    0    0
     8    4    8    4
     1    1
5.52      4.43      0.0       374.90    0.5
.0001     .10000E+091.1       .10000E+091.0
1.0       0.1591549
0.00004   0.00004   0.35      0.
0.1       0.1       0.30      0.
0.        0.        .15       .03       .20       .09       .25       .2
.28       .33       .30       .5        .32       .96       .35       1.0
.04       1000.     .10       500.      .15       200.      .35       0.
0.        0.        .13       .03       .17       .09       .22       .2
.24       .33       .26       .5        .28       .96       .30       1.0
.05       1000.     .10       50.       .28       10.       .30       0.
     1    2    5.52      0.0     374.90      0.0
     9    2    5.52    137.16    237.74      0.0
    25    2    5.52    374.90      0.0       0.0
    26    0    6.77      0.0     137.16      0.0
    34    0    6.77    137.16      0.0       0.0
    50    0    6.77    374.90   -237.74      0.0
    51    0    8.65      0.0     137.16      0.0
    59    0    8.65    137.16      0.0       0.0
    75    0    8.65    374.90   -237.74      0.0
    76    0   11.43      0.0     137.16      0.0
    84    0   11.43    137.16      0.0       0.0
   100    0   11.43    374.90   -237.74      0.0
   101    0   15.03      0.0     137.16      0.0
   105    0   15.03    137.16      0.0       0.0
   113    0   15.03    374.90   -237.74      0.0
   114    0   20.42      0.0     137.16      0.0
   118    0   20.42    137.16      0.0       0.0
   126    0   20.42    374.90   -237.74      0.0
   127    0   28.50      0.0     137.16      0.0
   129    0   28.50    137.16      0.0       0.0
   133    0   28.50    374.90   -237.74      0.0
   134    0   40.62      0.0     137.16      0.0
   136    0   40.62    137.16      0.0       0.0
   140    0   40.62    374.90   -237.74      0.0
   141    0   58.79      0.0     137.16      0.0
   142    0   58.79    137.16      0.0       0.0
   144    0   58.79    374.90   -237.74      0.0
   145    0   86.04      0.0     137.16      0.0
   146    0   86.04    137.16      0.0       0.0
   148    0   86.04    374.90   -237.74      0.0
   149    0  126.91      0.0     137.16      0.0
   150    0  126.91    137.16      0.0       0.0
   152    0  126.91    374.90   -237.74      0.0
   153    0  188.21      0.0     137.16      0.0
   154    0  188.21    137.16      0.0       0.0
   156    0  188.21    374.90   -237.74      0.0
```

```
157   0     280.16        0.0      137.16      0.0
158   0     280.16      137.16       0.0       0.0
159   0     280.16      374.90    -237.74      0.0
160   0     418.08        0.0      137.16      0.0
161   0     418.08      374.90    -237.74      0.0
162   0     624.96        0.0      137.16      0.0
163   0     624.96      374.90    -237.74      0.0
164   0     935.27        0.0      137.16      0.0
165   0     935.27      374.90    -237.74      0.0
166   0    1400.73        0.0      137.16      0.0
167   0    1400.73      374.90    -237.74      0.0
168   0    2098.92        0.0      137.16      0.0
169   0    2098.92      374.90    -237.74      0.0
170   0    3146.20        0.0      137.16      0.0
171   0    3146.20      374.90    -237.74      0.0
172   0    4717.12        0.0      137.16      0.0
173   0    4717.12      374.90    -237.74      0.0
174   0    7073.50        0.0      137.16      0.0
175   0    7073.50      374.90    -237.74      0.0
176   0   10608.06        0.0      137.16      0.0
177   0   10608.06      374.90    -237.74      0.0
178   0   15909.90        0.0      137.16      0.0
179   0   15909.90      374.90    -237.74      0.0
180   0   23862.65        0.0      137.16      0.0
181   0   23862.65      374.90    -237.74      0.0
182   0   35791.77        0.0      137.16      0.0
183   0   35791.77      374.90    -237.74      0.0
184   0   53685.45        0.0      137.16      0.0
185   0   53685.45      374.90    -237.74      0.0
186   0   80525.96        0.0      137.16      0.0
187   0   80525.96      374.90    -237.74      0.0
188   0  120786.72        0.0      137.16      0.0
189   0  120786.72      374.90    -237.74      0.0
190   0  181177.85        0.0      137.16      0.0
191   0  181177.85      374.90    -237.74      0.0
192   0  271764.54        0.0      137.16      0.0
193   0  271764.54      374.90    -237.74      0.0
194   0  407644.57        0.0      137.16      0.0
195   0  407644.57      374.90    -237.74      0.0
196   0  611464.61        0.0      137.16      0.0
197   0  611464.61      374.90    -237.74      0.0
198   0  917194.66        0.0      137.16      0.0
199   0  917194.66      374.90    -237.74      0.0
200   01375789.73        0.0      137.16      0.0
201   01375789.73      374.90    -237.74      0.0
202   02063682.33        0.0      137.16      0.0
203   02063682.33      374.90    -237.74      0.0
204   13095521.23        0.0      137.16      0.0
205   13095521.23      374.90    -237.74      0.0
  1   1    26    27     2    2     0.0
 24  24    49    50    25    2     0.0
 25  26    51    52    27    2     0.0
 48  49    74    75    50    2     0.0
 49  51    76    77    52    2     0.0
 72  74    99   100    75    2     0.0
 73  76   101    77    77    1     0.0
 74  77   101   102   102    1     0.0
 75  77   102    78    78    1     0.0
 76  78   102    79    79    1     0.0
 77  79   102   103   103    1     0.0
 78  79   103    80    80    1     0.0
 79  80   103    81    81    1     0.0
 80  81   103   104   104    1     0.0
 81  81   104    82    82    1     0.0
 82  82   104    83    83    1     0.0
```

83	83	104	105	105	1	0.0
84	83	105	84	84	1	0.0
85	84	105	85	85	1	0.0
86	85	105	106	106	1	0.0
87	85	106	86	86	1	0.0
88	86	106	87	87	1	0.0
89	87	106	107	107	1	0.0
90	87	107	88	88	1	0.0
91	88	107	89	89	1	0.0
92	89	107	108	108	1	0.0
93	89	108	90	90	1	0.0
94	90	108	91	91	1	0.0
95	91	108	109	109	1	0.0
96	91	109	92	92	1	0.0
97	92	109	93	93	1	0.0
98	93	109	110	110	1	0.0
99	93	110	94	94	1	0.0
100	94	110	95	95	1	0.0
101	95	110	111	111	1	0.0
102	95	111	96	96	1	0.0
103	96	111	97	97	1	0.0
104	97	111	112	112	1	0.0
105	97	112	98	98	1	0.0
106	98	112	99	99	1	0.0
107	99	112	113	113	1	0.0
108	99	113	100	100	1	0.0
109	101	114	115	102	1	0.0
114	106	119	120	107	1	0.0
115	107	120	121	108	1	0.0
120	112	125	126	113	1	0.0
121	114	127	115	115	1	0.0
122	115	127	128	128	1	0.0
123	115	128	116	116	1	0.0
124	116	128	117	117	1	0.0
125	117	128	129	129	1	0.0
126	117	129	118	118	1	0.0
127	118	129	119	119	1	0.0
128	119	129	130	130	1	0.0
129	119	130	120	120	1	0.0
130	120	130	121	121	1	0.0
131	121	130	131	131	1	0.0
132	121	131	122	122	1	0.0
133	122	131	123	123	1	0.0
134	123	131	132	132	1	0.0
135	123	132	124	124	1	0.0
136	124	132	125	125	1	0.0
137	125	132	133	133	1	0.0
138	125	133	126	126	1	0.0
139	127	134	135	128	1	0.0
141	129	136	137	130	1	0.0
142	130	137	138	131	1	0.0
144	132	139	140	133	1	0.0
145	134	141	135	135	1	0.0
146	135	141	142	142	1	0.0
147	135	142	136	136	1	0.0
148	136	142	137	137	1	0.0
149	137	142	143	143	1	0.0
150	137	143	138	138	1	0.0
151	138	143	139	139	1	0.0
152	139	143	144	144	1	0.0
153	139	144	140	140	1	0.0
154	141	145	146	142	1	0.0
156	143	147	148	144	1	0.0
157	145	149	150	146	1	0.0
159	147	151	152	148	1	0.0

```
160  149  153  154  150  1     0.0
162  151  155  156  152  1     0.0
163  153  157  158  154  1     0.0
164  154  158  155  155  1     0.0
165  155  158  159  159  1     0.0
166  155  159  156  156  1     0.0
167  157  160  158  158  1     0.0
168  158  160  161  161  1     0.0
169  158  161  159  159  1     0.0
170  160  162  163  161  1     0.0
171  162  164  165  163  1     0.0
172  164  166  167  165  1     0.0
173  166  168  169  167  1     0.0
174  168  170  171  169  1     0.0
175  170  172  173  171  1     0.0
176  172  174  175  173  1     0.0
177  174  176  177  175  1     0.0
178  176  178  179  177  1     0.0
179  178  180  181  179  1     0.0
180  180  182  183  181  1     0.0
181  182  184  185  183  1     0.0
182  184  186  187  185  1     0.0
183  186  188  189  187  1     0.0
184  188  190  191  189  1     0.0
185  190  192  193  191  1     0.0
186  192  194  195  193  1     0.0
187  194  196  197  195  1     0.0
188  196  198  199  197  1     0.0
189  198  200  201  199  1     0.0
190  200  202  203  201  1     0.0
191  202  204  205  203  1     0.0
END
```

Table 7. Output from UNSAT2 for a slug test for well NC7-25.

TIME =   .11639E+00   TIME STEP = 50

MAX CHANGE IN PRESS HEAD DURING ITERATION 2 WAS   .98828E+00 AT NODE   26

CUMULATIVE INFLOW INTO SYSTEM IS =   .35090E+04
DISCHARGE FROM WELL = 0.
WATER LEVEL IN WELL =   .28010E+03

O NODE	HEAD	PRESS HEAD	DISCHARGE	NODE	HEAD	PRESS HEAD	DISCHARGE
1	.280E+03	.280E+03	.114E+00	2	.280E+03	.263E+03	.264E+00
3	.280E+03	.246E+03	.267E+00	4	.280E+03	.229E+03	.298E+00
5	.280E+03	.212E+03	.291E+00	6	.280E+03	.194E+03	.374E+00
7	.280E+03	.177E+03	.872E+00	8	.280E+03	.160E+03	.933E+01
9	.280E+03	.143E+03	.130E+03	10	.280E+03	.128E+03	.148E+04
11	.280E+03	.113E+03	.181E+04	12	.280E+03	.984E+02	.188E+04
13	.280E+03	.835E+02	.147E+04	14	.280E+03	.686E+02	.128E+04
15	.280E+03	.538E+02	.117E+04	16	.280E+03	.389E+02	.109E+04
17	.280E+03	.241E+02	.118E+04	18	.280E+03	.921E+01	.790E+03
19	.277E+03	-.881E+01	0.	20	.281E+03	-.193E+02	0.
21	.289E+03	-.268E+02	0.	22	.296E+03	-.339E+02	0.
23	.299E+03	-.460E+02	0.	24	.300E+03	-.596E+02	0.
25	.295E+03	-.794E+02	0.	26	.281E+03	.281E+03	0.
27	.281E+03	.263E+03	0.	28	.281E+03	.246E+03	0.
29	.281E+03	.229E+03	0.	30	.281E+03	.212E+03	0.
31	.281E+03	.195E+03	0.	32	.281E+03	.178E+03	0.
33	.280E+03	.160E+03	0.	34	.278E+03	.141E+03	0.
35	.248E+03	.962E+02	0.	36	.241E+03	.742E+02	0.
37	.240E+03	.579E+02	0.	38	.249E+03	.520E+02	0.
39	.253E+03	.412E+02	0.	40	.255E+03	.288E+02	0.
41	.256E+03	.153E+02	0.	42	.251E+03	-.541E+01	0.
43	.252E+03	-.185E+02	0.	44	.261E+03	-.243E+02	0.
45	.268E+03	-.326E+02	0.	46	.272E+03	-.430E+02	0.
47	.268E+03	-.619E+02	0.	48	.249E+03	-.966E+02	0.
49	.219E+03	-.141E+03	0.	50	.214E+03	-.161E+03	0.
51	.281E+03	.281E+03	0.	52	.281E+03	.263E+03	0.
53	.281E+03	.246E+03	0.	54	.281E+03	.229E+03	0.
55	.281E+03	.212E+03	0.	56	.281E+03	.195E+03	0.
57	.281E+03	.178E+03	0.	58	.280E+03	.160E+03	0.
59	.275E+03	.138E+03	0.	60	.209E+03	.571E+02	0.
61	.194E+03	.267E+02	0.	62	.179E+03	-.311E+01	0.
63	.179E+03	-.171E+02	0.	64	.185E+03	-.262E+02	0.
65	.193E+03	-.337E+02	0.	66	.198E+03	-.435E+02	0.
67	.190E+03	-.663E+02	0.	68	.170E+03	-.101E+03	0.
69	.156E+03	-.130E+03	0.	70	.150E+03	-.150E+03	0.
71	.146E+03	-.169E+03	0.	72	.144E+03	-.186E+03	0.
73	.144E+03	-.202E+03	0.	74	.142E+03	-.218E+03	0.
75	.142E+03	-.233E+03	0.	76	.281E+03	.281E+03	0.
77	.281E+03	.263E+03	0.	78	.281E+03	.246E+03	0.
79	.281E+03	.229E+03	0.	80	.281E+03	.212E+03	0.
81	.281E+03	.195E+03	0.	82	.280E+03	.178E+03	0.
83	.280E+03	.160E+03	0.	84	.273E+03	.136E+03	0.
85	.168E+03	.164E+02	0.	86	.146E+03	-.212E+02	0.
87	.141E+03	-.412E+02	0.	88	.140E+03	-.565E+02	0.
89	.138E+03	-.731E+02	0.	90	.138E+03	-.879E+02	0.
91	.138E+03	-.103E+03	0.	92	.138E+03	-.118E+03	0.
93	.137E+03	-.133E+03	0.	94	.137E+03	-.148E+03	0.
95	.137E+03	-.163E+03	0.	96	.137E+03	-.178E+03	0.

97	.137E+03	-.193E+03	0.	98	.137E+03	-.208E+03	0.
99	.137E+03	-.223E+03	0.	100	.137E+03	-.238E+03	0.
101	.266E+03	.266E+03	0.	102	.263E+03	.229E+03	0.
103	.262E+03	.193E+03	0.	104	.257E+03	.154E+03	0.
105	.137E+03	.542E-01	0.	106	.137E+03	-.297E+02	0.
107	.137E+03	-.594E+02	0.	108	.137E+03	-.892E+02	0.
109	.137E+03	-.119E+03	0.	110	.137E+03	-.149E+03	0.
111	.137E+03	-.178E+03	0.	112	.137E+03	-.208E+03	0.
113	.137E+03	-.238E+03	0.	114	.250E+03	.250E+03	0.
115	.244E+03	.209E+03	0.	116	.240E+03	.172E+03	0.
117	.217E+03	.114E+03	0.	118	.137E+03	.358E-02	0.
119	.137E+03	-.297E+02	0.	120	.137E+03	-.594E+02	0.
121	.137E+03	-.892E+02	0.	122	.137E+03	-.119E+03	0.
123	.137E+03	-.149E+03	0.	124	.137E+03	-.178E+03	0.
125	.137E+03	-.208E+03	0.	126	.137E+03	-.238E+03	0.
127	.230E+03	.230E+03	0.	128	.217E+03	.148E+03	0.
129	.137E+03	.250E-02	0.	130	.137E+03	-.594E+02	0.
131	.137E+03	-.119E+03	0.	132	.137E+03	-.178E+03	0.
133	.137E+03	-.238E+03	0.	134	.211E+03	.211E+03	0.
135	.189E+03	.121E+03	0.	136	.137E+03	.680E-03	0.
137	.137E+03	-.594E+02	0.	138	.137E+03	-.119E+03	0.
139	.137E+03	-.178E+03	0.	140	.137E+03	-.238E+03	0.
141	.191E+03	.191E+03	0.	142	.137E+03	.454E-03	0.
143	.137E+03	-.119E+03	0.	144	.137E+03	-.238E+03	0.
145	.172E+03	.172E+03	0.	146	.137E+03	.680E-04	0.
147	.137E+03	-.119E+03	0.	148	.137E+03	-.238E+03	0.
149	.156E+03	.156E+03	0.	150	.137E+03	.374E-04	0.
151	.137E+03	-.119E+03	0.	152	.137E+03	-.238E+03	0.
153	.146E+03	.146E+03	0.	154	.137E+03	.398E-04	0.
155	.137E+03	-.119E+03	0.	156	.137E+03	-.238E+03	0.
157	.140E+03	.140E+03	0.	158	.137E+03	.432E-05	0.
159	.137E+03	-.238E+03	0.	160	.137E+03	.137E+03	0.
161	.137E+03	-.238E+03	0.	162	.137E+03	.137E+03	0.
163	.137E+03	-.238E+03	0.	164	.137E+03	.137E+03	0.
165	.137E+03	-.238E+03	0.	166	.137E+03	.137E+03	0.
167	.137E+03	-.238E+03	0.	168	.137E+03	.137E+03	0.
169	.137E+03	-.238E+03	0.	170	.137E+03	.137E+03	0.
171	.137E+03	-.238E+03	0.	172	.137E+03	.137E+03	0.
173	.137E+03	-.238E+03	0.	174	.137E+03	.137E+03	0.
175	.137E+03	-.238E+03	0.	176	.137E+03	.137E+03	0.
177	.137E+03	-.238E+03	0.	178	.137E+03	.137E+03	0.
179	.137E+03	-.238E+03	0.	180	.137E+03	.137E+03	0.
181	.137E+03	-.238E+03	0.	182	.137E+03	.137E+03	0.
183	.137E+03	-.238E+03	0.	184	.137E+03	.137E+03	0.
185	.137E+03	-.238E+03	0.	186	.137E+03	.137E+03	0.
187	.137E+03	-.238E+03	0.	188	.137E+03	.137E+03	0.
189	.137E+03	-.238E+03	0.	190	.137E+03	.137E+03	0.
191	.137E+03	-.238E+03	0.	192	.137E+03	.137E+03	0.
193	.137E+03	-.238E+03	0.	194	.137E+03	.137E+03	0.
195	.137E+03	-.238E+03	0.	196	.137E+03	.137E+03	0.
197	.137E+03	-.238E+03	0.	198	.137E+03	.137E+03	0.
199	.137E+03	-.238E+03	0.	200	.137E+03	.137E+03	0.
201	.137E+03	-.238E+03	0.	202	.137E+03	.137E+03	0.
203	.137E+03	-.238E+03	0.	204	.137E+03	.137E+03	.547E-07
205	.137E+03	-.238E+03	.249E-06	0	0.	0.	0.

MOISTURE CONTENT AT UNSATURATED NODES CORRESPONDING TO MATERIAL 1

86	.32879E+00	87	.30880E+00	88	.29353E+00
89	.27689E+00	90	.26207E+00	91	.24660E+00
92	.23182E+00	93	.21657E+00	94	.20171E+00
95	.18672E+00	96	.17190E+00	97	.15697E+00
98	.14869E+00	99	.14621E+00	100	.14373E+00
106	.32028E+00	107	.29057E+00	108	.26085E+00
109	.23113E+00	110	.20141E+00	111	.17170E+00

112	.14866E+00	113	.14371E+00	119	.32028E+00
120	.29057E+00	121	.26085E+00	122	.23113E+00
123	.20141E+00	124	.17170E+00	125	.14866E+00
126	.14371E+00	130	.29056E+00	131	.23113E+00
132	.17170E+00	133	.14371E+00	137	.29057E+00
138	.23113E+00	139	.17170E+00	140	.14371E+00
143	.23113E+00	144	.14371E+00	147	.23113E+00
148	.14371E+00	151	.23113E+00	152	.14371E+00
155	.23113E+00	156	.14371E+00	159	.14371E+00
161	.14371E+00	163	.14371E+00	165	.14371E+00
167	.14371E+00	169	.14371E+00	171	.14371E+00
173	.14371E+00	175	.14371E+00	177	.14371E+00
179	.14371E+00	181	.14371E+00	183	.14371E+00
185	.14371E+00	187	.14371E+00	189	.14371E+00
191	.14371E+00	193	.14371E+00	195	.14371E+00
197	.14371E+00	199	.14371E+00	201	.14371E+00
203	.14371E+00	205	.14371E+00	0	0.

MOISTURE CONTENT AT UNSATURATED NODES CORRESPONDING TO MATERIAL 2

19	.28239E+00	20	.23821E+00	21	.20425E+00
22	.17243E+00	23	.11813E+00	24	.99495E-01
25	.98451E-01	42	.28917E+00	43	.24153E+00
44	.21567E+00	45	.17822E+00	46	.13142E+00
47	.99374E-01	48	.97545E-01	49	.95231E-01
50	.94172E-01	62	.29378E+00	63	.24802E+00
64	.20695E+00	65	.17344E+00	66	.12944E+00
67	.99140E-01	68	.97298E-01	69	.95790E-01
70	.94726E-01	71	.93730E-01	72	.92848E-01
73	.92024E-01	74	.91163E-01	75	.90392E-01
86	.22955E+00	87	.13958E+00	88	.99660E-01
89	.98784E-01	90	.98004E-01	91	.97189E-01
92	.96412E-01	93	.95609E-01	94	.94827E-01
95	.94038E-01	96	.93258E-01	97	.92472E-01
98	.91693E-01	99	.90907E-01	100	.90126E-01
0	0.	0	0.	0	0.

TIME =   .13780E+02   TIME STEP = 100

MAX CHANGE IN PRESS HEAD DURING ITERATION 2 WAS   .11887E+00 AT NODE   26

CUMULATIVE INFLOW INTO SYSTEM IS =   .57649E+04
DISCHARGE FROM WELL = 0.
WATER LEVEL IN WELL =   .21628E+03

0 NODE	HEAD	PRESS HEAD	DISCHARGE	NODE	HEAD	PRESS HEAD	DISCHARGE
1	.216E+03	.216E+03	.631E-01	2	.216E+03	.199E+03	.146E+00
3	.216E+03	.182E+03	.148E+00	4	.216E+03	.165E+03	.164E+00
5	.216E+03	.148E+03	.160E+00	6	.216E+03	.131E+03	.197E+00
7	.216E+03	.113E+03	.236E+00	8	.216E+03	.963E+02	.698E+00
9	.216E+03	.791E+02	.976E+00	10	.216E+03	.643E+02	.797E+00
11	.216E+03	.494E+02	.795E+00	12	.216E+03	.345E+02	.466E+00
13	.216E+03	.197E+02	.104E+01	14	.216E+03	.483E+01	.629E+01
15	.212E+03	-.147E+02	0.	16	.201E+03	-.401E+02	0.
17	.199E+03	-.567E+02	0.	18	.184E+03	-.865E+02	0.
19	.184E+03	-.101E+03	0.	20	.177E+03	-.124E+03	0.
21	.180E+03	-.135E+03	0.	22	.175E+03	-.156E+03	0.
23	.174E+03	-.171E+03	0.	24	.166E+03	-.194E+03	0.
25	.162E+03	-.212E+03	0.	26	.216E+03	.216E+03	0.
27	.216E+03	.199E+03	0.	28	.216E+03	.182E+03	0.
29	.216E+03	.165E+03	0.	30	.216E+03	.148E+03	0.
31	.216E+03	.131E+03	0.	32	.216E+03	.113E+03	0.
33	.216E+03	.963E+02	0.	34	.216E+03	.792E+02	0.

35	.216E+03	.643E+02	0.	36	.216E+03	.494E+02	0.
37	.216E+03	.346E+02	0.	38	.216E+03	.197E+02	0.
39	.216E+03	.474E+01	0.	40	.212E+03	-.147E+02	0.
41	.201E+03	-.401E+02	0.	42	.199E+03	-.567E+02	0.
43	.184E+03	-.867E+02	0.	44	.184E+03	-.102E+03	0.
45	.177E+03	-.124E+03	0.	46	.180E+03	-.135E+03	0.
47	.175E+03	-.156E+03	0.	48	.174E+03	-.171E+03	0.
49	.166E+03	-.194E+03	0.	50	.162E+03	-.212E+03	0.
51	.216E+03	.216E+03	0.	52	.216E+03	.199E+03	0.
53	.216E+03	.182E+03	0.	54	.216E+03	.165E+03	0.
55	.216E+03	.148E+03	0.	56	.216E+03	.131E+03	0.
57	.216E+03	.113E+03	0.	58	.216E+03	.963E+02	0.
59	.216E+03	.791E+02	0.	60	.216E+03	.643E+02	0.
61	.216E+03	.494E+02	0.	62	.216E+03	.346E+02	0.
63	.216E+03	.197E+02	0.	64	.216E+03	.461E+01	0.
65	.212E+03	-.148E+02	0.	66	.201E+03	-.402E+02	0.
67	.199E+03	-.571E+02	0.	68	.184E+03	-.873E+02	0.
69	.184E+03	-.102E+03	0.	70	.176E+03	-.124E+03	0.
71	.180E+03	-.136E+03	0.	72	.174E+03	-.156E+03	0.
73	.174E+03	-.172E+03	0.	74	.165E+03	-.195E+03	0.
75	.162E+03	-.213E+03	0.	76	.216E+03	.216E+03	0.
77	.216E+03	.199E+03	0.	78	.216E+03	.182E+03	0.
79	.216E+03	.165E+03	0.	80	.216E+03	.148E+03	0.
81	.216E+03	.131E+03	0.	82	.216E+03	.113E+03	0.
83	.216E+03	.963E+02	0.	84	.216E+03	.791E+02	0.
85	.216E+03	.643E+02	0.	86	.216E+03	.494E+02	0.
87	.216E+03	.346E+02	0.	88	.216E+03	.197E+02	0.
89	.216E+03	.454E+01	0.	90	.212E+03	-.148E+02	0.
91	.201E+03	-.404E+02	0.	92	.198E+03	-.578E+02	0.
93	.182E+03	-.887E+02	0.	94	.184E+03	-.102E+03	0.
95	.176E+03	-.125E+03	0.	96	.180E+03	-.136E+03	0.
97	.174E+03	-.156E+03	0.	98	.174E+03	-.172E+03	0.
99	.165E+03	-.195E+03	0.	100	.162E+03	-.213E+03	0.
101	.208E+03	.208E+03	0.	102	.207E+03	.172E+03	0.
103	.206E+03	.137E+03	0.	104	.203E+03	.100E+03	0.
105	.144E+03	.722E+01	0.	106	.139E+03	-.279E+02	0.
107	.139E+03	-.580E+02	0.	108	.138E+03	-.881E+02	0.
109	.138E+03	-.118E+03	0.	110	.137E+03	-.148E+03	0.
111	.137E+03	-.178E+03	0.	112	.137E+03	-.208E+03	0.
113	.137E+03	-.238E+03	0.	114	.199E+03	.199E+03	0.
115	.196E+03	.162E+03	0.	116	.194E+03	.126E+03	0.
117	.181E+03	.779E+02	0.	118	.138E+03	.591E+00	0.
119	.137E+03	-.297E+02	0.	120	.137E+03	-.594E+02	0.
121	.137E+03	-.892E+02	0.	122	.137E+03	-.119E+03	0.
123	.137E+03	-.149E+03	0.	124	.137E+03	-.178E+03	0.
125	.137E+03	-.208E+03	0.	126	.137E+03	-.238E+03	0.
127	.189E+03	.189E+03	0.	128	.181E+03	.112E+03	0.
129	.137E+03	.143E+00	0.	130	.137E+03	-.594E+02	0.
131	.137E+03	-.119E+03	0.	132	.137E+03	-.178E+03	0.
133	.137E+03	-.238E+03	0.	134	.178E+03	.178E+03	0.
135	.166E+03	.974E+02	0.	136	.137E+03	.399E-01	0.
137	.137E+03	-.594E+02	0.	138	.137E+03	-.119E+03	0.
139	.137E+03	-.178E+03	0.	140	.137E+03	-.238E+03	0.
141	.167E+03	.167E+03	0.	142	.137E+03	.259E-01	0.
143	.137E+03	-.119E+03	0.	144	.137E+03	-.238E+03	0.
145	.156E+03	.156E+03	0.	146	.137E+03	.391E-02	0.
147	.137E+03	-.119E+03	0.	148	.137E+03	-.238E+03	0.
149	.148E+03	.148E+03	0.	150	.137E+03	.214E-02	0.
151	.137E+03	-.119E+03	0.	152	.137E+03	-.238E+03	0.
153	.142E+03	.142E+03	0.	154	.137E+03	.227E-02	0.
155	.137E+03	-.119E+03	0.	156	.137E+03	-.238E+03	0.
157	.139E+03	.139E+03	0.	158	.137E+03	.247E-03	0.
159	.137E+03	-.238E+03	0.	160	.137E+03	.137E+03	0.
161	.137E+03	-.238E+03	0.	162	.137E+03	.137E+03	0.
163	.137E+03	-.238E+03	0.	164	.137E+03	.137E+03	0.

```
165  .137E+03  -.238E+03  0.        166  .137E+03  .137E+03  0.
167  .137E+03  -.238E+03  0.        168  .137E+03  .137E+03  0.
169  .137E+03  -.238E+03  0.        170  .137E+03  .137E+03  0.
171  .137E+03  -.238E+03  0.        172  .137E+03  .137E+03  0.
173  .137E+03  -.238E+03  0.        174  .137E+03  .137E+03  0.
175  .137E+03  -.238E+03  0.        176  .137E+03  .137E+03  0.
177  .137E+03  -.238E+03  0.        178  .137E+03  .137E+03  0.
179  .137E+03  -.238E+03  0.        180  .137E+03  .137E+03  0.
181  .137E+03  -.238E+03  0.        182  .137E+03  .137E+03  0.
183  .137E+03  -.238E+03  0.        184  .137E+03  .137E+03  0.
185  .137E+03  -.238E+03  0.        186  .137E+03  .137E+03  0.
187  .137E+03  -.238E+03  0.        188  .137E+03  .137E+03  0.
189  .137E+03  -.238E+03  0.        190  .137E+03  .137E+03  0.
191  .137E+03  -.238E+03  0.        192  .137E+03  .137E+03  0.
193  .137E+03  -.238E+03  0.        194  .137E+03  .137E+03  0.
195  .137E+03  -.238E+03  0.        196  .137E+03  .137E+03  0.
197  .137E+03  -.238E+03  0.        198  .137E+03  .137E+03  0.
199  .137E+03  -.238E+03  0.        200  .137E+03  .137E+03  0.
201  .137E+03  -.238E+03  0.        202  .137E+03  .137E+03  0.
203  .137E+03  -.238E+03  0.        204  .137E+03  .137E+03  .547E-07
205  .137E+03  -.238E+03  .249E-06    0  0.        0.        0.
```

MOISTURE CONTENT AT UNSATURATED NODES CORRESPONDING TO MATERIAL 1

```
 90  .33520E+00   91  .30961E+00   92  .29223E+00
 93  .26128E+00   94  .24780E+00   95  .22491E+00
 96  .21415E+00   97  .19355E+00   98  .17838E+00
 99  .15525E+00  100  .14789E+00  106  .32211E+00
107  .29204E+00  108  .26190E+00  109  .23160E+00
110  .20162E+00  111  .17185E+00  112  .14868E+00
113  .14372E+00  119  .32029E+00  120  .29057E+00
121  .26085E+00  122  .23113E+00  123  .20141E+00
124  .17170E+00  125  .14866E+00  126  .14371E+00
130  .29056E+00  131  .23113E+00  132  .17170E+00
133  .14371E+00  137  .29057E+00  138  .23113E+00
139  .17170E+00  140  .14371E+00  143  .23113E+00
144  .14371E+00  147  .23113E+00  148  .14371E+00
151  .23113E+00  152  .14371E+00  155  .23113E+00
156  .14371E+00  159  .14371E+00  161  .14371E+00
163  .14371E+00  165  .14371E+00  167  .14371E+00
169  .14371E+00  171  .14371E+00  173  .14371E+00
175  .14371E+00  177  .14371E+00  179  .14371E+00
181  .14371E+00  183  .14371E+00  185  .14371E+00
187  .14371E+00  189  .14371E+00  191  .14371E+00
193  .14371E+00  195  .14371E+00  197  .14371E+00
199  .14371E+00  201  .14371E+00  203  .14371E+00
205  .14371E+00    0  0.            0  0.
```

MOISTURE CONTENT AT UNSATURATED NODES CORRESPONDING TO MATERIAL 2

```
 15  .25872E+00   16  .14462E+00   17  .99649E-01
 18  .98078E-01   19  .97291E-01   20  .96120E-01
 21  .95503E-01   22  .94435E-01   23  .93607E-01
 24  .92397E-01   25  .91451E-01   40  .25869E+00
 41  .14460E+00   42  .99645E-01   43  .98070E-01
 44  .97288E-01   45  .96115E-01   46  .95501E-01
 47  .94432E-01   48  .93607E-01   49  .92396E-01
 50  .91450E-01   65  .25860E+00   66  .14426E+00
 67  .99626E-01   68  .98034E-01   69  .97274E-01
 70  .96092E-01   71  .95493E-01   72  .94420E-01
 73  .93603E-01   74  .92391E-01   75  .91447E-01
 90  .25839E+00   91  .14324E+00   92  .99591E-01
 93  .97962E-01   94  .97253E-01   95  .96048E-01
 96  .95482E-01   97  .94398E-01   98  .93599E-01
 99  .92382E-01  100  .91440E-01    0  0.
```

TIME = .92708E+02 _ TIME STEP = 120

MAX CHANGE IN PRESS HEAD DURING ITERATION 2 WAS .23235E+00 AT NODE 26

CUMULATIVE INFLOW INTO SYSTEM IS = .61904E+04
DISCHARGE FROM WELL = 0.
WATER LEVEL IN WELL = .20466E+03

O NODE	HEAD	PRESS HEAD	DISCHARGE	NODE	HEAD	PRESS HEAD	DISCHARGE
1	.205E+03	.205E+03	.540E-01	2	.205E+03	.188E+03	.125E+00
3	.205E+03	.170E+03	.127E+00	4	.205E+03	.153E+03	.140E+00
5	.205E+03	.136E+03	.136E+00	6	.205E+03	.119E+03	.182E+00
7	.205E+03	.102E+03	.216E+00	8	.205E+03	.846E+02	.431E+00
9	.205E+03	.675E+02	.552E+00	10	.205E+03	.526E+02	.610E+00
11	.205E+03	.378E+02	.678E+00	12	.205E+03	.229E+02	.497E+00
13	.205E+03	.806E+01	-.402E+00	14	.205E+03	-.626E+01	0.
15	.205E+03	-.209E+02	0.	16	.204E+03	-.367E+02	0.
17	.198E+03	-.585E+02	0.	18	.187E+03	-.842E+02	0.
19	.182E+03	-.104E+03	0.	20	.178E+03	-.122E+03	0.
21	.177E+03	-.139E+03	0.	22	.174E+03	-.156E+03	0.
23	.171E+03	-.174E+03	0.	24	.168E+03	-.192E+03	0.
25	.166E+03	-.209E+03	0.	26	.205E+03	.205E+03	0.
27	.205E+03	.188E+03	0.	28	.205E+03	.170E+03	0.
29	.205E+03	.153E+03	0.	30	.205E+03	.136E+03	0.
31	.205E+03	.119E+03	0.	32	.205E+03	.102E+03	0.
33	.205E+03	.847E+02	0.	34	.205E+03	.676E+02	0.
35	.205E+03	.527E+02	0.	36	.205E+03	.379E+02	0.
37	.205E+03	.230E+02	0.	38	.205E+03	.816E+01	0.
39	.205E+03	-.626E+01	0.	40	.205E+03	-.209E+02	0.
41	.204E+03	-.367E+02	0.	42	.198E+03	-.585E+02	0.
43	.187E+03	-.842E+02	0.	44	.182E+03	-.104E+03	0.
45	.178E+03	-.122E+03	0.	46	.177E+03	-.139E+03	0.
47	.174E+03	-.156E+03	0.	48	.171E+03	-.174E+03	0.
49	.168E+03	-.192E+03	0.	50	.166E+03	-.209E+03	0.
51	.205E+03	.205E+03	0.	52	.205E+03	.188E+03	0.
53	.205E+03	.170E+03	0.	54	.205E+03	.153E+03	0.
55	.205E+03	.136E+03	0.	56	.205E+03	.119E+03	0.
57	.205E+03	.102E+03	0.	58	.205E+03	.847E+02	0.
59	.205E+03	.676E+02	0.	60	.205E+03	.527E+02	0.
61	.205E+03	.378E+02	0.	62	.205E+03	.230E+02	0.
63	.205E+03	.816E+01	0.	64	.205E+03	-.626E+01	0.
65	.205E+03	-.209E+02	0.	66	.204E+03	-.367E+02	0.
67	.198E+03	-.585E+02	0.	68	.187E+03	-.843E+02	0.
69	.182E+03	-.104E+03	0.	70	.178E+03	-.123E+03	0.
71	.177E+03	-.139E+03	0.	72	.174E+03	-.156E+03	0.
73	.171E+03	-.174E+03	0.	74	.168E+03	-.192E+03	0.
75	.166E+03	-.209E+03	0.	76	.205E+03	.205E+03	0.
77	.205E+03	.188E+03	0.	78	.205E+03	.170E+03	0.
79	.205E+03	.153E+03	0.	80	.205E+03	.136E+03	0.
81	.205E+03	.119E+03	0.	82	.205E+03	.102E+03	0.
83	.205E+03	.847E+02	0.	84	.205E+03	.676E+02	0.
85	.205E+03	.527E+02	0.	86	.205E+03	.378E+02	0.
87	.205E+03	.230E+02	0.	88	.205E+03	.816E+01	0.
89	.205E+03	-.627E+01	0.	90	.205E+03	-.209E+02	0.
91	.204E+03	-.368E+02	0.	92	.197E+03	-.587E+02	0.
93	.186E+03	-.845E+02	0.	94	.181E+03	-.104E+03	0.
95	.178E+03	-.123E+03	0.	96	.177E+03	-.139E+03	0.
97	.174E+03	-.156E+03	0.	98	.171E+03	-.174E+03	0.
99	.168E+03	-.192E+03	0.	100	.166E+03	-.209E+03	0.
101	.198E+03	.198E+03	0.	102	.196E+03	.162E+03	0.
103	.196E+03	.127E+03	0.	104	.191E+03	.885E+02	0.
105	.165E+03	.282E+02	0.	106	.147E+03	-.201E+02	0.
107	.145E+03	-.513E+02	0.	108	.144E+03	-.823E+02	0.
109	.141E+03	-.115E+03	0.	110	.139E+03	-.147E+03	0.

```
111   .138E+03  -.177E+03  0.        112   .138E+03  -.207E+03  0.
113   .138E+03  -.237E+03  0.        114   .190E+03   .190E+03  0.
115   .187E+03   .153E+03  0.        116   .186E+03   .117E+03  0.
117   .174E+03   .709E+02  0.        118   .146E+03   .877E+01  0.
119   .137E+03  -.294E+02  0.        120   .137E+03  -.592E+02  0.
121   .137E+03  -.891E+02  0.        122   .137E+03  -.119E+03  0.
123   .137E+03  -.149E+03  0.        124   .137E+03  -.178E+03  0.
125   .137E+03  -.208E+03  0.        126   .137E+03  -.238E+03  0.
127   .181E+03   .181E+03  0.        128   .174E+03   .106E+03  0.
129   .138E+03   .995E+00  0.        130   .137E+03  -.594E+02  0.
131   .137E+03  -.119E+03  0.        132   .137E+03  -.178E+03  0.
133   .137E+03  -.238E+03  0.        134   .172E+03   .172E+03  0.
135   .162E+03   .931E+02  0.        136   .137E+03   .274E+00  0.
137   .137E+03  -.594E+02  0.        138   .137E+03  -.119E+03  0.
139   .137E+03  -.178E+03  0.        140   .137E+03  -.238E+03  0.
141   .162E+03   .162E+03  0.        142   .137E+03   .151E+00  0.
143   .137E+03  -.119E+03  0.        144   .137E+03  -.238E+03  0.
145   .153E+03   .153E+03  0.        146   .137E+03   .240E-01  0.
147   .137E+03  -.119E+03  0.        148   .137E+03  -.238E+03  0.
149   .146E+03   .146E+03  0.        150   .137E+03   .127E-01  0.
151   .137E+03  -.119E+03  0.        152   .137E+03  -.238E+03  0.
153   .141E+03   .141E+03  0.        154   .137E+03   .133E-01  0.
155   .137E+03  -.119E+03  0.        156   .137E+03  -.238E+03  0.
157   .138E+03   .138E+03  0.        158   .137E+03   .147E-02  0.
159   .137E+03  -.238E+03  0.        160   .137E+03   .137E+03  0.
161   .137E+03  -.238E+03  0.        162   .137E+03   .137E+03  0.
163   .137E+03  -.238E+03  0.        164   .137E+03   .137E+03  0.
165   .137E+03  -.238E+03  0.        166   .137E+03   .137E+03  0.
167   .137E+03  -.238E+03  0.        168   .137E+03   .137E+03  0.
169   .137E+03  -.238E+03  0.        170   .137E+03   .137E+03  0.
171   .137E+03  -.238E+03  0.        172   .137E+03   .137E+03  0.
173   .137E+03  -.238E+03  0.        174   .137E+03   .137E+03  0.
175   .137E+03  -.238E+03  0.        176   .137E+03   .137E+03  0.
177   .137E+03  -.238E+03  0.        178   .137E+03   .137E+03  0.
179   .137E+03  -.238E+03  0.        180   .137E+03   .137E+03  0.
181   .137E+03  -.238E+03  0.        182   .137E+03   .137E+03  0.
183   .137E+03  -.238E+03  0.        184   .137E+03   .137E+03  0.
185   .137E+03  -.238E+03  0.        186   .137E+03   .137E+03  0.
187   .137E+03  -.238E+03  0.        188   .137E+03   .137E+03  0.
189   .137E+03  -.238E+03  0.        190   .137E+03   .137E+03  0.
191   .137E+03  -.238E+03  0.        192   .137E+03   .137E+03  0.
193   .137E+03  -.238E+03  0.        194   .137E+03   .137E+03  0.
195   .137E+03  -.238E+03  0.        196   .137E+03   .137E+03  0.
197   .137E+03  -.238E+03  0.        198   .137E+03   .137E+03  0.
199   .137E+03  -.238E+03  0.        200   .137E+03   .137E+03  0.
201   .137E+03  -.238E+03  0.        202   .137E+03   .137E+03  0.
203   .137E+03  -.238E+03  0.        204   .137E+03   .137E+03   .547E-07
205   .137E+03  -.238E+03  .249E-06    0   0.        0.        0.
```

MOISTURE CONTENT AT UNSATURATED NODES CORRESPONDING TO MATERIAL 1

```
 89   .34373E+00    90   .32907E+00    91   .31323E+00
 92   .29135E+00    93   .26552E+00    94   .24573E+00
 95   .22742E+00    96   .21104E+00    97   .19382E+00
 98   .17590E+00    99   .15753E+00   100   .14854E+00
106   .32988E+00   107   .29867E+00   108   .26765E+00
109   .23504E+00   110   .20315E+00   111   .17295E+00
112   .14880E+00   113   .14383E+00   119   .32060E+00
120   .29075E+00   121   .26091E+00   122   .23117E+00
123   .20142E+00   124   .17170E+00   125   .14866E+00
126   .14371E+00   130   .29056E+00   131   .23113E+00
132   .17170E+00   133   .14371E+00   137   .29057E+00
138   .23113E+00   139   .17169E+00   140   .14371E+00
143   .23113E+00   144   .14371E+00   147   .23113E+00
148   .14371E+00   151   .23113E+00   152   .14371E+00
```

155	.23113E+00	156	.14371E+00	159	.14371E+00
161	.14371E+00	163	.14371E+00	165	.14371E+00
167	.14371E+00	169	.14371E+00	171	.14371E+00
173	.14371E+00	175	.14371E+00	177	.14371E+00
179	.14371E+00	181	.14371E+00	183	.14371E+00
185	.14371E+00	187	.14371E+00	189	.14371E+00
191	.14371E+00	193	.14371E+00	195	.14371E+00
197	.14371E+00	199	.14371E+00	201	.14371E+00
203	.14371E+00	205	.14371E+00	0	0.

MOISTURE CONTENT AT UNSATURATED NODES CORRESPONDING TO MATERIAL 2

14	.28748E+00	15	.23103E+00	16	.15986E+00
17	.99555E-01	18	.98198E-01	19	.97150E-01
20	.96185E-01	21	.95320E-01	22	.94413E-01
23	.93470E-01	24	.92504E-01	25	.91646E-01
39	.28748E+00	40	.23102E+00	41	.15984E+00
42	.99555E-01	43	.98198E-01	44	.97150E-01
45	.96185E-01	46	.95320E-01	47	.94413E-01
48	.93469E-01	49	.92504E-01	50	.91646E-01
64	.28747E+00	65	.23097E+00	66	.15976E+00
67	.99552E-01	68	.98194E-01	69	.97148E-01
70	.96183E-01	71	.95320E-01	72	.94412E-01
73	.93469E-01	74	.92503E-01	75	.91645E-01
89	.28746E+00	90	.23083E+00	91	.15954E+00
92	.99545E-01	93	.98185E-01	94	.97144E-01
95	.96180E-01	96	.95318E-01	97	.94412E-01
98	.93468E-01	99	.92501E-01	100	.91643E-01
0	0.	0	0.	0	0.

Table 8. Input data file for a bail test for well NC7-25.

```
NC7-25   BAIL TEST
  205  25  191    1    2    0   30    1    1   25
    1   1   25    0    9    0    0    0    0
    8   4    8    4
   25  -1
1    2    3    4    5    6    7    8    9   10   11   12   13   14
15   16   17   18   19   20   21   22   23   24   25
1    1
5.52      0.0       0.0         10.36      0.5
.01       .10000E+091.1         .10000E+091.0
1.0       0.1591549
0.00004   0.00004   0.35       0.
0.1       0.1       0.30       0.
0.        0.        .15        .03       .20       .09       .25       .2
.28       .33       .30        .5        .32       .96       .35       1.0
.04       1000.     .10        500.      .15       200.      .35       0.
0.        0.        .13        .03       .17       .09       .22       .2
.24       .33       .26        .5        .28       .96       .30       1.0
.05       1000.     .10        50.       .28       10.       .30       0.
      1    2    5.52       0.0      10.36        0.0
      9    2    5.52      10.36      0.00        0.0
     25    2    5.52     134.11      0.0         0.0
     26    0    6.77       0.0     134.11        0.0
     34    0    6.77      10.36    123.75        0.0
     50    0    6.77     134.11      0.0         0.0
     51    0    8.65       0.0     134.11        0.0
     59    0    8.65      10.36    123.75        0.0
     75    0    8.65     134.11      0.0         0.0
     76    0   11.43       0.0     134.11        0.0
     84    0   11.43      10.36    123.75        0.0
    100    0   11.43     134.11      0.0         0.0
    101    0   15.03       0.0     134.11        0.0
    105    0   15.03      10.36    123.75        0.0
    113    0   15.03     134.11      0.0         0.0
    114    0   20.42       0.0     134.11        0.0
    118    0   20.42      10.36    123.75        0.0
    126    0   20.42     134.11      0.0         0.0
    127    0   28.50       0.0     134.11        0.0
    129    0   28.50      10.36    123.75        0.0
    133    0   28.50     134.11      0.0         0.0
    134    0   40.62       0.0     134.11        0.0
    136    0   40.62      10.36    123.75        0.0
    140    0   40.62     134.11      0.0         0.0
    141    0   58.79       0.0     134.11        0.0
    142    0   58.79      10.36    123.75        0.0
    144    0   58.79     134.11      0.0         0.0
    145    0   86.04       0.0     134.11        0.0
    146    0   86.04      10.36    123.75        0.0
    148    0   86.04     134.11      0.0         0.0
    149    0  126.91       0.0     134.11        0.0
    150    0  126.91      10.36    123.75        0.0
    152    0  126.91     134.11      0.0         0.0
    153    0  188.21       0.0     134.11        0.0
    154    0  188.21      10.36    123.75        0.0
    156    0  188.21     134.11      0.0         0.0
    157    0  280.16       0.0     134.11        0.0
    158    0  280.16      10.36    123.75        0.0
    159    0  280.16     134.11      0.0         0.0
```

160	0	418.08	0.0	134.11	0.0
161	0	418.08	134.11	0.0	0.0
162	0	624.96	0.0	134.11	0.0
163	0	624.96	134.11	0.0	0.0
164	0	935.27	0.0	134.11	0.0
165	0	935.27	134.11	0.0	0.0
166	0	1400.73	0.0	134.11	0.0
167	0	1400.73	134.11	0.0	0.0
168	0	2098.92	0.0	134.11	0.0
169	0	2098.92	134.11	0.0	0.0
170	0	3146.20	0.0	134.11	0.0
171	0	3146.20	134.11	0.0	0.0
172	0	4717.12	0.0	134.11	0.0
173	0	4717.12	134.11	0.0	0.0
174	0	7073.50	0.0	134.11	0.0
175	0	7073.50	134.11	0.0	0.0
176	0	10608.06	0.0	134.11	0.0
177	0	10608.06	134.11	0.0	0.0
178	0	15909.90	0.0	134.11	0.0
179	0	15909.90	134.11	0.0	0.0
180	0	23862.65	0.0	134.11	0.0
181	0	23862.65	134.11	0.0	0.0
182	0	35791.77	0.0	134.11	0.0
183	0	35791.77	134.11	0.0	0.0
184	0	53685.45	0.0	134.11	0.0
185	0	53685.45	134.11	0.0	0.0
186	0	80525.96	0.0	134.11	0.0
187	0	80525.96	134.11	0.0	0.0
188	0	120786.72	0.0	134.11	0.0
189	0	120786.72	134.11	0.0	0.0
190	0	181177.85	0.0	134.11	0.0
191	0	181177.85	134.11	0.0	0.0
192	0	271764.54	0.0	134.11	0.0
193	0	271764.54	134.11	0.0	0.0
194	0	407644.57	0.0	134.11	0.0
195	0	407644.57	134.11	0.0	0.0
196	0	611464.61	0.0	134.11	0.0
197	0	611464.61	134.11	0.0	0.0
198	0	917194.66	0.0	134.11	0.0
199	0	917194.66	134.11	0.0	0.0
200	0	1375789.73	0.0	134.11	0.0
201	0	1375789.73	134.11	0.0	0.0
202	0	2063682.33	0.0	134.11	0.0
203	0	2063682.33	134.11	0.0	0.0
204	1	3095521.23	0.0	134.11	0.0
205	1	3095521.23	134.11	0.0	0.0
1	1	26	27	2	2	0.0
24	24	49	50	25	2	0.0
25	26	51	52	27	2	0.0
48	49	74	75	50	2	0.0
49	51	76	77	52	2	0.0
72	74	99	100	75	2	0.0
73	76	101	77	77	1	0.0
74	77	101	102	102	1	0.0
75	77	102	78	78	1	0.0
76	78	102	79	79	1	0.0
77	79	102	103	103	1	0.0
78	79	103	80	80	1	0.0
79	80	103	81	81	1	0.0
80	81	103	104	104	1	0.0
81	81	104	82	82	1	0.0
82	82	104	83	83	1	0.0
83	83	104	105	105	1	0.0
84	83	105	84	84	1	0.0
85	84	105	85	85	1	0.0

86	85	105	106	106	1	0.0
87	85	106	86	86	1	0.0
88	86	106	87	87	1	0.0
89	87	106	107	107	1	0.0
90	87	107	88	88	1	0.0
91	88	107	89	89	1	0.0
92	89	107	108	108	1	0.0
93	89	108	90	90	1	0.0
94	90	108	91	91	1	0.0
95	91	108	109	109	1	0.0
96	91	109	92	92	1	0.0
97	92	109	93	93	1	0.0
98	93	109	110	110	1	0.0
99	93	110	94	94	1	0.0
100	94	110	95	95	1	0.0
101	95	110	111	111	1	0.0
102	95	111	96	96	1	0.0
103	96	111	97	97	1	0.0
104	97	111	112	112	1	0.0
105	97	112	98	98	1	0.0
106	98	112	99	99	1	0.0
107	99	112	113	113	1	0.0
108	99	113	100	100	1	0.0
109	101	114	115	102	1	0.0
114	106	119	120	107	1	0.0
115	107	120	121	108	1	0.0
120	112	125	126	113	1	0.0
121	114	127	115	115	1	0.0
122	115	127	128	128	1	0.0
123	115	128	116	116	1	0.0
124	116	128	117	117	1	0.0
125	117	128	129	129	1	0.0
126	117	129	118	118	1	0.0
127	118	129	119	119	1	0.0
128	119	129	130	130	1	0.0
129	119	130	120	120	1	0.0
130	120	130	121	121	1	0.0
131	121	130	131	131	1	0.0
132	121	131	122	122	1	0.0
133	122	131	123	123	1	0.0
134	123	131	132	132	1	0.0
135	123	132	124	124	1	0.0
136	124	132	125	125	1	0.0
137	125	132	133	133	1	0.0
138	125	133	126	126	1	0.0
139	127	134	135	128	1	0.0
141	129	136	137	130	1	0.0
142	130	137	138	131	1	0.0
144	132	139	140	133	1	0.0
145	134	141	135	135	1	0.0
146	135	141	142	142	1	0.0
147	135	142	136	136	1	0.0
148	136	142	137	137	1	0.0
149	137	142	143	143	1	0.0
150	137	143	138	138	1	0.0
151	138	143	139	139	1	0.0
152	139	143	144	144	1	0.0
153	139	144	140	140	1	0.0
154	141	145	146	142	1	0.0
156	143	147	148	144	1	0.0
157	145	149	150	146	1	0.0
159	147	151	152	148	1	0.0
160	149	153	154	150	1	0.0
162	151	155	156	152	1	0.0
163	153	157	158	154	1	0.0

164	154	158	155	155	1	0.0
165	155	158	159	159	1	0.0
166	155	159	156	156	1	0.0
167	157	160	158	158	1	0.0
168	158	160	161	161	1	0.0
169	158	161	159	159	1	0.0
170	160	162	163	161	1	0.0
171	162	164	165	163	1	0.0
172	164	166	167	165	1	0.0
173	166	168	169	167	1	0.0
174	168	170	171	169	1	0.0
175	170	172	173	171	1	0.0
176	172	174	175	173	1	0.0
177	174	176	177	175	1	0.0
178	176	178	179	177	1	0.0
179	178	180	181	179	1	0.0
180	180	182	183	181	1	0.0
181	182	184	185	183	1	0.0
182	184	186	187	185	1	0.0
183	186	188	189	187	1	0.0
184	188	190	191	189	1	0.0
185	190	192	193	191	1	0.0
186	192	194	195	193	1	0.0
187	194	196	197	195	1	0.0
188	196	198	199	197	1	0.0
189	198	200	201	199	1	0.0
190	200	202	203	201	1	0.0
191	202	204	205	203	1	0.0

END

Table 9. Output from UNSAT2 for a bail test for well NC7-25.

TIME =   .11639E+02   TIME STEP = 50

MAX CHANGE IN PRESS HEAD DURING ITERATION 2 WAS   .87860E-01 AT NODE   26

CUMULATIVE INFLOW INTO SYSTEM IS = -.38260E+03
DISCHARGE FROM WELL = 0.
WATER LEVEL IN WELL =   .13893E+02

NODE	HEAD	PRESS HEAD	DISCHARGE	NODE	HEAD	PRESS HEAD	DISCHARGE
1	.139E+02	.139E+02	-.215E+00	2	.139E+02	.126E+02	-.434E+00
3	.139E+02	.113E+02	-.489E+00	4	.139E+02	.100E+02	-.588E+00
5	.139E+02	.871E+01	-.739E+00	6	.139E+02	.742E+01	-.960E+00
7	.139E+02	.612E+01	-.128E+01	8	.139E+02	.483E+01	-.176E+01
9	.139E+02	.353E+01	-.102E+02	10	.181E+02	0.	-.126E+02
11	.258E+02	0.	-.221E+01	12	.336E+02	0.	-.509E+00
13	.413E+02	0.	-.785E-01	14	.490E+02	-.306E-01	0.
15	.567E+02	-.112E+00	0.	16	.642E+02	-.265E+00	0.
17	.717E+02	-.542E+00	0.	18	.790E+02	-.999E+00	0.
19	.860E+02	-.175E+01	0.	20	.925E+02	-.291E+01	0.
21	.985E+02	-.468E+01	0.	22	.104E+03	-.725E+01	0.
23	.108E+03	-.109E+02	0.	24	.111E+03	-.152E+02	0.
25	.113E+03	-.210E+02	0.	26	.140E+02	.140E+02	0.
27	.140E+02	.127E+02	0.	28	.140E+02	.114E+02	0.
29	.140E+02	.101E+02	0.	30	.140E+02	.885E+01	0.
31	.141E+02	.761E+01	0.	32	.142E+02	.640E+01	0.
33	.143E+02	.522E+01	0.	34	.145E+02	.411E+01	0.
35	.186E+02	.482E+00	0.	36	.259E+02	.924E-01	0.
37	.336E+02	.213E-01	0.	38	.413E+02	.368E-02	0.
39	.490E+02	-.302E-01	0.	40	.567E+02	-.111E+00	0.
41	.642E+02	-.264E+00	0.	42	.717E+02	-.541E+00	0.
43	.790E+02	-.998E+00	0.	44	.860E+02	-.175E+01	0.
45	.925E+02	-.291E+01	0.	46	.985E+02	-.468E+01	0.
47	.104E+03	-.725E+01	0.	48	.108E+03	-.109E+02	0.
49	.111E+03	-.152E+02	0.	50	.113E+03	-.209E+02	0.
51	.141E+02	.141E+02	0.	52	.141E+02	.128E+02	0.
53	.141E+02	.115E+02	0.	54	.142E+02	.103E+02	0.
55	.142E+02	.905E+01	0.	56	.143E+02	.786E+01	0.
57	.145E+02	.672E+01	0.	58	.147E+02	.564E+01	0.
59	.150E+02	.464E+01	0.	60	.190E+02	.915E+00	0.
61	.260E+02	.189E+00	0.	62	.336E+02	.445E-01	0.
63	.413E+02	.881E-02	0.	64	.490E+02	-.282E-01	0.
65	.567E+02	-.109E+00	0.	66	.642E+02	-.261E+00	0.
67	.717E+02	-.538E+00	0.	68	.790E+02	-.993E+00	0.
69	.860E+02	-.175E+01	0.	70	.925E+02	-.290E+01	0.
71	.985E+02	-.467E+01	0.	72	.104E+03	-.723E+01	0.
73	.108E+03	-.109E+02	0.	74	.111E+03	-.151E+02	0.
75	.113E+03	-.209E+02	0.	76	.141E+02	.141E+02	0.
77	.141E+02	.128E+02	0.	78	.142E+02	.116E+02	0.
79	.142E+02	.104E+02	0.	80	.143E+02	.915E+01	0.
81	.145E+02	.799E+01	0.	82	.147E+02	.688E+01	0.
83	.149E+02	.584E+01	0.	84	.152E+02	.487E+01	0.
85	.192E+02	.112E+01	0.	86	.261E+02	.242E+00	0.
87	.336E+02	.602E-01	0.	88	.413E+02	.147E-01	0.
89	.490E+02	-.233E-01	0.	90	.567E+02	-.104E+00	0.
91	.642E+02	-.253E+00	0.	92	.717E+02	-.530E+00	0.
93	.790E+02	-.977E+00	0.	94	.860E+02	-.173E+01	0.
95	.926E+02	-.287E+01	0.	96	.985E+02	-.465E+01	0.

97	.104E+03	-.718E+01	0.	98	.108E+03	-.108E+02	0.
99	.111E+03	-.150E+02	0.	100	.113E+03	-.207E+02	0.
101	.325E+02	.325E+02	0.	102	.325E+02	.299E+02	0.
103	.326E+02	.275E+02	0.	104	.330E+02	.253E+02	0.
105	.337E+02	.233E+02	0.	106	.429E+02	.171E+02	0.
107	.552E+02	.139E+02	0.	108	.692E+02	.124E+02	0.
109	.826E+02	.103E+02	0.	110	.976E+02	.993E+01	0.
111	.112E+03	.848E+01	0.	112	.133E+03	.145E+02	0.
113	.134E+03	-.371E+00	0.	114	.521E+02	.521E+02	0.
115	.523E+02	.497E+02	0.	116	.524E+02	.472E+02	0.
117	.528E+02	.450E+02	0.	118	.532E+02	.428E+02	0.
119	.617E+02	.359E+02	0.	120	.707E+02	.294E+02	0.
121	.830E+02	.262E+02	0.	122	.942E+02	.220E+02	0.
123	.109E+03	.211E+02	0.	124	.122E+03	.188E+02	0.
125	.134E+03	.154E+02	0.	126	.134E+03	-.178E-02	0.
127	.729E+02	.729E+02	0.	128	.731E+02	.679E+02	0.
129	.740E+02	.636E+02	0.	130	.879E+02	.466E+02	0.
131	.107E+03	.347E+02	0.	132	.134E+03	.308E+02	0.
133	.134E+03	-.674E-04	0.	134	.922E+02	.922E+02	0.
135	.925E+02	.873E+02	0.	136	.929E+02	.826E+02	0.
137	.105E+03	.641E+02	0.	138	.120E+03	.476E+02	0.
139	.134E+03	.309E+02	0.	140	.134E+03	-.835E-05	0.
141	.110E+03	.110E+03	0.	142	.110E+03	.100E+03	0.
143	.134E+03	.618E+02	0.	144	.134E+03	-.478E-05	0.
145	.122E+03	.122E+03	0.	146	.123E+03	.112E+03	0.
147	.134E+03	.619E+02	0.	148	.134E+03	-.547E-06	0.
149	.130E+03	.130E+03	0.	150	.130E+03	.119E+03	0.
151	.134E+03	.619E+02	0.	152	.134E+03	-.200E-06	0.
153	.133E+03	.133E+03	0.	154	.133E+03	.123E+03	0.
155	.134E+03	.619E+02	0.	156	.134E+03	-.372E-07	0.
157	.134E+03	.134E+03	0.	158	.134E+03	.124E+03	0.
159	.134E+03	-.430E-08	0.	160	.134E+03	.134E+03	0.
161	.134E+03	-.235E-10	0.	162	.134E+03	.134E+03	0.
163	.134E+03	-.385E-14	0.	164	.134E+03	.134E+03	0.
165	.134E+03	-.377E-14	0.	166	.134E+03	.134E+03	0.
167	.134E+03	-.442E-14	0.	168	.134E+03	.134E+03	0.
169	.134E+03	-.434E-14	0.	170	.134E+03	.134E+03	0.
171	.134E+03	-.425E-14	0.	172	.134E+03	.134E+03	0.
173	.134E+03	-.254E-14	0.	174	.134E+03	.134E+03	0.
175	.134E+03	-.364E-14	0.	176	.134E+03	.134E+03	0.
177	.134E+03	-.342E-14	0.	178	.134E+03	.134E+03	0.
179	.134E+03	-.309E-14	0.	180	.134E+03	.134E+03	0.
181	.134E+03	-.353E-14	0.	182	.134E+03	.134E+03	0.
183	.134E+03	-.333E-14	0.	184	.134E+03	.134E+03	0.
185	.134E+03	-.393E-14	0.	186	.134E+03	.134E+03	0.
187	.134E+03	-.337E-14	0.	188	.134E+03	.134E+03	0.
189	.134E+03	-.361E-14	0.	190	.134E+03	.134E+03	0.
191	.134E+03	-.333E-14	0.	192	.134E+03	.134E+03	0.
193	.134E+03	-.371E-14	0.	194	.134E+03	.134E+03	0.
195	.134E+03	-.357E-14	0.	196	.134E+03	.134E+03	0.
197	.134E+03	-.363E-14	0.	198	.134E+03	.134E+03	0.
199	.134E+03	-.412E-14	0.	200	.134E+03	.134E+03	0.
201	.134E+03	-.438E-14	0.	202	.134E+03	.134E+03	0.
203	.134E+03	-.513E-14	0.	204	.134E+03	.134E+03	-.165E-05
205	.134E+03	0.	.202E-15	0	0.	0.	0.

MOISTURE CONTENT AT UNSATURATED NODES CORRESPONDING TO MATERIAL 1

89	.34998E+00	90	.34990E+00	91	.34975E+00
92	.34947E+00	93	.34902E+00	94	.34827E+00
95	.34713E+00	96	.34535E+00	97	.34282E+00
98	.33917E+00	99	.33498E+00	100	.32925E+00
113	.34963E+00	126	.35000E+00	133	.35000E+00
140	.35000E+00	144	.35000E+00	148	.35000E+00
152	.35000E+00	156	.35000E+00	159	.35000E+00

```
161  .35000E+00   163  .35000E+00   165  .35000E+00
167  .35000E+00   169  .35000E+00   171  .35000E+00
173  .35000E+00   175  .35000E+00   177  .35000E+00
179  .35000E+00   181  .35000E+00   183  .35000E+00
185  .35000E+00   187  .35000E+00   189  .35000E+00
191  .35000E+00   193  .35000E+00   195  .35000E+00
197  .35000E+00   199  .35000E+00   201  .35000E+00
203  .35000E+00     0  0.            0  0.
```

MOISTURE CONTENT AT UNSATURATED NODES CORRESPONDING TO MATERIAL 2

```
14  .29994E+00   15  .29978E+00   16  .29947E+00
17  .29892E+00   18  .29800E+00   19  .29649E+00
20  .29418E+00   21  .29063E+00   22  .28550E+00
23  .27589E+00   24  .25680E+00   25  .23065E+00
39  .29994E+00   40  .29978E+00   41  .29947E+00
42  .29892E+00   43  .29800E+00   44  .29650E+00
45  .29419E+00   46  .29064E+00   47  .28550E+00
48  .27591E+00   49  .25681E+00   50  .23073E+00
64  .29994E+00   65  .29978E+00   66  .29948E+00
67  .29892E+00   68  .29801E+00   69  .29651E+00
70  .29421E+00   71  .29066E+00   72  .28554E+00
73  .27601E+00   74  .25696E+00   75  .23097E+00
89  .29995E+00   90  .29979E+00   91  .29949E+00
92  .29894E+00   93  .29805E+00   94  .29654E+00
95  .29426E+00   96  .29071E+00   97  .28564E+00
98  .27626E+00   99  .25740E+00  100  .23163E+00
 0  0.            0  0.            0  0.
```

TIME =   .13780E+04   TIME STEP = 100

MAX CHANGE IN PRESS HEAD DURING ITERATION 2 WAS   .42006E+00 AT NODE   27

CUMULATIVE INFLOW INTO SYSTEM IS = -.53393E+04
DISCHARGE FROM WELL = 0.
WATER LEVEL IN WELL =   .61671E+02

0 NODE	HEAD	PRESS HEAD	DISCHARGE	NODE	HEAD	PRESS HEAD	DISCHARGE
1	.617E+02	.617E+02	-.586E-02	2	.617E+02	.604E+02	-.113E-01
3	.617E+02	.591E+02	-.113E-01	4	.617E+02	.578E+02	-.113E-01
5	.617E+02	.565E+02	-.113E-01	6	.617E+02	.552E+02	-.113E-01
7	.617E+02	.539E+02	-.113E-01	8	.617E+02	.526E+02	-.113E-01
9	.617E+02	.513E+02	-.405E-01	10	.617E+02	.436E+02	-.717E-01
11	.617E+02	.358E+02	-.717E-01	12	.617E+02	.281E+02	-.776E-01
13	.617E+02	.204E+02	-.881E-01	14	.617E+02	.126E+02	-.153E+00
15	.617E+02	.490E+01	-.551E+00	16	.617E+02	-.282E+01	0.
17	.618E+02	-.104E+02	0.	18	.621E+02	-.179E+02	0.
19	.626E+02	-.251E+02	0.	20	.636E+02	-.318E+02	0.
21	.652E+02	-.380E+02	0.	22	.677E+02	-.432E+02	0.
23	.707E+02	-.479E+02	0.	24	.730E+02	-.534E+02	0.
25	.736E+02	-.605E+02	0.	26	.615E+02	.615E+02	0.
27	.615E+02	.602E+02	0.	28	.615E+02	.589E+02	0.
29	.615E+02	.576E+02	0.	30	.615E+02	.563E+02	0.
31	.615E+02	.550E+02	0.	32	.615E+02	.537E+02	0.
33	.615E+02	.524E+02	0.	34	.615E+02	.511E+02	0.
35	.615E+02	.434E+02	0.	36	.615E+02	.357E+02	0.
37	.615E+02	.279E+02	0.	38	.615E+02	.202E+02	0.
39	.615E+02	.125E+02	0.	40	.615E+02	.476E+01	0.
41	.617E+02	-.282E+01	0.	42	.618E+02	-.104E+02	0.
43	.621E+02	-.179E+02	0.	44	.626E+02	-.251E+02	0.
45	.636E+02	-.318E+02	0.	46	.652E+02	-.380E+02	0.
47	.677E+02	-.432E+02	0.	48	.707E+02	-.479E+02	0.
49	.730E+02	-.534E+02	0.	50	.736E+02	-.605E+02	0.

51	.615E+02	.615E+02	0.	52	.615E+02	.602E+02	0.
53	.615E+02	.589E+02	0.	54	.615E+02	.576E+02	0.
55	.615E+02	.563E+02	0.	56	.615E+02	.550E+02	0.
57	.615E+02	.537E+02	0.	58	.615E+02	.524E+02	0.
59	.615E+02	.511E+02	0.	60	.615E+02	.434E+02	0.
61	.615E+02	.357E+02	0.	62	.615E+02	.279E+02	0.
63	.615E+02	.202E+02	0.	64	.615E+02	.125E+02	0.
65	.615E+02	.478E+01	0.	66	.617E+02	-.282E+01	0.
67	.618E+02	-.104E+02	0.	68	.621E+02	-.179E+02	0.
69	.626E+02	-.251E+02	0.	70	.637E+02	-.318E+02	0.
71	.652E+02	-.379E+02	0.	72	.677E+02	-.432E+02	0.
73	.708E+02	-.478E+02	0.	74	.731E+02	-.533E+02	0.
75	.737E+02	-.604E+02	0.	76	.615E+02	.615E+02	0.
77	.615E+02	.602E+02	0.	78	.615E+02	.589E+02	0.
79	.615E+02	.576E+02	0.	80	.615E+02	.563E+02	0.
81	.615E+02	.550E+02	0.	82	.615E+02	.537E+02	0.
83	.615E+02	.524E+02	0.	84	.615E+02	.512E+02	0.
85	.615E+02	.434E+02	0.	86	.615E+02	.357E+02	0.
87	.615E+02	.280E+02	0.	88	.615E+02	.202E+02	0.
89	.615E+02	.125E+02	0.	90	.616E+02	.479E+01	0.
91	.617E+02	-.282E+01	0.	92	.618E+02	-.104E+02	0.
93	.621E+02	-.179E+02	0.	94	.627E+02	-.250E+02	0.
95	.637E+02	-.317E+02	0.	96	.653E+02	-.379E+02	0.
97	.679E+02	-.430E+02	0.	98	.710E+02	-.476E+02	0.
99	.733E+02	-.530E+02	0.	100	.740E+02	-.602E+02	0.
101	.711E+02	.711E+02	0.	102	.710E+02	.684E+02	0.
103	.710E+02	.658E+02	0.	104	.710E+02	.633E+02	0.
105	.711E+02	.607E+02	0.	106	.717E+02	.459E+02	0.
107	.719E+02	.306E+02	0.	108	.724E+02	.156E+02	0.
109	.713E+02	-.983E+00	0.	110	.775E+02	-.102E+02	0.
111	.859E+02	-.173E+02	0.	112	.984E+02	-.203E+02	0.
113	.103E+03	-.316E+02	0.	114	.815E+02	.815E+02	0.
115	.816E+02	.790E+02	0.	116	.815E+02	.763E+02	0.
117	.816E+02	.738E+02	0.	118	.815E+02	.711E+02	0.
119	.830E+02	.572E+02	0.	120	.835E+02	.422E+02	0.
121	.853E+02	.286E+02	0.	122	.858E+02	.136E+02	0.
123	.940E+02	.629E+01	0.	124	.103E+03	-.118E+00	0.
125	.116E+03	-.253E+01	0.	126	.122E+03	-.124E+02	0.
127	.931E+02	.931E+02	0.	128	.931E+02	.879E+02	0.
129	.932E+02	.829E+02	0.	130	.966E+02	.553E+02	0.
131	.101E+03	.291E+02	0.	132	.120E+03	.165E+02	0.
133	.131E+03	-.352E+01	0.	134	.105E+03	.105E+03	0.
135	.105E+03	.995E+02	0.	136	.105E+03	.945E+02	0.
137	.110E+03	.688E+02	0.	138	.116E+03	.438E+02	0.
139	.129E+03	.263E+02	0.	140	.134E+03	-.513E+00	0.
141	.116E+03	.116E+03	0.	142	.116E+03	.106E+03	0.
143	.130E+03	.581E+02	0.	144	.134E+03	-.146E+00	0.
145	.125E+03	.125E+03	0.	146	.125E+03	.115E+03	0.
147	.133E+03	.613E+02	0.	148	.134E+03	-.107E-01	0.
149	.131E+03	.131E+03	0.	150	.131E+03	.120E+03	0.
151	.134E+03	.617E+02	0.	152	.134E+03	-.247E-02	0.
153	.133E+03	.133E+03	0.	154	.133E+03	.123E+03	0.
155	.134E+03	.618E+02	0.	156	.134E+03	-.457E-03	0.
157	.134E+03	.134E+03	0.	158	.134E+03	.124E+03	0.
159	.134E+03	-.530E-04	0.	160	.134E+03	.134E+03	0.
161	.134E+03	-.331E-06	0.	162	.134E+03	.134E+03	0.
163	.134E+03	-.990E-10	0.	164	.134E+03	.134E+03	0.
165	.134E+03	-.111E-11	0.	166	.134E+03	.134E+03	0.
167	.134E+03	-.113E-11	0.	168	.134E+03	.134E+03	0.
169	.134E+03	-.116E-11	0.	170	.134E+03	.134E+03	0.
171	.134E+03	-.115E-11	0.	172	.134E+03	.134E+03	0.
173	.134E+03	-.925E-12	0.	174	.134E+03	.134E+03	0.
175	.134E+03	-.114E-11	0.	176	.134E+03	.134E+03	0.
177	.134E+03	-.103E-11	0.	178	.134E+03	.134E+03	0.
179	.134E+03	-.965E-12	0.	180	.134E+03	.134E+03	0.

```
181   .134E+03   -.907E-12   0.        182   .134E+03   .134E+03   0.
183   .134E+03   -.876E-12   0.        184   .134E+03   .134E+03   0.
185   .134E+03   -.102E-11   0.        186   .134E+03   .134E+03   0.
187   .134E+03   -.105E-11   0.        188   .134E+03   .134E+03   0.
189   .134E+03   -.940E-12   0.        190   .134E+03   .134E+03   0.
191   .134E+03   -.931E-12   0.        192   .134E+03   .134E+03   0.
193   .134E+03   -.876E-12   0.        194   .134E+03   .134E+03   0.
195   .134E+03   -.909E-12   0.        196   .134E+03   .134E+03   0.
197   .134E+03   -.974E-12   0.        198   .134E+03   .134E+03   0.
199   .134E+03   -.108E-11   0.        200   .134E+03   .134E+03   0.
201   .134E+03   -.105E-11   0.        202   .134E+03   .134E+03   0.
203   .134E+03   -.128E-11   0.        204   .134E+03   .134E+03   -.165E-05
205   .134E+03   0.          .502E-13   0   0.         0.         0.
```

MOISTURE CONTENT AT UNSATURATED NODES CORRESPONDING TO MATERIAL 1

```
 91   .34718E+00    92   .33961E+00    93   .33212E+00
 94   .32496E+00    95   .31827E+00    96   .31212E+00
 97   .30698E+00    98   .30238E+00    99   .29697E+00
100   .28984E+00   109   .34902E+00   110   .33976E+00
111   .33269E+00   112   .32972E+00   113   .31842E+00
124   .34988E+00   125   .34747E+00   126   .33762E+00
133   .34648E+00   140   .34949E+00   144   .34985E+00
148   .34999E+00   152   .35000E+00   156   .35000E+00
159   .35000E+00   161   .35000E+00   163   .35000E+00
165   .35000E+00   167   .35000E+00   169   .35000E+00
171   .35000E+00   173   .35000E+00   175   .35000E+00
177   .35000E+00   179   .35000E+00   181   .35000E+00
183   .35000E+00   185   .35000E+00   187   .35000E+00
189   .35000E+00   191   .35000E+00   193   .35000E+00
195   .35000E+00   197   .35000E+00   199   .35000E+00
201   .35000E+00   203   .35000E+00     0   0.
```

MOISTURE CONTENT AT UNSATURATED NODES CORRESPONDING TO MATERIAL 2

```
 16   .29436E+00    17   .27820E+00    18   .24449E+00
 19   .21221E+00    20   .18194E+00    21   .15409E+00
 22   .13047E+00    23   .10942E+00    24   .99820E-01
 25   .99448E-01    41   .29436E+00    42   .27820E+00
 43   .24449E+00    44   .21222E+00    45   .18195E+00
 46   .15411E+00    47   .13051E+00    48   .10949E+00
 49   .99821E-01    50   .99449E-01    66   .29436E+00
 67   .27821E+00    68   .24450E+00    69   .21225E+00
 70   .18202E+00    71   .15423E+00    72   .13074E+00
 73   .10981E+00    74   .99826E-01    75   .99454E-01
 91   .29437E+00    92   .27822E+00    93   .24453E+00
 94   .21233E+00    95   .18220E+00    96   .15456E+00
 97   .13142E+00    98   .11070E+00    99   .99840E-01
100   .99465E-01     0   0.            0   0.
```

TIME =   .92708E+04   TIME STEP = 120

MAX CHANGE IN PRESS HEAD DURING ITERATION 2 WAS   .76829E+00 AT NODE   32

CUMULATIVE INFLOW INTO SYSTEM IS = -.95462E+04
DISCHARGE FROM WELL = 0.
WATER LEVEL IN WELL =   .10388E+03

```
0 NODE   HEAD    PRESS HEAD  DISCHARGE  NODE    HEAD    PRESS HEAD  DISCHARGE

     1   .104E+03   .104E+03  -.212E-02    2   .104E+03   .103E+03  -.409E-02
     3   .104E+03   .101E+03  -.409E-02    4   .104E+03   .100E+03  -.409E-02
     5   .104E+03   .987E+02  -.408E-02    6   .104E+03   .974E+02  -.408E-02
     7   .104E+03   .961E+02  -.407E-02    8   .104E+03   .948E+02  -.407E-02
```

9	.104E+03	.935E+02	-.146E-01	10	.104E+03	.858E+02	-.254E-01
11	.104E+03	.781E+02	-.248E-01	12	.104E+03	.703E+02	-.256E-01
13	.104E+03	.626E+02	-.248E-01	14	.104E+03	.549E+02	-.259E-01
15	.104E+03	.471E+02	-.254E-01	16	.104E+03	.394E+02	-.261E-01
17	.104E+03	.316E+02	-.249E-01	18	.104E+03	.239E+02	-.251E-01
19	.104E+03	.162E+02	-.205E-01	20	.104E+03	.845E+01	0.
21	.104E+03	.712E+00	0.	22	.104E+03	-.731E+01	0.
23	.104E+03	-.151E+02	0.	24	.104E+03	-.228E+02	0.
25	.104E+03	-.306E+02	0.	26	.104E+03	.104E+03	0.
27	.104E+03	.102E+03	0.	28	.104E+03	.101E+03	0.
29	.104E+03	.997E+02	0.	30	.104E+03	.984E+02	0.
31	.104E+03	.971E+02	0.	32	.104E+03	.958E+02	0.
33	.104E+03	.943E+02	0.	34	.104E+03	.933E+02	0.
35	.104E+03	.855E+02	0.	36	.104E+03	.778E+02	0.
37	.104E+03	.700E+02	0.	38	.104E+03	.623E+02	0.
39	.104E+03	.546E+02	0.	40	.104E+03	.468E+02	0.
41	.104E+03	.391E+02	0.	42	.104E+03	.314E+02	0.
43	.104E+03	.236E+02	0.	44	.104E+03	.159E+02	0.
45	.104E+03	.817E+01	0.	46	.104E+03	.430E+00	0.
47	.104E+03	-.731E+01	0.	48	.104E+03	-.151E+02	0.
49	.104E+03	-.228E+02	0.	50	.104E+03	-.306E+02	0.
51	.104E+03	.104E+03	0.	52	.104E+03	.102E+03	0.
53	.104E+03	.101E+03	0.	54	.104E+03	.997E+02	0.
55	.104E+03	.984E+02	0.	56	.104E+03	.971E+02	0.
57	.104E+03	.958E+02	0.	58	.104E+03	.945E+02	0.
59	.104E+03	.933E+02	0.	60	.104E+03	.855E+02	0.
61	.104E+03	.778E+02	0.	62	.104E+03	.700E+02	0.
63	.104E+03	.623E+02	0.	64	.104E+03	.546E+02	0.
65	.104E+03	.468E+02	0.	66	.104E+03	.391E+02	0.
67	.104E+03	.314E+02	0.	68	.104E+03	.236E+02	0.
69	.104E+03	.159E+02	0.	70	.104E+03	.817E+01	0.
71	.104E+03	.430E+00	0.	72	.104E+03	-.731E+01	0.
73	.104E+03	-.151E+02	0.	74	.104E+03	-.228E+02	0.
75	.104E+03	-.306E+02	0.	76	.104E+03	.104E+03	0.
77	.104E+03	.102E+03	0.	78	.104E+03	.101E+03	0.
79	.104E+03	.997E+02	0.	80	.104E+03	.984E+02	0.
81	.104E+03	.971E+02	0.	82	.104E+03	.958E+02	0.
83	.104E+03	.945E+02	0.	84	.104E+03	.933E+02	0.
85	.104E+03	.855E+02	0.	86	.104E+03	.778E+02	0.
87	.104E+03	.701E+02	0.	88	.104E+03	.623E+02	0.
89	.104E+03	.546E+02	0.	90	.104E+03	.468E+02	0.
91	.104E+03	.391E+02	0.	92	.104E+03	.314E+02	0.
93	.104E+03	.236E+02	0.	94	.104E+03	.159E+02	0.
95	.104E+03	.817E+01	0.	96	.104E+03	.431E+00	0.
97	.104E+03	-.731E+01	0.	98	.104E+03	-.151E+02	0.
99	.104E+03	-.228E+02	0.	100	.104E+03	-.306E+02	0.
101	.107E+03	.107E+03	0.	102	.107E+03	.104E+03	0.
103	.107E+03	.102E+03	0.	104	.107E+03	.993E+02	0.
105	.107E+03	.967E+02	0.	106	.107E+03	.813E+02	0.
107	.107E+03	.658E+02	0.	108	.107E+03	.505E+02	0.
109	.107E+03	.349E+02	0.	110	.107E+03	.195E+02	0.
111	.107E+03	.336E+01	0.	112	.106E+03	-.129E+02	0.
113	.106E+03	-.278E+02	0.	114	.111E+03	.111E+03	0.
115	.111E+03	.108E+03	0.	116	.111E+03	.106E+03	0.
117	.111E+03	.103E+03	0.	118	.111E+03	.100E+03	0.
119	.111E+03	.853E+02	0.	120	.111E+03	.697E+02	0.
121	.111E+03	.545E+02	0.	122	.111E+03	.389E+02	0.
123	.111E+03	.236E+02	0.	124	.111E+03	.737E+01	0.
125	.110E+03	-.860E+01	0.	126	.111E+03	-.234E+02	0.
127	.115E+03	.115E+03	0.	128	.115E+03	.110E+03	0.
129	.115E+03	.105E+03	0.	130	.115E+03	.742E+02	0.
131	.116E+03	.434E+02	0.	132	.115E+03	.123E+02	0.
133	.117E+03	-.168E+02	0.	134	.119E+03	.119E+03	0.
135	.119E+03	.114E+03	0.	136	.119E+03	.109E+03	0.
137	.120E+03	.788E+02	0.	138	.120E+03	.482E+02	0.

```
139  .122E+03  .185E+02  0.        140  .125E+03  -.938E+01  0.
141  .124E+03  .124E+03  0.        142  .124E+03   .114E+03  0.
143  .125E+03  .531E+02  0.        144  .130E+03  -.374E+01  0.
145  .128E+03  .128E+03  0.        146  .128E+03   .118E+03  0.
147  .130E+03  .581E+02  0.        148  .133E+03  -.750E+00  0.
149  .131E+03  .131E+03  0.        150  .132E+03   .121E+03  0.
151  .133E+03  .608E+02  0.        152  .134E+03  -.126E+00  0.
153  .133E+03  .133E+03  0.        154  .133E+03   .123E+03  0.
155  .134E+03  .617E+02  0.        156  .134E+03  -.192E-01  0.
157  .134E+03  .134E+03  0.        158  .134E+03   .124E+03  0.
159  .134E+03  -.218E-02 0.        160  .134E+03   .134E+03  0.
161  .134E+03  -.230E-04 0.        162  .134E+03   .134E+03  0.
163  .134E+03  -.472E-07 0.        164  .134E+03   .134E+03  0.
165  .134E+03  -.449E-10 0.        166  .134E+03   .134E+03  0.
167  .134E+03  -.899E-11 0.        168  .134E+03   .134E+03  0.
169  .134E+03  -.895E-11 0.        170  .134E+03   .134E+03  0.
171  .134E+03  -.912E-11 0.        172  .134E+03   .134E+03  0.
173  .134E+03  -.752E-11 0.        174  .134E+03   .134E+03  0.
175  .134E+03  -.932E-11 0.        176  .134E+03   .134E+03  0.
177  .134E+03  -.814E-11 0.        178  .134E+03   .134E+03  0.
179  .134E+03  -.809E-11 0.        180  .134E+03   .134E+03  0.
181  .134E+03  -.732E-11 0.        182  .134E+03   .134E+03  0.
183  .134E+03  -.732E-11 0.        184  .134E+03   .134E+03  0.
185  .134E+03  -.844E-11 0.        186  .134E+03   .134E+03  0.
187  .134E+03  -.819E-11 0.        188  .134E+03   .134E+03  0.
189  .134E+03  -.740E-11 0.        190  .134E+03   .134E+03  0.
191  .134E+03  -.783E-11 0.        192  .134E+03   .134E+03  0.
193  .134E+03  -.659E-11 0.        194  .134E+03   .134E+03  0.
195  .134E+03  -.708E-11 0.        196  .134E+03   .134E+03  0.
197  .134E+03  -.755E-11 0.        198  .134E+03   .134E+03  0.
199  .134E+03  -.826E-11 0.        200  .134E+03   .134E+03  0.
201  .134E+03  -.806E-11 0.        202  .134E+03   .134E+03  0.
203  .134E+03  -.943E-11 0.        204  .134E+03   .134E+03  -.165E-05
205  .134E+03  0.        .371E-12   0  0.         0.         0.
```

MOISTURE CONTENT AT UNSATURATED NODES CORRESPONDING TO MATERIAL 1

```
 97  .34269E+00    98  .33494E+00    99  .32719E+00
100  .31944E+00   112  .33713E+00   113  .32219E+00
125  .34140E+00   126  .32663E+00   133  .33322E+00
140  .34062E+00   144  .34626E+00   148  .34925E+00
152  .34987E+00   156  .34998E+00   159  .35000E+00
161  .35000E+00   163  .35000E+00   165  .35000E+00
167  .35000E+00   169  .35000E+00   171  .35000E+00
173  .35000E+00   175  .35000E+00   177  .35000E+00
179  .35000E+00   181  .35000E+00   183  .35000E+00
185  .35000E+00   187  .35000E+00   189  .35000E+00
191  .35000E+00   193  .35000E+00   195  .35000E+00
197  .35000E+00   199  .35000E+00   201  .35000E+00
203  .35000E+00     0  0.             0  0.
```

MOISTURE CONTENT AT UNSATURATED NODES CORRESPONDING TO MATERIAL 2

```
 22  .28537E+00    23  .25723E+00    24  .22233E+00
 25  .18748E+00    47  .28537E+00    48  .25723E+00
 49  .22233E+00    50  .18748E+00    72  .28537E+00
 73  .25723E+00    74  .22234E+00    75  .18748E+00
 97  .28537E+00    98  .25723E+00    99  .22235E+00
100  .18750E+00     0  0.             0  0.
```

APPENDIX C. VARIABLES USED IN CALCULATING HYDRAULIC
CONDUCTIVITY FOR FIELD TESTS

Table 10. Variables used in the Hvorslev method (1951)
to calculate hydraulic conductivity for Site 300 wells.

Variables	NC7-25 Slug Test	NC7-25 Bail Test	NC7-23 Slug Test	NC7-23 Bail Test	NC2-08 Slug Test	NC2-08 Bail Test
Hvorslev:						
To (sec)	4500	10000	35000	44000	420	420
R (cm)	6.46	6.46	3.35	3.35	7.45	7.45
r (cm)	6.46	6.46	3.35	3.35	7.45	7.45
L (cm)	173.2	88.3	203.9	74.14	881.2	827.2
Hvorslev modified:						
To (sec)	6000	14000	40000	45000	425	400
R (cm)	6.46	6.46	3.35	3.35	7.45	7.45
r (cm)	6.46	6.46	3.35	3.35	7.45	7.45
L (cm)	173.20	88.3	203.9	74.14	881.2	827.2

Table 11.   Variables used in the method of Bouwer and
Rice (1976) to calculate hydraulic conductivity for Site 300
wells.

Variables		NC7-25 Slug Test	NC7-25 Bail Test	NC7-23 Slug Test	NC7-23 Bail Test	NC2-08 Slug Test	NC2-08 Bail Test
Bouwer and Rice:							
r	(cm)	6.46	6.46	3.35	3.35	7.45	7.45
L	(cm)	173.20	88.30	203.90	120.20	881.20	827.20
ln (Re/r)	( )	2.40	2.40	3.20	3.20	4.20	4.20
Yo	(cm)	237.70	134.11	182.88	166.12	213.36	182.88
Yt	(cm)	14.30	17.40	18.30	33.20	21.30	36.60
t	(sec)	12000.00	20000.00	80000.00	70000.00	880.00	680.00
Bouwer and Rice modified:							
r	(cm)	6.46	6.46	3.35	3.35	7.45	7.45
L	(cm)	173.20	88.30	203.90	120.20	881.20	827.20
ln (Re/r)	( )	2.40	2.40	3.20	3.20	4.20	4.20
Yo	(cm)	61.80	73.80	115.20	132.90	64.00	54.90
Yt	(cm)	11.12	7.40	28.80	33.20	16.00	13.70
t	(sec)	10000.00	30000.00	54000.00	64000.00	560.00	580.00